

AD _____

Award Number: W81XWH-07-1-0134

TITLE: S-Nitrosylation and the Development of Pulmonary Hypertension

PRINCIPAL INVESTIGATOR: Lisa A. Palmer Ph.D.

CONTRACTING ORGANIZATION:
University of Virginia
Charlottesville, VA 22904

REPORT DATE: February 2011

TYPE OF REPORT: Final

PREPARED FOR: U. S. Army Medical Research and Materiel Command
Fort Detrick, Maryland 21702-5012

DISTRIBUTION STATEMENT:

Approved for public release; distribution unlimited

The views, opinions and/or finding contained in this report are those of the author(s) and should not be construed as an official Department of the Army position, policy or decision unless so designated by other documentation.

REPORT DOCUMENTATION PAGE

Form Approved
OMB No. 0704-0188

Public reporting burden for this collection of information is estimated to average 1 hour per response, including the time for reviewing instructions, searching existing data sources, gathering and maintaining the data needed, and completing and reviewing this collection of information. Send comments regarding this burden estimate or any other aspect of this collection of information, including suggestions for reducing this burden to Department of Defense, Washington Headquarters Services, Directorate for Information Operations and Reports (0704-0188), 1215 Jefferson Davis Highway, Suite 1204, Arlington, VA 22202-4302. Respondents should be aware that notwithstanding any other provision of law, no person shall be subject to any penalty for failing to comply with a collection of information if it does not display a currently valid OMB control number. **PLEASE DO NOT RETURN YOUR FORM TO THE ABOVE ADDRESS.**

1. REPORT DATE (DD-MM-YYYY) 01-02-2011		2. REPORT TYPE Final		3. DATES COVERED (From - To) 15 Jan 2007 -14 Jan 2011	
4. TITLE AND SUBTITLE S-Nitrosylation and the Development of Pulmonary Hypertension				5a. CONTRACT NUMBER	
				5b. GRANT NUMBER W81XWH-07-1-0134	
				5c. PROGRAM ELEMENT NUMBER	
6. AUTHOR(S) Lisa A. Palmer r r 7y B xki kplc Qf w				5d. PROJECT NUMBER	
				5e. TASK NUMBER	
				5f. WORK UNIT NUMBER	
7. PERFORMING ORGANIZATION NAME(S) AND ADDRESS(ES) University of Virginia Charlottesville, VA 22904				8. PERFORMING ORGANIZATION REPORT NUMBER	
9. SPONSORING / MONITORING AGENCY NAME(S) AND ADDRESS(ES) U.S. Army Medical Research And Materiel Command Fort Detrick, Maryland 21702				10. SPONSOR/MONITOR'S ACRONYM(S)	
				11. SPONSOR/MONITOR'S REPORT NUMBER(S)	
12. DISTRIBUTION / AVAILABILITY STATEMENT Approved for public release; distribution unlimited.					
13. SUPPLEMENTARY NOTES					
14. ABSTRACT Pulmonary hypertension (PH), high blood pressure in the lungs, is a disease with no known cure. Left untreated, this disease results in right heart failure and death. The studies performed during the past four years have focused on defining the role of S-nitrosothiols in the development and progression of PH. In the pulmonary vascular endothelium, endothelial nitric oxide synthase (eNOS) activity is associated with the formation of S-nitrosothiols. S-nitrosothiol catabolism is mediated, in part, through the action of S-nitrosoglutathione reductase (GSNOR). The relationship between these two enzymes to net S-nitrosothiol bioavailability and the development of this disease is unknown. Our studies using N-acetyl cysteine as a tracer to monitor S-nitrosothiol abundance have implicated S-nitrosothiols in the development of hypoxia-induced pulmonary hypertension in male but not female C57BL6 mice. Moreover, the observed gender differences in pulmonary vascular response are due to gender differences in the activity of GSNOR. GSNOR activity in females is controlled by the hormonal regulation of eNOS. In contrast, GSNOR activity in males is negatively controlled by testosterone in an eNOS-independent manner. Lastly, smooth muscle/endothelial cell communication in resistance arteries was found to be mediated by S-nitrosylation /denitrosylation of connexin 43 (Cx 43) at the myoendothelial junction. Cx43 is constitutively S-nitrosylated on Cys 270 by eNOS and denitrosylated by GSNOR in this cellular compartment. The importance of this interaction to that of the pulmonary vascular disease is currently unknown, but suggests the importance of these post-translational modifications in the vascular response.					
15. SUBJECT TERMS S-nitrosothiols, S-nitrosoglutathione reductase, pulmonary hypertension					
16. SECURITY CLASSIFICATION OF:			17. LIMITATION OF ABSTRACT UU	18. NUMBER OF PAGES 88	19a. NAME OF RESPONSIBLE PERSON USAMRMC
a. REPORT U	b. ABSTRACT U	c. THIS PAGE U			19b. TELEPHONE NUMBER (include area code)

Table of Contents

	<u>Page</u>
Introduction.....	4
Body.....	5-14
Key Research Accomplishments.....	14-16
Reportable Outcomes.....	16-17
Personelle Receiving Pay for this Research Effort.....	17
Conclusion.....	17-18
References.....	18-21

Appendices.....

(1) Manuscripts:

Palmer LA, Doctor A, Chhabra P, Sheram ML, Laubach VE, Karlinsky MZ, Forbes MS, Macdonald T, Gaston B. 2007 S-nitrosothiols signal hypoxia-mimetic vascular pathology J. Clin Investigation 117: (9) 2592-2601, 2007.

Brown-Steinke K, deRonde K, Yemen S, **Palmer LA**. Gender differences in S-nitrosoglutathione reductase activity in the lung. PLoS One 5:e14007, 2010.

Straub, AC, Billaud M, Johnstone SR, Best AL, Yemen S, Dwyer ST, Looft-Wilson R, Lysiak, JJ, Gaston B, **Palmer LA**, Isakson BE. Compartmentalized connexin 43 S-nitrosylation/ denitrosylation regulates heterocellular communication in the vessel Wall. Arterioscler Thromb Vasc Biol 31: 399-407, 2011.

(2) Abstracts:

Palmer LA, Que L, Brown-Steinke K, de Ronde K, Gaston B. S-nitrosoglutathione Reductase, Gender, and the Development of Pulmonary Arterial Hypertension. American Thoracic Society International Conference Toronto Canada May 2008.

Palmer LA, Brown-Steinke K, deRonde K, Que L, and Gaston B S-nitrosylation/denitrosylation coupling and the Regulation of Endothelial Nitric Oxide synthase. Thoracic Society International Conference, San Diego CA, 2009.

Brown-Steinke K, de Ronde K, Sullivan S, Yeman, S, **Palmer LA** S-nitrosoglutathione Reductase and its role in pulmonary arterial hypertension. Thoracic Society International Conference, New Orleans LA, 2010.

Lewis SJ, May W, Young S, Yenam S, **Palmer LA**. Gender differences in the ventilatory responses to hypoxia. Thoracic Society International Conference, New Orleans LA, 2010.

Yeman S, Marozkina NV, **Palmer LA**, Gaston B Therapeutic ultrasound decreases mean right ventricular pressure in hypoxic mice. Thoracic Society International Conference, New Orleans LA, 2010.

Kavoussi PK, Ellen JH, Oliver JL, Woodson RI, Costabile RA, Steers WD, **Palmer LA**, Lysiak JJ. eNOS S-nitrosylation and Erectile Function J. American Urological Association Annual Meeting 2010.

Palmer LA, May WJ, de Ronde Km, Young AP, Gaston B, Lewis SJ. Ventilatory Responses during and following exposure to hypoxia in conscious mice deficient or null in S-nitrosoglutathione Reductase. American Thoracic Society International Conference, Denver Colorado, May 2011

Sundararajan S, **Palmer L**, Gaston B. Hemoglobin β -93 signal increased pulmonary endothelial NOS expression in hypoxia. American Thoracic Society International Conference, Denver, Colorado, May 2011

(3) Patents

Therapeutic application of the effect of androgens on S-nitrosothiol metabolism in pulmonary disease.

Introduction:

Pulmonary arterial hypertension (PAH), high blood pressure within the lung, is a progressive disease which is characterized by an increase in pulmonary arterial pressure and the formation of muscle around normally non-muscular small pulmonary arteries. Without treatment, PAH progresses rapidly to right heart failure and death. The mechanism(s) sensing the initiating event and transducing this signal into changes in protein expression to alter pulmonary physiology are unclear. The role S-nitrosothiols (SNO) play in the development of PAH is examined in this research project. In the pulmonary circulation, erythrocytes deliver SNOs to recipient target proteins on the surface of the endothelium as a function of oxygen saturation. In this context, erythrocytes can act as a molecular switch, monitoring changes in oxygen saturation to deliver SNOs to the vascular endothelium. We have developed a model in which N-acetyl cysteine (NAC) is used as a tracer to 1) monitor SNO formation, transfer and metabolism *in vivo*, 2) address the physiological and pathological consequences of SNO signaling in the pulmonary vasculature, and 3) identify SNO target proteins in this signaling pathway. Differences in SNO formation, transfer and metabolism and the role this pathway plays in gender specific differences associated with the development of PAH are examined. Studies for this award were focused on 1) defining the physiological pulmonary responses of S-nitrosothiols male and female mice using our NAC model; 2) analyzing the physiological responses to S-nitrosothiols using mice deficient and null for endothelial nitric oxide synthase (eNOS) and S-nitrosogluthione reductase (GSNOR), proteins known to be involved in the formation and metabolism of S-nitrosothiols and 3) identifying proteins and protein/protein interactions in the endothelium that are involved in this pathway.

Body:**Specific Aim 1: Aberrant formation/Transfer and/or delivery of S-nitrosothiols (SNOs) lead to the development of Pulmonary Hypertension.**

Dysregulated S-nitrosothiol (SNO) signaling contributes to a wide range of human pathologies including those within the cardiovascular, pulmonary, musculoskeletal, and neurological systems.¹ The majority of published work focuses on the formation and identification of specific protein SNOs and the impact of these modified proteins on disease development. PAH is a life threatening condition that remains poorly understood and is difficult to treat. The mechanisms that control pulmonary vascular tone and resistance are central to the pathology of PAH. NO bioactivity, mediated through the formation of SNOs, has a significant influence on vascular tone²⁻⁴. In health, these interactions are involved in maintaining low pulmonary vascular resistance and effective ventilation/perfusion matching³. The potential role of SNOs in the development of PAH has not been extensively studied. Deficiencies in S-nitroso-hemoglobin (SNO-Hb) levels has been reported in red blood cells (RBCs) from hypoxemic female patients with moderate to severe PAH⁵. Arterial SNO-Hb and Hb-bound NO levels were reduced compared to normoxic controls⁵. This defect is due to an impaired O₂-induced exchange of NO between the heme and the cysteine thiol⁵. In addition, studies performed in the monocrotaline rat model of PAH and monocrotaline pyrrole treated endothelial cells has suggested that disrupted intracellular membrane trafficking contributes to the development of PAH⁶⁻⁸. This is associated with a dramatic decrease in the S-

nitrosylation of N-ethylmaleimide-sensitive factor (NSF), eNOS, caveolin-1 and clathrin heavy chain⁶. Taken together, these results suggest that aberrant SNO bioavailability leads to the development of PAH.

In the first year of this award, we published a paper examining the role of S-nitrosothiols in the development of pulmonary hypertension using N-acetyl cysteine to monitor S-nitrosothiol transfer reactions. (Appendix; Manuscript 1).

Task 1: Characterize SNO formation/transfer/metabolism in vivo and in vitro in male animals following chronic N-acetyl cysteine (NAC) administration.

Nitric oxide (NO) transfer reactions between protein and peptide cysteine residues have been proposed to represent a regulated signaling process. To measure NO transfer reaction in the blood as well as study the vascular effects of these reactions in vivo, the antioxidant N-acetyl cysteine (NAC) was used as a bait reactant. Measurement of the ratio of total red blood cell S-nitrosothiol concentration of hemoglobin (Hb) in NAC-treated mice was lower than seen in untreated animals. (Appendix; Manuscript 1, Figure 3A). NAC was found to be converted to S-nitroso-N-acetyl cysteine (SNOAC) in blood both in vivo and ex vivo (Appendix; Manuscript 1, Figure 3B). Deoxygenation of human blood in the presence of NAC resulted in (1) the loss of SNO red blood cell content and (2) formation of SNOAC (Appendix; Manuscript 1, Figure 3C) The concentration of SNOAC increased as the fraction of oxygenated Hb decreased in the intact erythrocytes ex vivo. (Appendix Manuscript 1, Figure 3D). These findings are consistent with the idea that red blood cell SNO content is, in part, dependent on oxyhemoglobin saturation and thiols can accelerate the desaturation-induced loss of red blood SNO content.

Task 2. Identify the pathophysiological changes caused by NAC/SNOAC treatment in the pulmonary vasculature in vivo.

Chronic systemic treatment of high dose NAC in male mice for three weeks resulted in the development of pulmonary hypertension (Appendix; Manuscript 1, Figure 1). This was characterized by an increase in right ventricular weight, an increase in right ventricular pressure and muscularization of small pulmonary arterioles. Changes in right ventricular weight, right ventricular pressure and muscularization were indistinguishable from that obtained by exposure to hypoxia (10% O₂, normobaric hypoxia). Increases in right ventricular pressure were seen within 1 week of NAC exposure, and persisted during weeks 2 and 3. Changes in right ventricular weight occurred more slowly, with significant increase only seen at 3 weeks. The responses were also dose dependent. Low dose NAC (1 mg/ml) increased right ventricular pressure at three weeks, but no changes in right ventricular weight were seen within this time period.

Task 3. Identify significant components of the S-nitrosothiol signaling pathway Identification of proteins involved in S-nitrosothiol signaling in the pulmonary vasculature.

S-nitrosylation of proteins and peptides is a regulated process. Protein modification by S-nitrosylation often results in a change in protein function. eNOS has been shown to be an S-nitrosylated protein^{9,10}. In the S-nitrosylated form, eNOS is inactive⁹. In addition, we have shown that GSNOR is S-nitrosylated (Appendix; Manuscript 2, Figure 1D). In contrast to eNOS, GSNOR activity is increased in the S-nitrosylated form (Appendix; Manuscript 2, Figure 2). Since activation of nitric oxide

synthase isoforms is associated with the formation of S-nitrosothiols^{11,12}, we evaluated whether a relationship existed between these two proteins in endothelial cells. This relationship was explored in vitro using a static cell culture of primary mouse lung endothelial cells (MLECs).

GSNOR coimmunoprecipitates with eNOS (Figure 1). Under untreated conditions in murine pulmonary endothelial cells (MPEC), endothelial nitric oxide synthase (eNOS) is associated with GSNOR and caveolin-1, a protein involved in the regulation of eNOS activity. However, exogenous administration of SNO (SNOAC or GSNO) reduces eNOS/GSNOR interaction and reduces or eliminates its association with caveolin-1 (Figure 1).

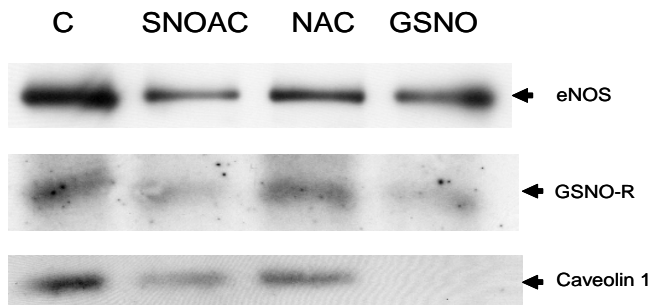


Figure 1. GSNOR and Caveolin-1 immunoprecipitate with eNOS. Mouse lung endothelial cells were treated with 50µM NAC, 1µM SNOAC or 100µM GSNO or were untreated (C) for a period of 4 hours. Whole cell homogenates were immunoprecipitated with antibody against eNOS. Western blot analysis was performed using eNOS, GSNOR and caveolin-1 antibodies. GSNOR immunoprecipitates with eNOS. This interaction is reduced by SNOAC and GSNO. The association with caveolin-1 is reduced or eliminated with SNOAC and GSNO respectively.

Overexpression of GSNOR in MLECs reduces eNOS activity (Figure 2). The activation of eNOS is associated with phosphorylation of serine 1177 (peNOS 1177)^{13,14}. Introduction of GSNOR into mouse pulmonary endothelial cells by transient transfections results in a dramatic loss of eNOS phosphorylation at serine 1177, suggesting that GSNOR influences the activity of eNOS.

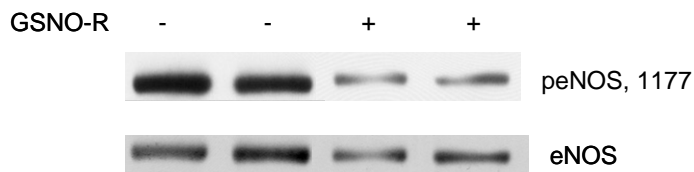


Figure 2. Overexpression of GSNOR-R reduces eNOS phosphorylation at serine 1177. MLECs were transfected with GSNOR-R. Whole cell lysates from transfected cells were subjected to Western blot analysis using antibodies against phosphorylated eNOS (peNOS, residue 1177) and total eNOS. Overexpression of GSNOR-R significantly reduced peNOS expression. eNOS expression was also reduced but not to the same extent

The ability of these two proteins, eNOS and GSNOR-R, to interact, either directly or indirectly, is a novel observation. In addition it appears that GSNOR may affect the activation of eNOS. The mechanism by which GSNOR modulates the activity is currently unknown. However, efficient production of NO is determined by the subcellular

location of eNOS with activity highest in the plasma membrane,¹⁵⁻¹⁸ lower in golgi¹⁷ and lowest in nucleus and mitochondrial matrix.¹⁹ Thus, one possibility is that this association is linked to to subcellular location of these proteins. In fact, formation of SNOs is linked to local NO production.²⁰ One examples can be seen with myristoylation-deficient eNOS (cytosol) which is hypo-S-nitrosylated compared to wild type eNOS.⁹

To determine the location of the interaction between eNOS and GSNO-R in cell lysates of MPECs, a 5-30% discontinuous sucrose gradient was used²¹ (Figure 3). GSNO-R was found to co-migrate with the golgi marker β COP (fractions 9-12) and was not present in the caveolar enriched fraction (fraction 3-5) suggesting that the interaction between eNOS and GSNO-R is not in the caveolae in cultured cells.

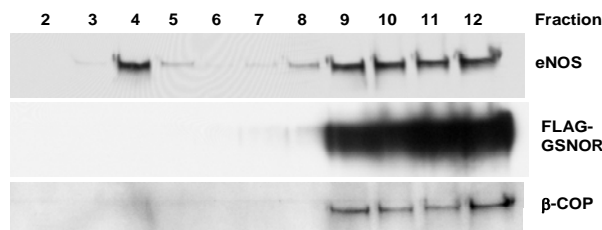


Figure 3. GSNO-R comigrates with the golgi marker β COP. Male MLEC were transfected with FLAG-tagged GSNO-R. Cell lysates were separated on a 5-30% discontinuous sucrose gradient²¹ to separate caveolar enriched membrane fractions from golgi fractions. 30 μ l of each fraction were separated on a 12% SDS PAGE and probed for eNOS, FLAG and β COP(golgi protein marker) and Cav-1 (not shown). FLAG-GSNO-R co localized with β COP.

Confocal microscopy was also used to identify the location of eNOS and GSNOR in intact MPECs (Figure 3). In subconfluent cells, GSNO-R expression is most prominent in the nucleus, but is also present in the perinuclear area and in punctuate regions within the cytoplasm. eNOS was primarily located in the perinuclear region. Colocalization of eNOS and GSNO-R was seen in the perinuclear regions and in punctate regions in the cytosol.

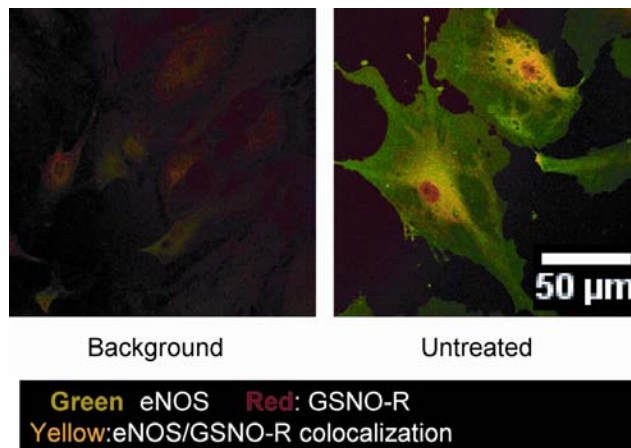


Figure 4. GSNO-R and eNOS colocalize to the perinuclear region in endothelial cells. MLECs were grown on coverslips, fixed in 3.7% formaldehyde and eNOS and GSNO-R expression visualized by immunofluorescence using Alexa Fluor 488 chicken anti mouse and Alexa fluor 568 goat anti-rabbit secondary antibodies respectively. eNOS was found primarily in the perinuclear region. GSNO-R was found in the nucleus and in punctuate regions throughout the cytoplasm. eNOS and GSNO-R appear to colocalize in the perinuclear region. Images collected using Zeiss510 META/NLO; 63X NA1.4 Oil lens; Multi-tract was used to avoid the fluorescence cross talk.

Although we have discovered a unique interaction between eNOS and GSNOR and believe that each of these proteins influences the activity of the other, their role in the development of diseases, such as pulmonary hypertension is not known.

Role of S-nitrosylation in communication between endothelium and smooth muscle.

Communication is essential for endothelial control of smooth muscle cell constriction, however the mechanism by which this occurs is not known. Nitric oxide and gap junctions have been shown to regulate heterocellular communication in the vessel wall. The myoendothelial junction (MEJ) is an anatomic structure that facilitates communication between endothelial cells and vascular smooth muscle within resistance arteries. Gap junctions at the MEJ provide a conduit for communication between endothelium and smooth muscle. Gap junctions are intracellular signaling channels made up of connexins. Of the 4 connexins identified, connexin 43 (Cx43) has been shown to proposed to play an important role at the myoendothelial junction²². Connexin 43 has been found to be constitutively S-nitrosylated at cysteine 271 in the MEJ (Appendix; Manuscript 3, Figure 3). This appears to be due to the presence of activated eNOS in the MEJ (Appendix/ Manuscript 3, Figure 2). Moreover, S-nitrosylation of Cx43 on cysteine 271 regulates gap junction communication. (Appendix; Manuscript 3, Figure 1). However, Cx 43 is rapidly denitrosylated at the myoendothelial junction upon phenylephrine stimulation (Appendix; Manuscript 3, Figure 4). Denitrosylation of Cx 43 at the myoendothelial junction is dependent on GSNOR (Appendix; Manuscript 3, Figure 5). Together, these data define a posttranslational mechanism by which endothelial cells and smooth muscle cells use to regulate heterocellular communication. Although these studies were performed on resistance arteries, muscularization of small arterioles increases in hypoxia- and NAC- induced pulmonary hypertension. It is not known whether these muscularized arteries contain MEJs. At this time, the importance of this interaction to the development of pulmonary arterial hypertension is unknown.

Specific Aim 2 NAC SNOAC signaling alters hypoxia Inducible factor (HIF) expression and activity

The ability of NAC to induce pulmonary hypertension was not significantly different from that induced by hypoxia (Appendix; Manuscript 1, Figure 1). This suggests that S-nitrosothiol transfer reactions can signal hypoxia in vivo. Hypoxia inducible factor-1 (HIF-1) is a protein known to be induced by hypoxia. Nitrogen oxides have been shown to stabilize the alpha subunit of HIF-1²³. HIF has also been shown to be S-

nitrosylated²⁴. Thus, one way in which NAC or SNOAC may mediate changes in the pulmonary vasculature is through the activation of hypoxia inducible transcription factors such as HIF-1.

Task 1. Determine if NAC/SNOAC signaling alters HIF expression and activity

Hypoxia regulated genes in the pulmonary endothelium may play a role in hypoxia and NAC induced pulmonary hypertension. S-nitrosothiols can have hypoxia mimetic gene regulatory effects that involved the expression of transcription factors pertinent to pulmonary vascular disease. HIF-1 along with Sp1 and Sp3 are upregulated in the lungs of mice treated chronically with NAC (Appendix, Manuscript 1, Figures 4 and 5B). This effect was more pronounced after treatment with SNOAC. In addition, NAC increased HIF-1 DNA binding activity in vivo (Appendix; Manuscript 1, Figure 5A).

HIF-1 has been shown to be stabilized in normoxia by GSNO²³. Stabilization was found to be due to S-nitrosylation preventing normoxic ubiquitination and degradation of HIF1 α (Appendix; Manuscript 1, Figure 5C). SNOAC was found to inhibit the coimmunoprecipitation of HIF1 α with its E3 ligase von Hippel-Lineau protein when overexpressed in COS cells (Appendix; Manuscript 1, Figure 5D). In addition, SNOAC was found to S-nitrosylate von Hippel Lindau protein in HeLa cells (Appendix; Manuscript 1, Figure 5E) and 786-O renal carcinoma cells stably overexpressing von Hippel Lindau protein (Appendix; Manuscript 1 Figure 5F). Cysteine 162 was identified as being critical for S-nitrosylation (Appendix; Manuscript 1, Figure 5G). Thus, one mechanism by which S-nitrosothiols may be hypoxia mimetic may involve the stabilization of HIF1 α through the S-nitrosylation of von Hippel Lindau protein cysteine residue 162.

Task 2. Determine if NAC/SNOAC modifies the expression of HIF-1 responsive genes implicated in the development of PH.

The expression of several proteins, known to be induced by HIF-1 and identified to be associated with the development of pulmonary hypertension were evaluated in lungs of mice exposed to NAC or SNOAC. Fibronectin, eNOS and hypoxia inducible mitogenic factor protein expression were found to increase with NAC or hypoxia exposure (Appendix; Manuscript 1, Figure 2A-C). However, vascular endothelial growth factor (VEGF) and endothelin protein expression was not significantly altered (Appendix; Manuscript 1, Figure 2 E,F).

Specific Aim 3 Gender differences in pulmonary hypertension arise from an imbalance of SNO formation and metabolism.

Gender is an important risk factor in the development of PAH^{25,26}. Human females are twice as likely to get this disease as males^{25,26}. Oral contraceptives and estrogens are thought to be unlikely risk factors in the development of PAH^{27,28}. However, recent data indicate a role for the estrogen metabolizing gene CYP1B1²⁹. Chronic hypoxia can cause PAH in humans and animals³⁰⁻³⁶ and as such, can be used as a model system to examine the gender differences associated with the development of this disease. In humans, there is no apparent difference in pulmonary artery pressures seen between

male and female children and adolescents living at high altitude^{37,38}. However, menarchal humans are better able to adapt to high altitude than males and non-menarchal females^{37,38} suggesting the response to hypoxia can be modulated by sex hormones. Female rats^{39,40} and swine⁴¹ develop less severe PAH in response to chronic hypoxia compared to males. To date, little research has focused on examining the gender dependent regulation of S-nitrosothiol formation and its relationship to the development of pulmonary hypertension.

In the last two years of this award, we examined the hypothesis that S-nitrosothiol bioavailability, mediated through the actions of S-nitrosoglutathione reductase (GSNOR), may play a role in the gender predilection seen in this disease (Appendix; Manuscript 2). Studies were performed in our novel mouse model of PAH induced by N-acetyl cysteine (Appendix Manuscript 1),

Task 1. Measure to pathophysiological parameters of PH following chronic administration of NAC/SNOAC to female animals for comparison to that measured in males. Pulmonary hypertension is characterized by an increase in right ventricular pressure, an increase in right ventricular weight and muscularization of the small pulmonary arterioles. The data obtained from our studies in female C57BL6/129SvEv mice reveal female mice have higher resting right ventricular pressures and right ventricular weights than males, but are protected from the NAC-induced increases in right ventricular pressure and weight observed in males. (Appendix, Manuscript 2; Figure 5)

Task 2 Identify differences in SNO formation/ transfer/metabolism between male and female animals. In the NAC model, NAC is used as a tracer to monitor the formation of S-nitrosothiols. In vivo, NAC is converted to S-nitrosylated N acetyl cysteine (SNOAC) which can be measured in the serum using liquid chromatography/ mass spectroscopy (LC/MS) (Appendix, Manuscript 1, Figure 3B). SNOAC levels present in the serum of NAC-treated female animals were greater than that seen in the male animals (Appendix; Manuscript 1, Figure 6), suggesting that differential S-nitrosothiol metabolism may be responsible for these observations. Analysis of the activity and expression of GSNOR demonstrated GSNOR activity was greater in female compared to the male animals with no changes in mRNA or protein expression (Appendix; Manuscript 2, Figure 1. Tables 1 and 2). This suggested that a post-translational modification of GSNOR may be responsible for the increased activity of GSNOR. Therefore, we evaluated the S-nitrosylation state of GSNOR and the effect it has on GSNOR activity. GSNOR was found to be an S-nitrosylated protein (Appendix; Manuscript 2 Figures 1). Moreover, S-nitrosoglutathione was found to increase the activity of GSNOR (Appendix; Manuscript 2, figure 2). Lastly, in the lung, GSNOR S-nitrosylation was greater in female mice

Task 3 Evaluate the effect of estrogen and testosterone in modulating the SNO signaling pathway. S-nitrosothiol abundance in the endothelium is determined, in part, through the activities of eNOS (S-nitrosothiol production) and GSNOR (S-nitrosothiol catabolism). Estrogen is known to increase the expression and activity of eNOS⁴². As

such, lung homogenates from female mice have more eNOS protein expression when compared to lung homogenates obtained from male mice (Appendix; Manuscript 2, Figure 3). Increases in eNOS activation is associated with the formation of S-nitrosothiols. GSNO-R is an S-nitrosylated protein (Appendix; Manuscript 2, Figure 1D). Therefore, we evaluated the effects of estrogen on GSNOR S-nitrosylation. In vitro studies using primary pulmonary endothelial cells isolated from female mice show that estrogen increases the levels of S-nitrosylated GSNOR compared to untreated cells. This increase in S-nitrosylated GSNOR by estrogen was abrogated by L-NAME, a non-specific nitric oxide synthase inhibitor. (Appendix Manuscript 2 Figure 3), suggesting that the activity of eNOS contributes to the S-nitrosylation and activation of GSNOR. This is consistent with the observation that eNOS knockout (eNOS^{-/-}) mice have reduced GSNOR activity (Appendix Manuscript 2, Figure 4).

Female mice are protected from NAC induced pulmonary hypertension (Appendix; Manuscript 2, Figure 5). To determine if estrogen is responsible for this protective effect, the ability of NAC to induce pulmonary hypertension was evaluated in ovariectomized and castrated mice. In contrast to what was expected, ovariectomized animals did not show increases in right heart weight or right ventricular pressure in response to NAC. Castrated animals, on the other hand, were found to be protected from the increases in right ventricular weight and pressures in response to NAC (Appendix; Manuscript 2, Figure 7). Castration was accompanied by an increase in GSNOR activity (Appendix; Manuscript 2, Figure 8) Moreover, GSNOR activity in the castrated animals was now comparable to that seen in female animals. (Appendix; Manuscript 2, Figure 8). To further evaluate the role of androgens on the activation of GSNO-R, eNOS^{-/-} animals were castrated and the activity of GSNOR evaluated. GSNO-R activity in eNOS^{-/-} castrated animals was increased compared to that of the gonad intact animals (Appendix, Manuscript 2, Figure 9). This suggests the presence of an eNOS independent androgen mediated effect on GSNOR activity.

How does this data relate to humans with pulmonary hypertension? In humans, the genetic basis for approximately half of the familial cases and a one quarter of the sporadic cases of pulmonary arterial hypertension include the autosomal dominant mutation in the cell-surface localized bone morphogenetic receptor type 2 (BMPR2)^{43, 44}. The low penetrance of these mutations (10-20%) lead to a search for a “second hit” or modifier gene^{45,46} and the possibility that GSNO-reductase is a modifier gene associated with the development of pulmonary arterial hypertension was examined. Human genetic analysis examined the effect of an SNP locus in exon 1 (ADH5^SNP1; rs1154400)⁴⁷ of the human adh5 gene (which encodes GSNO-reductase). In a cohort of 209 individuals tested (89 unaffected, 120 affected) collected by the Vanderbilt PAH center, absence or presence of familial PAH did not correlate with the presence for this particular SNP. However, within the population of 55 BMPR2+ subjects (18 male, 37 female) for which the age of diagnosis was known, the data suggested that the presence of a T in the allele correlated with the age of onset of the disease. This was true only for the males (Table 1) and did not appear to hold true for the females. These are preliminary data on a small cohort using just one SNP. The data are consistent

with the idea that GSNOR may be a sex steroid responsive gene product that modifies age of presentation for PAH.

Table 1. GSNOR in Individuals with BMPR2 mutations correlated with age of Diagnosis

Allele	Male			Female		
	N (%)	Mean Age (years) At diagnosis	95% CI	N (%)	Mean Age (years) At diagnosis	95% CI
CT	10 (53%)	43.5	35.5 to 51.5	18 (43%)	35.4	29.9 to 40.9
TT	8 (42%)	25.7	16.7 to 34.7	19 (45%)	2.6	26.0 to 39.3
Total	18 (100%)			37 (100%)		

P < 0.019 Kruskal-Wallis

p < 0.587 Kruskal-Wallis

Treatment with GSNO disrupts the interaction between eNOS and GSNOR (Figure 1). GSNOR activity is greater in female mice compared to males. (Appendix; Manuscript 2, Figure 1. Tables 1 and 2). Sodium carbonate is known to release peripheral membrane proteins from membranes. Sodium carbonate extraction was used to determine if (1) GSNOR is a peripheral membrane protein, (2) subcellular location is altered in the presence of GSNO and (3) if we can detect and differences between male and female MLECs. GSNOR was present in both the cytosolic (supernatant) and membrane (pellet) fractions, suggesting GSNO-R may be a peripheral membrane protein. Treatment of MLECs with GSNO did not alter the expression of GSNOR in cells isolated from either gender (Figure 5). However, treatment with GSNO does influence its association with the membrane (Figure 5). It is interesting to note that the association of GSNO-R with the membrane is not determined by gender. However, treatment with GSNO alters the affinity of this association, which is gender dependent, suggesting that changes in membrane affinity may occur through S-nitrosylation.

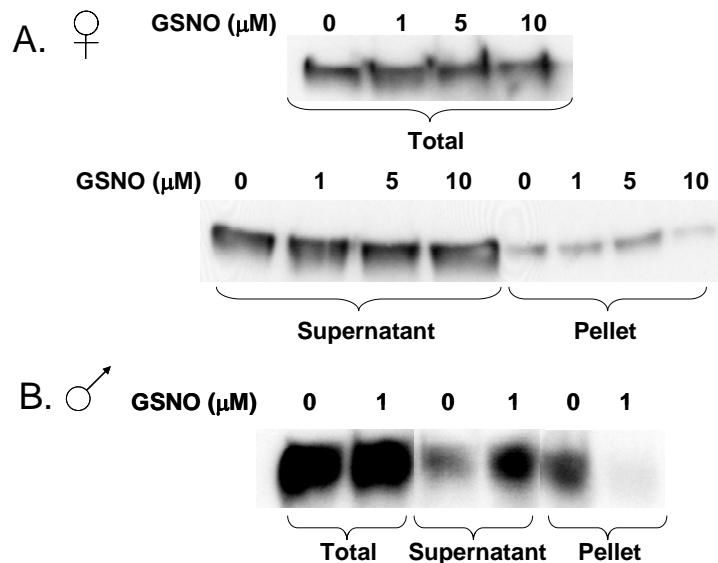


Figure 5. Affinity of GSNO-R for membrane is gender dependent. Female (A) and male (B) MLECs were transfected with FLAG-tagged GSNO-R, treated with various concentrations of GSNO (4 h) and subjected to sodium carbonate extraction. Similar

levels of GSNO-R were expressed in each treatment group (Total). GSNO-R protein was found in both the cytoplasmic fraction (supernatant) as well as the membrane fraction (pellet), suggesting that GSNO-R is a peripheral membrane protein. GSNO treatment with altered the affinity of GSNO-R for the membrane fraction (pellet), which is gender dependent.

Key Research Accomplishments

Specific Aim 1: Aberrant formation/Transfer and/or delivery of S-nitrosothiols (SNOs) lead to the development of Pulmonary Hypertension.

Task 1: Characterize SNO formation/transfer/metabolism in vivo and in vitro in male animals following chronic N-acetyl cysteine (NAC) administration.

- Red blood cell SNO content is dependent on oxyhemoglobin saturation
- Thiols can accelerate the desaturation-induced loss of red blood SNO content.

Task 2. Identify the pathophysiological changes caused by NAC/SNOAC treatment in the pulmonary vasculature in vivo.

- NAC/ SNOAC treatment increase right ventricular pressure.
- NAC/SNOAC treatment increases right ventricular weight.
- NAC/SNOAC treatment increases the muscularization of small pulmonary arterioles.
- Chronic systemic treatment of NAC/SNOAC in male mice results in the development of pulmonary hypertension which is indistinguishable from that induced by hypoxia.

Task 3. Identify significant components of the S-nitrosothiol signaling pathway. Identification of proteins involved in S-nitrosothiol signaling in the pulmonary vasculature.

- GSNOR coimmunoprecipitates with eNOS.
- Treatment with an S-nitrosothiol disrupts the interaction between eNOS and GSNOR.
- eNOS activity influences the activity of GSNOR
- GSNOR activity influences the activity of eNOS.
- eNOS and GSNO-R colocalize in intact endothelial cells to the perinuclear regions and in punctate regions in the cytosol.
- The interaction between eNOS and GSNO-R is not in the caveolae in cultured cells.
- S-nitrosylation is posttranslational mechanism by which endothelial cells and smooth muscle cells use to regulate heterocellular communication.
- Heterocellular communication between endothelial cells and smooth muscle cells is regulated through the S-nitrosylation of connexin 43.

Specific Aim 2 NAC/SNOAC signaling alters hypoxia Inducible factor (HIF) expression and activity.

Task 1. Determine if NAC/SNOAC signaling alters HIF expression and activity

- HIF-1 along with Sp1 and Sp3 are upregulated in the lungs of mice treated chronically with NAC.
- HIF-1 DNA binding activity was increased by NAC.
- SNOAC was found to inhibit the coimmunoprecipitation of HIF1 α with its E3 ligase von Hippel-Lindau protein.
- SNOAC was found to S-nitrosylate von Hippel Lindau protein, the E3 ligase for HIF1 α .
- Cysteine 162 of protein von Hippel Lindau was identified as being critical for S-nitrosylation.

Task 2. Determine if NAC/SNOAC modifies the expression of HIF-1 responsive genes implicated in the development of PH.

- Fibronectin, eNOS and hypoxia inducible mitogenic factor protein expression were found to increase with NAC or hypoxia exposure.
- The protein expression of vascular endothelial growth factor (VEGF) and endothelin protein expression were not significantly altered by NAC.

Specific Aim 3 Gender differences in pulmonary hypertension arise from an imbalance of SNO formation and metabolism.

Task 1. Measure to pathophysiological parameters of PH following chronic administration of NAC/SNOAC to female animals for comparison to that measured in males.

- NAC does not increase right ventricular pressure in female mice.
- NAC does not increase right ventricular weight in female mice.
- Female mice are protected from NAC induced pulmonary hypertension.

Task 2. Identify differences in SNO formation/ transfer/metabolism between male and female animals.

- SNOAC levels present in the serum of NAC-treated female animals were greater than that seen in the male animals.
- GSNOR activity was greater in female compared to the male animals.
- Changes in GSNOR activity were not due to changes in mRNA or protein expression.
- GSNOR was found to be an S-nitrosylated protein.
- S-nitrosylation increases GSNOR activity.

Task 3. Evaluate the effect of estrogen and testosterone in modulating the SNO signaling pathway.

- Estrogen increases the levels of S-nitrosylated GSNOR.
- Estrogen induced increased in S-nitrosylated GSNOR is abrogated by L-NAME.
- eNOS knockout (eNOS^{-/-}) mice have reduced GSNOR activity.

- Castrated animals are protected from the increases in right ventricular weight and pressures in response to NAC.
- Castration was accompanied by an increase in GSNOR activity.
- GSNOR activity in the castrated animals is similar to that seen in female animals.
- GSNOR activity in eNOS^{-/-} castrated animals was increased compared to that of the gonad intact eNOS^{-/-} animals.
- GSNOR may be a sex steroid responsive gene product that modifies age of presentation for PAH in male humans.

Reportable Outcomes.

Manuscripts:

(1) **Palmer LA**, Doctor A, Chhabra,P, Sheram ML, Laubach VE, Karlinsey MZ, Forbes MS, Macdonald T, and Gaston B.S-nitrosothiols signal hypoxia-mimetic vascular pathology. *J. Clin Invest* 117: 2592-601, 2007.

(2) Brown-Steinke K, de Ronde K, Yemen, **Palmer LA** Gender differences in S-nitrosogluthione Reductase Activity in the Lung. *PLos One* 5:e14007, 2010.

(3) Straub AC, Billaud M, Johnstone SR, Best AK, Yemen S, Dweyer ST, Looft-Wilson R, Gaston B, **Palmer L**, Isakson BE. Cellular localization and regulation of S-nitrosylation mediates heterocellular communication. *Arteriosclerosis, Thrombosis and Vascular Biology* 31: 399-407, 2011.

Abstracts

(1) Palmer LA, Que L, Brown-Stenke, deRonde K, Gaston B S-nitrosothiol Reductase, Gender, and the development of Pulmonary Arterial Hypertension. American Thoracic Society International Conference, Toronto Canada, 2008.

(2) Palmer L.A. Brown-Steinke K, deRonde K, Que L, and Gaston B S-nitrosylation/denitrosylation coupling and the Regulation of Endothelial Nitric Oxide synthase. Thoracic Society International Conference, San Diego CA, 2009.

(3) Palmer LA, S-nitrosothiols: Their role in the development of Pulmonary Arterial Hypertension. Military Health Research Forum, Kansas City, MO 2009.

(4) Brown-Steinke K, de Ronde K, Sullivan S, Yeman, S, Palmer LA S-nitrosogluthione Reductase and its role in pulmonary arterial hypertension. Thoracic Society International Conference, New Orleans LA, 2010.

Patent disclosure:

Therapeutic Application of the Effects of Androgens on S-nitrosothiol metabolism in pulmonary disease. L. A. Palmer and B. Gaston

Grant applications submitted as a result of this work

R21 National Institutes of Health: Gender, GSNO-Reductase and the Development of Pulmonary Hypertension: Submission November 2007; Resubmission November 2008

Program Project Grant: Cellular S-nitrosothiol signaling in respiratory biology; Project 2: S-nitrosothiol Signaling in the Pulmonary Endothelium. Original Submission: May 2009, Resubmission: May 2010.

NIH RO1 S-nitrosylation in the Regulation of the Erectile Response: Original Submission June 2009; Resubmission July 2010.

American Heart Association Grant in Aid: S-nitrosylation in the Regulation of the Erectile Response. Original Submission January 2010; Resubmission: January 2011

NIH RO1 The role of S-nitrosothiols in the erectile response. Submitted February 2011.

Personnel receiving pay for this research effort.

Dr. Lisa Palmer

Ms. Kathleen Brown-Steinke

Conclusions

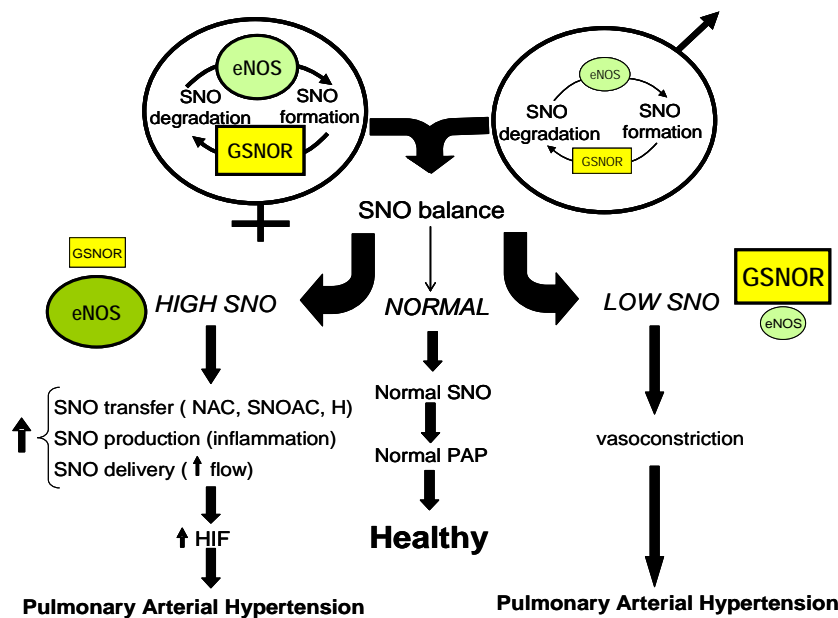


Figure 6. Mismatch between SNO-production/delivery and SNO-metabolism may contribute to the development of PAH. The importance of maintaining a balance between SNO production and degradation is illustrated in the schematic diagram. The relative expression and/or activity of eNOS and GSNOR are different in male and female mice, with females having increased expression and/or activity of both proteins. An imbalance in SNO bioavailability in the pulmonary vasculature could lead to the activation of downstream events that contribute to the development of pulmonary arterial hypertension.

Women are more likely than men to develop PAH^{25,26}. However, the molecular basis for this gender difference is not known. Abnormal blood SNO levels have been implicated in the development of this disease. Components (eNOS expression and activation, oxygen affinity of red blood cells, and GSNO-R activity) necessary in the formation, transfer and metabolism of endogenously produced SNOs are generally greater in females than in males. Our data suggest that the expression and/or activities of GSNO-R may be the key since GSNOR associates with eNOS; overexpression of GSNO-R alters eNOS phosphorylation at serine 1177, a residue implicated in eNOS activation; castration prevents the development of PAH in response to unregulated delivery of SNOs; and GSNOR activity in castrated mice is equal to that of female mice. The mechanism by which GSNO-R alters eNOS function and the role that it may play in the gender differences seen in PAH are not known. Based on the data we obtained during this 4 year funding period, we propose hormonally regulated S-nitrosylation/denitrosylation coupling may be involved (Figure 6). This forms a local compartmentalized regulatory loop. Target proteins involved in this regulation may be used to aid in the identification of individuals susceptible to develop this disease as well as lead to the discovery of new therapeutics for the treatment of this disease.

References

1. Foster MW, Hess DT, Stamler JS. Protein S-nitrosylation in health and disease: a current perspective. *Trends in Molecular Medicine* 15: 391-404, 2009.
2. Singel DJ and Stamler JS. Chemical Physiology of blood flow regulation by red blood cells: The role of nitric oxide and S-nitrosohemoglobin. *Annu. Rev. Physiol.* 67: 99-145, 2005.
3. Gaston B, Singel D, Doctor A, Stamler JS. S-nitrosothiols signaling in Respiratory Biology. *AmJ. Respir Crit Care Med* 173: 1186-1193, 2006
4. Sonveaux P, Kaz AM, Snyder SA, Richardson RA, Cardenas-Navia LI, Braun RD, PawloskiJR, tozer GM, Bonaventura J, McMahon TJ, Stamler JS, Dewhirst MW. Oxygen regulation of tumor perfusion by S-nitrosohemoglobin reveals a pressure activity of nitric oxide. *Circ Res* 96: 1119-1126, 2005.
5. McMahon TJ, Ahearn GS, Moya MP, Gow AJ, Huang YC, Luchsinger BP, Nudelman R, Yan Y, Krichman AD, Bashore TM, Califf RM, Singel DJ, Piantadosi CA, Tapon VF, Stamler JS. A nitric oxide processing defect of red blood cells created by hypoxia: deficiency of S-nitrosohemoglobin in pulmonary hypertension. *Proc Natl Acad Sci U S A.* 102:14801-6, 2005.
6. Mukhopadhyay S, Lee J, Sehgal PB. Depletion of the ATPase NSF from Golgi membranes with hypo-S-nitrosylation of vasorelevant proteins in endothelial cells exposed to monocrotaline pyrrole. *Am. J. Physiol* 295: H1943-1955, 2008.
7. Mukhopadhyay S, Xu F, Sehgal PB. Aberrant cytoplasmic sequestration of eNOS in endothelial cells after monocrotaline, hypoxia, and senescence: subcellular eNOS localization and live-cell caveolar and cytoplasmic NO imaging studies. *Am J. Physiol* 292:1373-89, 2007.
8. Sehgal PB and Mukhopadhyay S. Pulmonary arterial hypertension: a disease of tethers, SNARES and SNAPS. *Am J Physiol* 293: 77-85, 2007.

9. Erwin PA, Lin AJ, Golan DE, Michel T Receptor-regulated dynamic S-nitrosylation of endothelial nitric-oxide synthase in vascular endothelial cells. *J. Biol Chem.* 280: 19888-19894, 2005.
10. Ravi K, Brennan LA, Levic S, Ross PA, Black SM S-nitrosylation of endothelial nitric oxide synthase is associated with monomerization and decreased enzyme activity. *PNAS* 101: 2619-2624, 2004
11. Gow, A. J., Chen, Q., Hess, B. J., Day, H., Ischiropoulos, H., and Stamler J. S. Basal and stimulated protein S-nitrosylation in multiple cell types and tissues. *J. Biol. Chem.* 277, 9637-9640, 2002.
12. Jaffrey SR, Erdjument-Bromage H, Ferris CD Tempst P, Snyder SH Protein S-nitrosylation: a physiological signal for neuronal nitric oxide. *Nature Cell Biol* 3: 193-97, 2001
13. Dimmler, S., Fleming, I., Fisslthaler, B., Hermann, C., Busse, R., Zeiher, A.M. Activation of nitric oxide synthase in endothelial cells by Akt dependent phosphorylation. *Nature* 399, 601-5 1999.
14. McCabe, T.J., Fulton, D., Roman, L.J. Sessa, W.C. Enhanced electron flux and reduced calmodulin dissociation may explain "Calcium -independent" eNOS activation by phosphorylation. *J Biol Chem* 275, 6123-6128, 2000.
15. Oess S, Icking A, Fulton D, Govers R, Muller-Esterl W Subcellular targeting and trafficking of nitric oxide synthases *Biochem J* 396: 401-409, 2006.
16. Govers R, Bevers L, de Bree P and Rabelink TJ. Endothelial nitric oxide synthase activity is linked to its presence at cell-cell contacts. *Biochem J.* 361: 193-201 2002.
17. Fulton D, Babbitt R, Zoellner S, Fontant J, Acevedo L, McCabe TJ, Iwakiri Y, and Sessa WC. Targeting of endothelial nitric oxide synthase to the cytoplasmic face of the Golgi complex or plasma membrane regulates Akt versus calcium dependent mechanism for nitric oxide release. *J. Biol Chem* 279: 30349-30357, 2004.
18. Liu J, Garcia-Cardena G, and Sessa WC. Biosynthesis and palmitoylation of endothelial nitric oxide synthase: mutagenesis of palmitoylation sites, cystines-15 and/or 26 argues against depalmitoylation-induced translocation of the enzyme. *Biochemistry* 34: 12333-12340, 1995.
19. Jagnandan D, Sessa WC, Fulton D. Intracellular location regulates calcium-calmodulin-dependent activation of organelle-restricted eNOS. *Am J. Physiol Cell Physiol* 289: C1024-C1033, 2005.
20. Iwakiri Y, Satoh A, Chatterjee S, Toomre DK, Chalouni CM, Fulton D, Groszmann RJ, Shah VH, Sessa WC. Nitric oxide synthase generates nitric oxide locally to regulate compartmentalized protein S-nitrosylation and protein trafficking. *Proc Natl Acad Sci* 103: 19777-19782, 2006.
21. Sowa G et al. Trafficking of endothelial nitric oxide synthases in living cells. Quantitative Evidence supporting a role of palmitoylation as a kinetic trapping mechanism limiting membrane diffusion. *J. Biol. Chem* 274: 22524-22531, 1999.
22. Heverlein KR, Straub AC, Isakson BE. The myoendothelial junction: breathing through the matrix! *Microcirculation* 16: 307-322, 2009.

23. Palmer LA, Gaston B and Johns RA Normoxic stabilization of hypoxia inducible factor 1 expression and activity: redox-dependent effect of nitrogen oxides. *Mol Pharmacology* 58:1197-1203, 2000.
24. Li F, Sonveaux P, Rabbani ZN, Liu S, Yan B, Huang Q, Vujaskovic Z, Dewhirst MW, Li CV, Regulation of HIF-1 alpha stability through S-nitrosylation. *Mol Cell.* 26:63-74, 2007.
25. Runo JR and Loyd JE. Primary pulmonary hypertension. *The Lancet* 361: 1533-44, 2003.
26. Gaine SP and Rubin JL Primary Pulmonary Hypertension 1998, 352-719-725.
27. Kleiger RE, Boxer M, Ingham RE and Harrison DC. Pulmonary hypertension in patients using oral contraceptives. *Chest* 69:143-147, 1976
28. Morse JH, Horn EM, Barst RJ. Hormone replacement therapy. A possible risk factor in carriers of familial primary pulmonary hypertension. *Chest* 116: 847, 1999.
29. West J, Cogan J, Geraci M, Robinson L, Newman J, Phillips JA, Lane K, Meyrick B, Loyd J. Gene expression in BMPR2 mutation carriers with and without evidence of pulmonary arterial hypertension suggests pathways relevant to disease penetrance. *BMC Medical Genomics* 1: 45-55., 2008
30. Grover RF, Reeves JT, Weir EK, McMurtry IF Alexander AF Genetic transmission of susceptibility to hypoxic pulmonary hypertension. *Prog Respir Res* 9: 112-117, 1975
31. Grover RE, Vogel JK, Averill KH, and Blount SC Pulmonary hypertension: individual and species variability relative to vascular reactivity. *Am Heart J.* 66: 1-3, 1963.
32. Rabinovitch M, Gamble W, Nadas AS, Miettinen OS, Reid L Rat pulmonary circulation after chronic hypoxia: hemodynamic and structural features. *Am J Physiol.* 236: 818-827, 1979.
33. Tucker A, McMurtry IF, Reeves JT, Alexander AF, Will DH, Grover RF Lung vascular smooth muscle as a determinant of pulmonary hypertension at high altitude. *Am J. Physiol.* 228: 762-76 1975.
34. Voelkel NF and Tuder RM. Hypoxia-induced pulmonary vascular remodeling: a model for what human disease. *J. Clin Invest* 106: 733-73, 2000.
35. Walker BR, Berend N, Voelkel NF Comparison of muscular pulmonary arteries in low and high altitude hamsters and rats. *Respir Physiol.* 56:34-50 1984.
36. Will DH Alexander AF, Reeves JT, Grover RF High altitude-induced pulmonary hypertension in normal cattle. *Circ Res* 10: 172-177, 1962.
37. Beall CM, Song K, Elston RC, Goldstein MC. Higher offspring survival among Tibetan women with high oxygen saturation genotypes residing at 4,000m [Multicenter Study] *Proc Natl Acad Sci USA* 101: 14300-14304, 2004.
38. Beall CM Decker MJ, Brittenham GM, Kushner I, Gebremedhin A, Strohl KP, An Ethiopian pattern of human adaptation to high-altitude hypoxia. *Proc Natl Acad Sci USA* 99: 17215-17218, 2002
39. Rabinovitch M, Gamble WJ, Miettinen OS, Reid L. Age and sex influence on pulmonary hypertension of chronic hypoxia and on recovery. *Am J. Physiol.* 240: 62-72 1981.

40. Resta TC, Kanagy NL, Walker BR. Estradiol-induced attenuation of pulmonary hypertension is not associated with altered eNOS expression. *Am J. Physiol.* 280: 88-97, 2001.
41. McMurtry IF, Frith CH, Will DH. Cardiopulmonary responses of male and female swine to simulated high altitude. *J. Appl. Physiol.* 45:459-462, 1973.
42. Chen Z, Yuhanna IS, Galcheva-Bargova Z, Karas RH, Mendelsohn ME, Shaul PW. Estrogen receptor alpha mediates nongenomic activation of eNOS by estrogen. *J Clin Invest* 103:401-6, 1999.
43. Deng Z, Morse JH, Slager SL, Cuervo N, Moore KJ, Venetos G, Kalachikov S, Cayanis E, Fisher SG, Barst RJ, Hodge SE, Knowles JA. Familial primary hypertension (gene PPH1) is caused by mutations in the bone morphogenetic protein receptor-II gene. *Am J. Hum Genet* 67: 737-744, 2000.
44. Lane KB, Machado RD, Pauciulo MW, Thompson JR, Phillips JA III, Loyd JE, Nichols WC, Trembathe RC. Heterozygous germline mutation in BMPR2 encoding a TGF- β receptor, cause familial pulmonary hypertension. *Nat Genet* 26: 81-84, 2000.
45. Machado RD, James V, Southwood M, Harrison RE, Atkinson C, Stewart S, Morrell NW, Trembath RC, Aldred MA. Investigation of second genetic hits at the BMPR2 locus as a modulator of disease progression in familial pulmonary arterial hypertension. *Circulation* 111: 607-613, 2005.
46. Yuan JX, Rubin LJ. Pathogenesis of pulmonary arterial hypertension: the need for multiple hits. *Circulation* 111: 534-538, 2005.
47. Wu H, Romieu T, Sienna-Morge JJ, Estela Del Rio-Navarro B, Anderson DM, Jenchura CA, Li H, Ramirez-Aquilar M, Del Corman Lara-Sanche I. Genetic variation in S-nitrosoglutathione reductase (GSNOR) and childhood asthma. *J. Allergy Clin Immunol.* 120: 322-8, 2007.



S-Nitrosothiols signal hypoxia-mimetic vascular pathology

Lisa A. Palmer,¹ Allan Doctor,¹ Preeti Chhabra,¹ Mary Lynn Sheram,¹ Victor E. Laubach,² Molly Z. Karlinsky,³ Michael S. Forbes,¹ Timothy Macdonald,³ and Benjamin Gaston¹

¹Department of Pediatrics and ²Department of Surgery, University of Virginia School of Medicine, and ³Department of Chemistry, University of Virginia, Charlottesville, Virginia, USA.

NO transfer reactions between protein and peptide cysteines have been proposed to represent regulated signaling processes. We used the pharmaceutical antioxidant *N*-acetylcysteine (NAC) as a bait reactant to measure NO transfer reactions in blood and to study the vascular effects of these reactions in vivo. NAC was converted to *S*-nitroso-*N*-acetylcysteine (SNOAC), decreasing erythrocytic *S*-nitrosothiol content, both during whole-blood deoxygenation ex vivo and during a 3-week protocol in which mice received high-dose NAC in vivo. Strikingly, the NAC-treated mice developed pulmonary arterial hypertension (PAH) that mimicked the effects of chronic hypoxia. Moreover, systemic SNOAC administration recapitulated effects of both NAC and hypoxia. eNOS-deficient mice were protected from the effects of NAC but not SNOAC, suggesting that conversion of NAC to SNOAC was necessary for the development of PAH. These data reveal an unanticipated adverse effect of chronic NAC administration and introduce a new animal model of PAH. Moreover, evidence that conversion of NAC to SNOAC during blood deoxygenation is necessary for the development of PAH in this model challenges conventional views of oxygen sensing and of NO signaling.

Introduction

NO transfer reactions between protein and peptide cysteines have been proposed to represent regulated signaling processes (1, 2). For example, NO transfer from deoxygenated erythrocytes to glutathione ex vivo forms *S*-nitrosoglutathione (GSNO) (3). GSNO can signal acute vascular and central ventilatory effects characteristic of oxyhemoglobin desaturation (3–4) that are regulated by γ -glutamyl transpeptidase (GGT), GSNO reductase (GSNOR), and other enzymes (1, 3–6). However, direct measurement of *S*-nitrosothiol signaling in vivo has proven challenging because of the metabolism and tissue-specific localization of endogenous *S*-nitrosothiol species (1, 3, 4, 6). We have addressed these challenges by using *N*-acetylcysteine (NAC) as a bait reactant, allowing the stable NO transfer product, *S*-nitroso-*N*-acetylcysteine (SNOAC), to be distinguished by mass spectrometry (MS) from endogenous *S*-nitrosothiols. We report that NAC is converted to SNOAC in mice in vivo. Furthermore, chronic, systemic administration of either NAC or SNOAC to mice causes hypoxia-mimetic pulmonary arterial hypertension (PAH). These data reveal a previously unappreciated vascular toxicity of NAC and of *S*-nitrosothiols. Moreover, they suggest that *S*-nitrosothiol transfer reactions can signal hypoxia in vivo.

PAH is characterized by increased pressure in the pulmonary arteries (PAs), increased RV weight, and thickening and remodeling of small PAs. Untreated human PAH can progress to right

heart failure and death (7, 8). Chronic hypoxia can cause PAH, and hypoxia-regulated genes in the pulmonary endothelium play a role (7, 9). The partial pressure of O₂ (pO₂) of blood in the hypoxic PA is not as low as that used to study the expression of hypoxia-modified genes in vitro (10). However, endothelium-derived NO in erythrocytes can be transferred as a nitrosonium (NO⁺) equivalent to cysteine thiolates on glutathione (GSH) and anion exchange protein 1 (AE1) – forming GSNO and *S*-nitroso-AE1 – during erythrocytic oxyhemoglobin desaturation in vitro; this effect is dependent on erythrocytic oxyhemoglobin saturation rather than pO₂ (3, 4, 11, 12). *S*-Nitrosothiols, in turn, can increase the expression of hypoxia-associated gene regulatory proteins in vitro (5, 13, 14), an effect regulated by *S*-nitrosothiol metabolic enzymes (5, 14). Here, we report a hypoxia-mimetic effect, pulmonary vascular remodeling, that is associated with chronic systemic conversion of NAC to SNOAC in vivo. Strikingly, chronic exogenous administration of SNOAC – a vasodilator (15) – recapitulates the effects of hypoxia on the lung, causing hypoxia-mimetic murine PAH. Furthermore, experiments in eNOS-deficient mice reveal that eNOS is necessary for NAC, but not SNOAC, to cause PAH. Taken together, these data demonstrate an unanticipated potential toxicity of chronic, systemic NAC and SNOAC administration and suggest a novel paradigm for understanding hypoxia-associated disease.

Results

NAC and SNOAC cause hypoxia-mimetic PAH. Three weeks of normobaric hypoxia (10%) increased RV systolic pressure, RV weight (relative to LV and septum [LV+S]) and muscularization of small (<80- μ m) pulmonary arterioles in both C57BL/6 and C57BL/6/129SvEv mice ($n = 4$ –14 each; Figure 1, A–E). The effects of 3 weeks' exposure to either NAC (10 mg/ml [52 mM]) or SNOAC (1 mM) in the drinking water were similar to those of 3 weeks' exposure to hypoxia in C57BL/6/129SvEv mice, increasing RV pressure ($n = 3$ –4 each, $P < 0.001$ relative to normoxia), RV/LV+S weight ratio ($n = 6$ –35 each; $P < 0.02$ relative to normoxia), and muscularization of the small pul-

Nonstandard abbreviations used: AE1, anion exchange protein 1; BPAEC, bovine pulmonary arterial cell; GGT, γ -glutamyl transpeptidase; Glut-1, glucose transport protein-1; GSNO, *S*-nitrosoglutathione; Hb, hemoglobin; HIF, hypoxia-inducible factor; HIME, hypoxia-inducible mitogenic factor; MS, mass spectrometry; NAC, *N*-acetylcysteine; PA, pulmonary artery; PAH, pulmonary arterial hypertension; pO₂, partial pressure of O₂; pVHL, von Hippel-Lindau protein; SNOAC, *S*-nitroso-*N*-acetylcysteine; SNO_{tb}, ratio of total erythrocytic *S*-nitrosothiol concentration to Hb; Sp, specificity protein.

Conflict of interest: B. Gaston is a consultant for, and has licensed intellectual property to, Galleon Pharmaceuticals Inc. and N30 Pharmaceuticals LLC.

Citation for this article: *J. Clin. Invest.* 117:2592–2601 (2007). doi:10.1172/JCI29444.

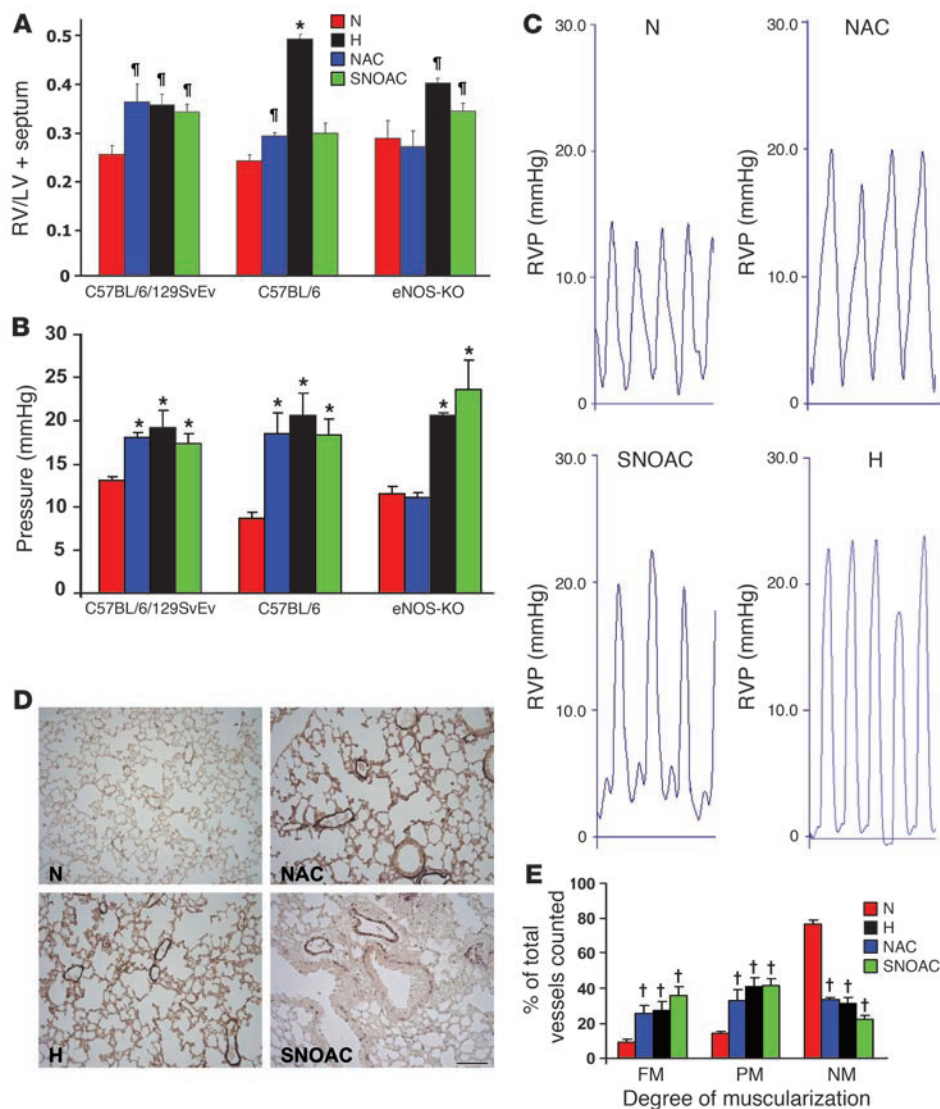


Figure 1 Systemic NAC and SNOAC cause hypoxia-mimetic PAH in mice. C57BL/6/129SvEv, C57BL/6, and eNOS^{-/-} male mice were maintained in normoxia (N, red; 21% O₂) or hypoxia (H, black; 10% O₂); or were treated with NAC (blue) or SNOAC (green) in their drinking water for 3 weeks. (A) Relative RV weight was determined as the ratio of the weight of the RV to the LV+S weight. (B) RV systolic pressures were measured in the closed chest using a Millar 1.4 F catheter/transducer. (C) Representative RV pressure (RVP) tracings (each = 1 s). (D) Lung section images from C57BL/6/129SvEv mice immunostained for von Willebrand factor and α -SMA to illustrate changes in muscularization after 3 weeks of exposure to normoxia, hypoxia, NAC, or SNOAC. Scale bar: 100 μ m (applies to all panels). (E) Changes in muscularization in C57BL/6/129SvEv mice in the small (<80- μ m) vessels from histological sections (as in D) counted by an observer blinded to the protocol. FM, fully muscular; PM, partly muscular, NM, nonmuscular. Significant increases in muscularization in each treatment group were seen in comparison to normoxic controls. Data are mean \pm SEM. †*P* < 0.02, **P* < 0.001, ††*P* < 0.003, by 1-way ANOVA followed by pairwise comparison, all compared with normoxic control.

monary arterioles. (*n* = 3–8; *P* < 0.003 relative to normoxia) (Figure 1, A–E). Of note, PA pressures in the treatment groups were greater than 125% those in controls in the hypoxia, NAC, and SNOAC groups, despite anesthesia, which can blunt PAH (ref. 8; Figure 1C). Similar results were obtained in C57BL/6 mice (*n* = 4–12 each); however, the increase in RV/LV+S ratio was not significant in these mice in the case of SNOAC (Figure 1, A and B).

In dose-response experiments, higher-dose NAC (10 mg/ml) increased RV weight relative to normoxia at 3 weeks in C57BL/6/129SvEv mice (Figure 1A); however, at a lower dose (1 mg/ml), RV/LV+S was normal at 3 weeks (0.27 ± 0.005 ; *n* = 5; *P* = NS compared with no treatment). On the other hand, low-dose NAC increased RV systolic pressure at 3 weeks to 27.5 mmHg (*n* = 4; *P* < 0.04 compared with normoxia).

In time course experiments performed using C57BL/6/129SvEv mice, there was a significant increase in RV pressure after 1 week of NAC exposure (10 mg/ml; mean RV pressure with NAC, 22.8 ± 3.3 mmHg, versus without NAC, 13.7 ± 0.7 mmHg; *n* = 5–8 each; *P* < 0.01), persisting at 2 and 3 weeks. RV/LV+S increased more slowly: a significant difference between NAC-

exposed and -unexposed animals was not observed until 3 weeks (*n* = 5–8 each at 1 and 2 weeks; *P* = NS). Concomitant 3-week exposure to both hypoxia and 10 mg/ml NAC did not result in a greater increase in mean RV/LV+S (0.35 ± 0.082 after NAC and hypoxia together versus 0.34 ± 0.020 after hypoxia alone; *n* = 4–6 each; *P* = NS) or RV pressure (21.4 ± 1.30 mmHg after NAC plus hypoxia versus 19.9 ± 1.03 mmHg after hypoxia alone; *n* = 4–6 each; *P* = NS), suggesting functional overlap between hypoxia- and NAC-stimulated pathways.

Whole-lung expression of hypoxia-inducible mitogenic factor (HIMF), fibronectin, and eNOS, proteins associated with the development of PAH in some models (16–20), was increased by hypoxia and by 3 weeks of NAC treatment (10 mg/ml; *n* = 3–6 each; *P* < 0.05 [HIMF and fibronectin] and *P* < 0.01 [eNOS]; Figure 2, A–D). Of note, VEGF-A and endothelin 1 protein expression did not increase significantly with hypoxia or NAC in our model (Figure 2, E and F). Though these proteins can be upregulated by low pO₂ in vitro, results are variable in PAH models (21–26), suggesting that PAH-associated vascular remodeling is more complex than would be predicted based on the effects of low pO₂ alone. Indeed, VEGF and

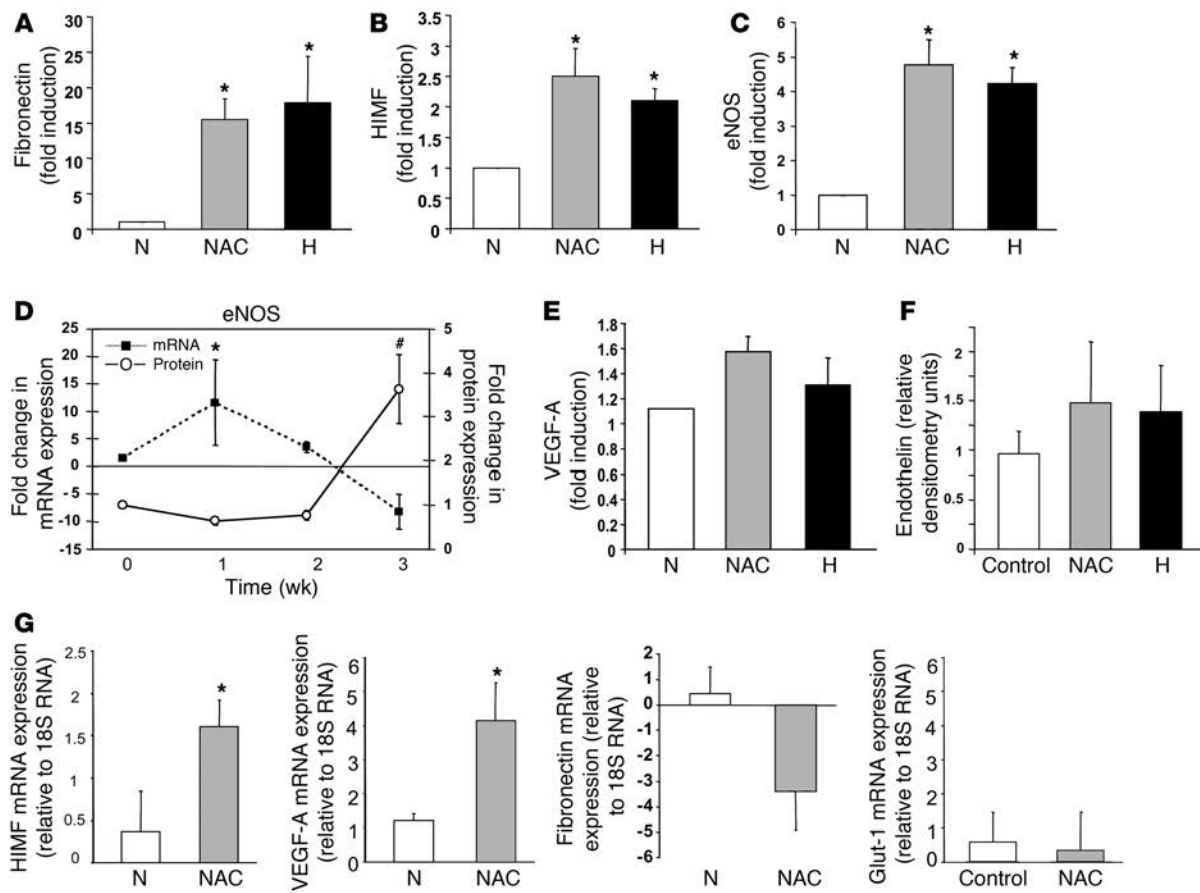


Figure 2

Three weeks of NAC treatment or hypoxia increases the whole-lung expression of certain genes associated with the development of PAH in mice. The expression of fibronectin (A), HIMF (B), eNOS (C and D), VEGF-A (E), and endothelin (F) in whole-lung homogenates from NAC-treated mice was examined by immunoblot. Fold increase in density relative to MAPK (equal loading control) was determined for each condition. The increases in fibronectin, HIMF, and eNOS ($n = 3-5$ each) were significant. (G) Three weeks of NAC treatment also increased whole-lung mRNA, assayed relative to 18S RNA by RT-PCR, for *HIMF* and *VEGF-A* but not *fibronectin* or *Glut-1* ($n = 3$ each). Time course analysis of NAC-treated mice (D) revealed that the increase in whole-lung *eNOS* mRNA (filled squares, left axis) preceded the increase in *eNOS* protein expression (open circles, right axis) but decreased by 3 weeks. * $P < 0.05$; # $P < 0.01$.

eNOS expression can be associated with both protection against PAH and development of PAH, depending on the model and time course (18–29). NAC did not change expression of neuronal or inducible NOS isoforms at 3 weeks (data not shown). NAC exposure increased whole-lung *HIMF* mRNA expression and transiently increased *eNOS* mRNA (Figure 2, D and G). Interestingly, parallel increases in lung protein and mRNA were not observed for the expression of some genes known to be upregulated in hypoxia in vitro, either because of nonvascular expression measured in whole-lung homogenates and/or because of the complexity of pathways involved in the response to hypoxia and the development of PAH in vivo. For example, mRNA levels for *VEGF-A* increased after 3 weeks of NAC treatment ($n = 3$; $P < 0.04$; Figure 2G), though there was no significant change in *VEGF-A* protein levels (Figure 2E). On the other hand, the change in mRNA expression for *fibronectin* was not significant ($n = 2-5$ each; $P = NS$; Figure 2G), though expression of the corresponding protein increased (described above; Figure 2A). Further, mRNA for glucose transport protein-1 (*Glut-1*), conventionally upregulated by hypoxia, did not increase ($n = 3$; $P = NS$). Consistent with this complexity, our time course analysis

revealed an NAC-induced increase in whole-lung *eNOS* mRNA that preceded the NAC-induced increase in *eNOS* protein expression but was transient (Figure 2D).

Three weeks of NAC (10 mg/ml) did not affect systemic or portal vascular morphology (Supplemental Data; supplemental material available online with this article; doi:10.1172/JCI29444DS1) or hemoglobin (Hb) (12.5 ± 0.64 g/dl after NAC treatment versus 12.1 ± 0.65 g/dl in controls). Likewise, 3 weeks of oral SNOAC (1 mM) did not affect the systemic or portal vasculature (Supplemental Data).

NAC is converted to SNOAC in vivo and during erythrocytic deoxygenation in vitro and in vivo. The chemical mechanisms, including both inhibition of nitrosative/oxidative stress (30–32) and NO transfer chemistry (1, 33), by which NAC could cause PAH were investigated. NAC did not affect pulmonary vascular immunostaining for 3-nitrotyrosine (Supplemental Data), suggesting that its ability to cause PAH was not simply the result of tissue injury associated with altered nitrosative or oxidative stress.

In contrast, the ratio of total erythrocytic S-nitrosothiol concentration to Hb (SNO_{rbc}) (11) in NAC-treated mice ($1.0 \times 10^{-4} \pm$

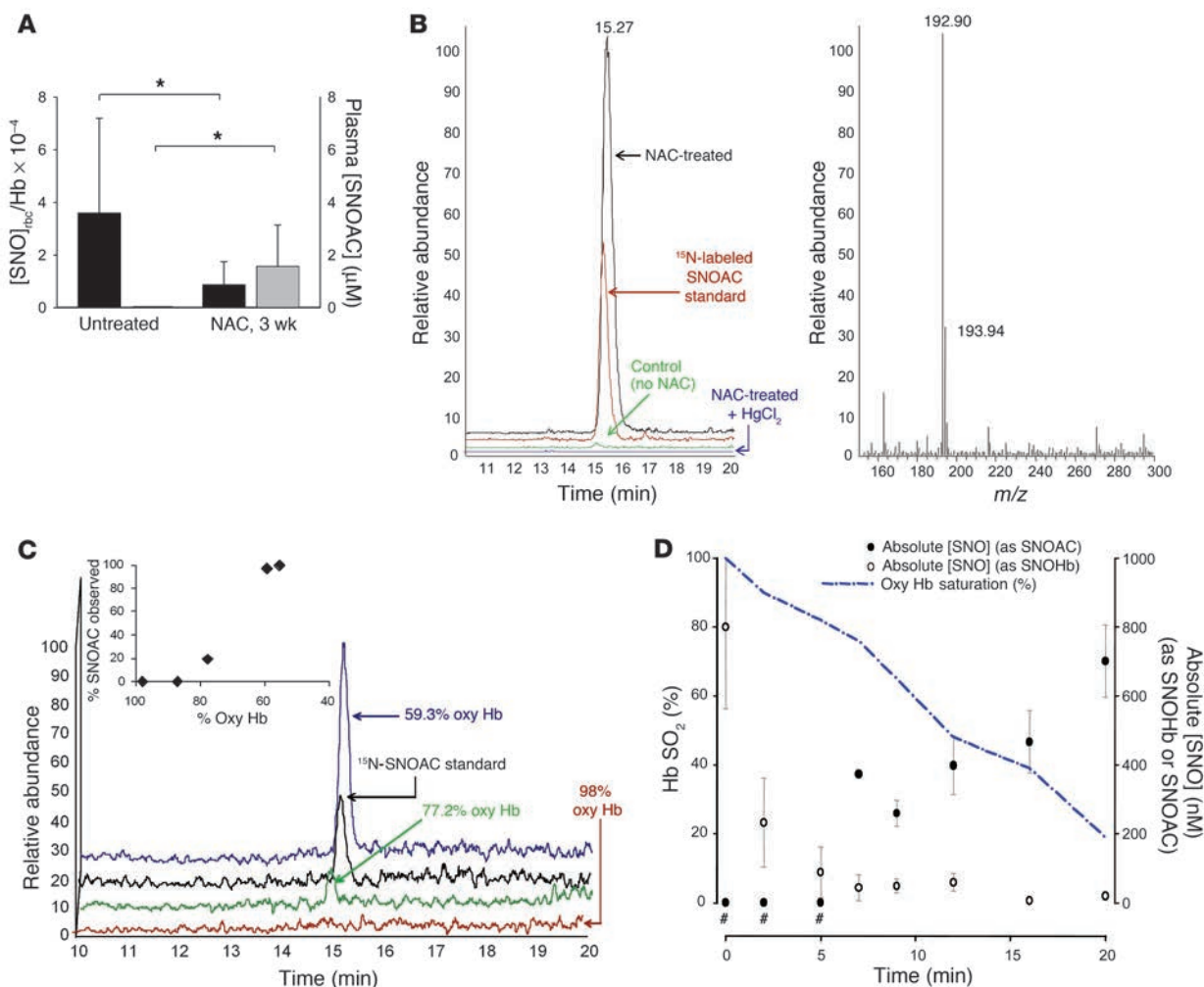


Figure 3

SNOAC is formed from NAC in blood ex vivo and in vivo. (A) The SNO_{rbc} in heparinized LV blood (black bars), measured by reductive chemiluminescence (11), was lower than normal following 3 weeks of treatment with 10 mg/ml NAC ($n = 3-4$ each). In the same mice, plasma SNOAC levels (gray bars; measured by MS) increased from undetectable to approximately 2 μM over the same time (* $P < 0.05$). (B) Serum SNOAC, measured by MS, formed in NAC-treated mice (3 weeks). Left: liquid chromatogram; right: MS spectrum. NAC-treated mice had a SNOAC peak (m/z 193; red) coeluting with ¹⁵N-labeled SNOAC standard (m/z 194; black) that was absent in untreated animals (green) and was not detected in NAC-treated mice after serum pretreatment with HgCl₂ to displace NO⁺ from the thiolate (blue). (C) Oxygenated erythrocytes were deoxygenated ex vivo (argon; ref. 11) in the presence of 100 μM NAC; supernatant SNOAC was measured by MS (above). SNOAC concentration increased with oxyhemoglobin (Oxy Hb) desaturation (co-oximetry: inset), being maximal at 59.3% saturation (blue), less at 77.2% saturation (green), and undetectable at 98% saturation. (D) SNOAC (filled circles) accumulated as the concentration of S-nitrosothiol-modified Hb (SNOHb; open circles) and oxyhemoglobin saturation (Hb SO₂; blue line) both decreased in heparinized whole blood using argon with 5% CO₂ (pH 7.3) in a tonometer. Both the increase in SNOAC and the loss of SNO_{rbc} between 0 and 20 minutes were significant ($P < 0.01$ by ANOVA followed by pairwise comparison to the maximum value; $n = 3$). #SNOAC levels were below the limit of detection when the oxyhemoglobin saturation was greater than 80%.

0.7×10^{-4} ; $n = 4$) was lower than that in control animals ($3.7 \times 10^{-4} \pm 3.2 \times 10^{-4}$; $n = 3$; $P < 0.05$; Figure 3A). Decreased SNO_{rbc} content in NAC-treated mice could be expected if the NO group on erythrocytic protein thiols were transferred (1, 33) to NAC according to the reaction: protein-S-NO + NAC → protein-SH + SNOAC. Therefore, the formation of plasma SNOAC was assayed by MS. SNOAC was identified in the RV plasma of the NAC-exposed animals ($1.6 \pm 0.9 \mu\text{M}$ versus 0 μM in unexposed animals; $P = 0.04$; Figure 3A), a finding confirmed both by coelution with ¹⁵N-labeled SNOAC and by NO displacement from the S-nitrosothiol bond using HgCl₂ (11) (Figure 3B). SNOAC was not detected in the LV

of NAC-treated animals ($n = 7$). Moreover, ex vivo human blood deoxygenation in the presence of NAC in a tonometer (in nitrogen with 5% CO₂; pH maintained at 7.3; ref. 11) resulted in both loss of SNO_{rbc} content and a nearly stoichiometric formation of SNOAC ($n = 3$; $P < 0.05$ by ANOVA followed by pairwise comparison with the maximal value; Figure 3, C and D). The concentration of SNOAC increased as the fraction of oxygenated Hb decreased in intact erythrocytes ex vivo (Figure 3D). There was no transfer from erythrocytes to NAC when blood was maintained at 100% saturation for 15 minutes (total SNO_{rbc} was $2.1 \times 10^{-4} \pm 0.7 \times 10^{-4}$ initially and $2.0 \times 10^{-4} \pm 0.6 \times 10^{-4}$ at 15 minutes; SNOAC

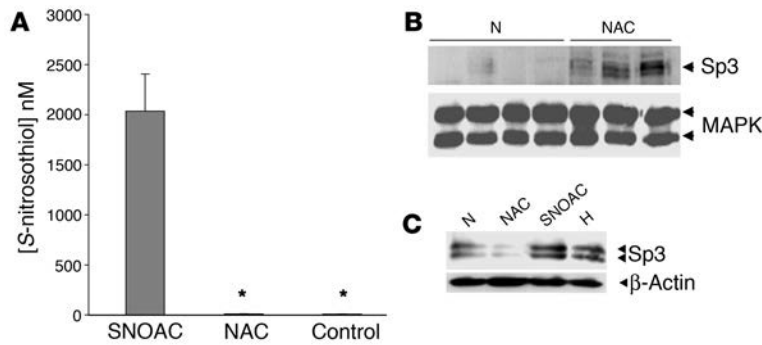


Figure 4
SNOAC recapitulates in primary pulmonary arterial endothelial cells the hypoxia-mimetic whole-lung effect of chronic NAC administration on Sp3 expression in vivo. (A) One micromolar SNOAC, but not 50 μ M NAC, treatment (4 hours each) increased intracellular S-nitrosothiol levels (assayed by Cu/cysteine chemiluminescence; ref. 11) in primary murine pulmonary endothelial cells (* $P < 0.05$ compared with SNOAC treatment). (B) Immunoblot showing increased Sp3 expression relative to MAPK in the whole-lung homogenates of mice treated for 3 weeks with 10 mg/ml NAC but not in those of control mice. By densitometry, this increase was significant ($P < 0.01$). (C) Paradoxically, however, NAC (50 μ M; 4 hours) did not increase Sp3 expression relative to β -actin in primary murine pulmonary endothelial cells in vitro, while both SNOAC (1 μ M; 4 hours) and hypoxia (10%; 4 hours) did.

assayed by MS was undetectable). These findings are consistent with evidence that SNO_{rbc} distribution is, in part, dependent on oxyhemoglobin saturation (3, 11, 12) and that thiols accelerate the desaturation-induced loss of SNO_{rbc} content (11). SNOAC formation was pseudo-first order (in excess NAC) and relatively slow ($k \sim 5.3 \times 10^{-10}$ M/s).

We also considered that NAC could be converted to circulating SNOAC by reacting with NO in endothelial cells. S-Nitrosothiol concentrations in whole-cell lysates (43 ± 7.3 nM) were not increased by 4 hours' exposure to 50 μ M NAC in the presence of 5 μ M exogenous NO (45 ± 3.1 nM; $P = \text{NS}$; $n = 3$). However, cellular levels were increased by exposure to 5 μ M SNOAC (2.0 ± 0.4 μ M; $n = 3$; $P < 0.05$ when compared with NAC alone and control; Figure 4A).

eNOS-deficient mice are protected from the hypoxia-mimetic effects of NAC. eNOS is proposed to be important for maintaining SNO_{rbc} content (34). We studied NAC-induced PAH in eNOS^{-/-} mice. The SNO_{rbc} content of these mice was $0.39 \times 10^{-4} \pm 0.15 \times 10^{-4}$ (nearly a log order lower than in wild-type mice; $P = 0.004$). At baseline, eNOS^{-/-} mice had slight increases in RV pressure and RV weight relative to those of the wild-type background (C57BL/6) mice, as reported previously (refs. 27–29; Figure 1, A and B). Strikingly, eNOS-deficient mice were completely protected from NAC-induced PAH – suggesting that the chronic effects of NAC to increase PAH are eNOS dependent – but they were not protected from SNOAC-induced PAH (Figure 1, A and B).

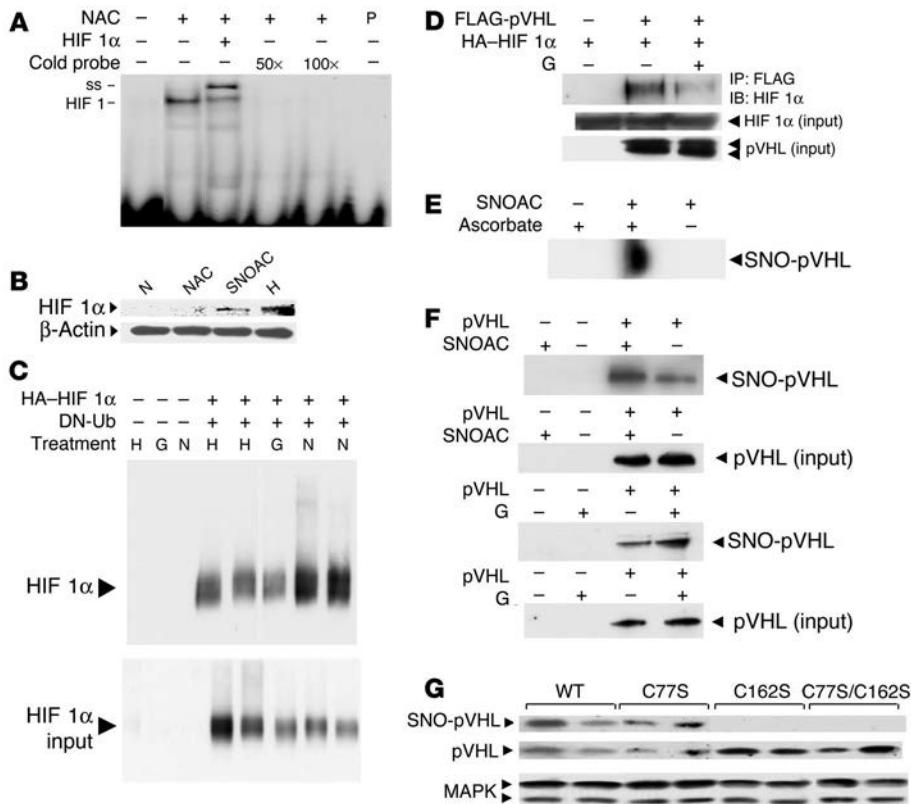
NAC could cause PAH in eNOS-replete mice by depleting endothelial NO or depleting eNOS-derived SNO_{rbc} (ref. 34; Figure 3). However, (a) NAC was not converted to SNOAC in eNOS-replete pulmonary endothelial cells in culture, even in the presence of exogenous NO; (b) SNO_{rbc} levels in eNOS^{-/-} mice at baseline were lower than those in wild-type, NAC-treated mice; and (c) SNOAC caused, rather than ameliorating, PAH in eNOS^{-/-} mice. Therefore, SNOAC excess, rather than endothelial NO or SNO_{rbc} depletion, appears most likely to have caused PAH in our model.

Chronic GSNO exposure in normoxia does not cause PAH. GSNO is an endogenous S-nitrosothiol that is similar to SNOAC in the kinetics of its homolytic decomposition (35). Normoxic C57BL/6/129SvEv mice receiving 1 mM GSNO in their drinking water for 3 weeks did not develop PAH as measured by any parameter ($n = 3$ in the GSNO group and 20 in the untreated control group; $P = \text{NS}$).

The molecular effects of S-nitrosothiols in vitro are hypoxia mimetic and recapitulate whole-lung effects of NAC in vivo. S-Nitrosothiols can have hypoxia-mimetic gene-regulatory effects involving the expression of transcription factors relevant to pulmonary vascular disease, including the hypoxia-inducible factor (HIF) (5, 13) and specificity protein (Sp) families (14). HIF 1, HIF 2, Sp1, and Sp3 are involved in regulating the expression of the genes upregulated in the lungs of mice treated chronically with NAC (9, 16, 17, 24, 25, 36). Because the expression and activity of the HIF and Sp families are affected by S-nitrosothiols in vitro (5, 13, 14, 37, 38), we tested whether chronic NAC or SNOAC could affect their pulmonary expression in mice. Interestingly, NAC increased whole-lung Sp3 expression in vivo but not in primary pulmonary vascular endothelial cells in vitro (Figure 4, B and C). SNOAC, on the other hand, increased both intracellular S-nitrosothiol levels and nuclear Sp3 expression in primary murine pulmonary vascular endothelial cells (Figure 4, A and C). Thus, conversion of NAC to SNOAC (as shown in Figure 3) could be one explanation for the paradox that NAC can increase Sp3 expression in vivo but not in vitro.

Similarly, NAC increased HIF 1 activity in whole-lung extracts in vivo (Figure 5A), though NAC suppresses upregulation of HIF 1 α , the oxygen-labile subunit of HIF 1, by both substance P (31) and by oxidized low-density lipoprotein (32) in vitro. As with Sp3, conversion of NAC to SNOAC may help to explain this paradox: SNOAC and hypoxia, but not NAC, increased HIF 1 α expression, relative to β actin, in primary pulmonary vascular endothelial cells in vitro (Figure 5B). This is consistent with previous work showing HIF 1 α stabilization by GSNO (5, 13); indeed, we found that GSNO reduced HIF 1 α monoubiquitination in bovine pulmonary arterial cells (BPAECs) expressing HA-tagged HIF 1 α and a histidine-tagged, dominant-negative ubiquitin that stops ubiquitin chain propagation (K48R DN-Ub) (Figure 5C).

Mechanisms by which S-nitrosothiols inhibit HIF 1 α ubiquitination and degradation are complex, involving both NO-radical reactions and transnitrosation reactions (1, 5, 13, 37–40). Low-micromolar SNOAC levels derived from NAC in vivo (Figure 3) would not generate concentrations of intravascular NO radical relevant to endothelial gene regulation (38) in the presence of millimolar concentrations of intravascular Hb (41); therefore, signaling through transnitrosation chemistry would seem more likely to be relevant to our in vivo model. NO transfer between thiols could stabilize HIF 1 α through effects on prolyl hydroxylase, Akt signaling, and HIF 1 α itself (13, 37–43). In addition, GSNO modifies E3 ubiquitin ligases through transnitrosation (44). Both SNOAC (Figure 5D) and GSNO (data not shown) inhibit the coimmunoprecipitation of HIF 1 α with its E3 ligase, von Hippel-Lindau protein (pVHL) (45) in COS cells overexpressing both FLAG-tagged pVHL and HA-tagged HIF 1 α . Strikingly, SNOAC S-nitrosylated native pVHL in HeLa cells (Figure 5E), and SNOAC and GSNO increased pVHL

**Figure 5**

S-Nitrosothiols prevent normoxic ubiquitination and degradation of HIF 1 α . (A) NAC treatment (10 mg/ml; 3 weeks) increased whole-lung HIF 1–DNA binding activity. Complexes were supershifted (ss) with anti-HIF 1 β and eliminated with excess cold probe (P). (B) SNOAC (1 μ M), like GSNO (5, 13, 38), increased normoxic HIF 1 α expression in nuclear extracts isolated from primary murine pulmonary endothelial cells. NAC alone (50 μ M) did not affect HIF 1 α expression. β -Actin was used as a protein load control. (C) In BPAECs transfected with HA-tagged HIF 1 α and dominant-negative His-6-Myc–tagged ubiquitin (DN-Ub), ubiquitinated proteins were isolated using a nickel column and immunoblotted for HIF 1 α . Both hypoxia and GSNO (G; 10 μ M) inhibited HIF 1 α ubiquitination relative to normoxia. (D) In COS cells cotransfected with HA-tagged HIF 1 α and FLAG-tagged pVHL, GSNO (10 μ M) prevented the coimmunoprecipitation of HIF 1 α with pVHL. (E) S-nitrosylation of pVHL by SNOAC (5 μ M) in equal protein aliquots isolated from HeLa cells was identified by biotin substitution (49); in the absence of ascorbate, S-nitrosylated pVHL was not detected. (F) Similarly, SNOAC and GSNO (5 μ M) increased pVHL S-nitrosylation in pVHL-overexpressing 786-O cells. (G) C162, but not C77, was identified by biotin substitution to be S-nitrosylated in BPAECs transfected with wild-type cysteine 77 to serine mutant (C77S), C162S, or combined C77S/C162S pVHL exposed to SNOAC (1 μ M). Native pVHL and MAPK immunoblots represented the pVHL expression and protein load controls, respectively. All *in vitro* treatments were for 4 hours.

S-nitrosylation in 786-O cells stably overexpressing pVHL (45), in which baseline NOS activity and/or NO transfer reactions (1) also resulted in baseline pVHL S-nitrosylation (Figure 5F). Therefore, we studied the 2 potential pVHL S-nitrosylation targets (C77 and C162; refs. 45, 46). In BPAECs transiently transfected with wild-type pVHL or with cysteine-to-serine mutants C77S, C162S, or C77S/C162S, mutation of C162 eliminated SNOAC-induced pVHL S-nitrosylation (Figure 5G), consistent with evidence that C162 is required for pVHL to bind elongin C and ubiquitinate HIF 1 α (46). Note that this effect could also reflect S-nitrosylation of a protein interacting with pVHL C162. Taken together, these data suggest that one element of the mechanism by which S-nitrosothiols may be hypoxia-mimetic involves prevention of HIF 1 α ubiquitination, possibly through S-nitrosylation of pVHL C162. Additional stud-

ies are needed to determine the extent to which each mechanism is involved in the hypoxia-mimetic vascular effects of SNOAC *in vivo*.

Discussion

In vitro evidence has suggested that NO transfer reactions occurring during erythrocyte deoxygenation may signal hypoxia (3–5, 11, 12). However, the relevance of these reactions to hypoxia-associated processes at the whole-organism level has not previously been directly demonstrated. Here, we used the pharmaceutical antioxidant NAC as a bait reactant to study this biochemistry *in vivo*. We report that chronic NAC administration to normoxic mice can cause increased RV pressure, RV hypertrophy, and pulmonary vascular remodeling that are indistinguishable from the effects of chronic hypoxia.

NAC must be converted to SNOAC to cause PAH. Several observations suggest that the chronic pulmonary vascular effects of NAC require conversion of NAC to SNOAC. To begin with, chronic treatment with both NAC and SNOAC caused PAH (Figure 1). Thus, PAH must have resulted from 1 of 4 pathways: (a) NAC was converted to SNOAC to cause PAH; (b) SNOAC was converted to NAC to cause PAH; (c) both NAC and SNOAC caused PAH, each by a separate mechanism; or (d) the generation of a third metabolite from both NAC and SNOAC caused PAH.

Second, eNOS^{-/-} mice had decreased circulating SNO_{rbc} content and were protected from NAC-induced PAH but were not protected from SNOAC-induced PAH. These data suggest that SNOAC formation from high concentrations of NAC and eNOS-derived NO, rather than reduction of lower concentrations of SNOAC to NAC, was necessary for the development of PAH. They suggest that neither NAC alone nor a common NAC/SNOAC metabolite causes PAH.

Third, we identified an oxyhemoglobin saturation-dependent mechanism by which NAC was converted to SNOAC under physiological conditions in blood. SNOAC concentrations, measured by MS, increased with the loss of SNO_{rbc} content during whole-blood deoxygenation in the presence of NAC *ex vivo* (Figure 3), consistent with previously reported NO transfer from deoxygenated erythrocytes to GSH to form GSNO (3). Neither SNOAC nor GSNO (3) were formed in the presence of oxygenated blood: deoxygenation was necessary. Alternative mechanisms by which NAC could be converted to SNOAC involve reactions in which NO radical either: (a) is oxidized in nonerythrocytic cells to an NO⁺ equivalent – a slow reaction under physiological conditions – that, in turn, reacts



with NAC thiolate; or (b) reacts directly with NAC as a thiol radical. These mechanisms are not kinetically favored in the context of competing reactions with excess heme or in the setting of hypoxia (1, 11, 40), and they were not observed experimentally in the current study: NAC had minimal reactivity with endogenous or exogenous endothelial NO. Taken together, these data suggest that erythrocyte deoxygenation resulted in conversion of NAC to SNOAC.

Fourth, NAC given systemically to the mice was converted to SNOAC *in vivo*, as identified by MS in RV (deoxygenated) blood. Levels of SNOAC were undetectable in LV (oxygenated) blood, suggesting that SNOAC was lost across the pulmonary vasculature and/or (consistent with our data) not formed from NAC in the presence of oxygenated erythrocytes. Further, chronic NAC administration depleted SNO_{rbc} content *in vivo* (Figure 3). Thus, the transnitrosation of an NO⁺ equivalent from erythrocyte to NAC can explain SNOAC formation from NAC *in vivo*, consistent with previous observations (3, 11).

Note that these data, coupled with evidence that low levels of NO radical react minimally with thiols in isolated endothelial cells and in oxygenated erythrocytes, argue against a model in which NAC causes PAH simply by depleting endothelial NO. They also argue against a model in which SNO_{rbc} depletion causes NAC-associated PAH. Humans with hypoxia-associated PAH are deficient in *S*-nitrosothiol-modified Hb (34); the relevance of this deficiency to PAH in hypoxic humans is not contradicted by our data. Indeed, we show that eNOS^{-/-} mice have a modest baseline increase in PA pressure associated with SNO_{rbc} depletion. However, chronic SNOAC treatment itself caused PAH in excess of that caused by SNO_{rbc} depletion.

Last, NAC-derived SNOAC is hypoxia-mimetic at the cellular level, whereas NAC itself opposes cellular effects associated with hypoxia (31, 32). SNOAC increases *S*-nitrosothiol levels in primary pulmonary vascular endothelial cells (Figure 4). *S*-nitrosothiols can upregulate hypoxia-associated genes *in vitro* through HIFs and/or Sp's (5, 13, 14, 38). In whole-lung homogenates, significant increases in mRNA and protein expression for genes associated with hypoxic pulmonary vascular remodeling were not uniform. This may reflect the use of whole-lung homogenates and the expression of genes in nonvascular cells. Nevertheless, mRNA and protein expression increased for several genes regulated by HIF 1, Sp3, and other hypoxia-associated factors. In the NAC-treated animals, it is unlikely that these effects on gene expression represented an effect of NAC alone: NAC (a) prevents hypoxia-mimetic cell injury in the absence of erythrocytes *in vitro* (31, 32); (b) did not cause PAH in the eNOS^{-/-} mice (Figure 1); and (c) did not increase Sp3 or HIF 1 α expression *in vitro* (Figures 4 and 5). Taken together, these data suggest that conversion of NAC to SNOAC was necessary for the hypoxia-mimetic effects of chronic, systemic NAC exposure.

Mechanisms by which S-nitrosothiols could be hypoxia mimetic at the cellular level. SNOAC could interact with cellular proteins to cause pulmonary vascular remodeling through: (a) homolytic cleavage to form NO radical, which reacts downstream with cellular free radicals or heme groups according to diffusion-limited kinetics; or (b) transnitrosation reactions, in which NO is transferred to a target cysteine thiol, conventionally represented as a covalent NO⁺ transfer between thiolate anions (1). The interactions of *S*-nitrosothiols with gene-regulatory proteins such as HIF 1 α are complex and likely involve both NO radical chemistry and transnitrosation chemistry (38). In the context of hypoxia and/or oxidative stress *in*

vitro, both NAC alone and *S*-nitrosothiol-derived NO radical can affect HIF 1 activation through mechanisms involving consumption of free radicals (38, 40). However, transnitrosation chemistry may be more relevant to our *in vivo* model because plasma *S*-nitrosothiols likely evolve little or no bioavailable NO radical in the presence of blood (1, 11, 41).

There are several potential targets of transnitrosation chemistry by which *S*-nitrosothiols might affect hypoxia-associated gene regulation. HIF 1 α and prolyl hydroxylases could be modified by transnitrosation chemistry (37–39); and there may be targets in the Akt signaling cascade (13). Our results demonstrate that pVHL is also a target for *S*-nitrosylation. This posttranslational modification of pVHL appears to alter pVHL–HIF 1 α interaction and decrease HIF 1 α ubiquitination. Of pVHL's 2 critical reactive cysteines, our data suggest that C162, which is necessary for the interaction of pVHL with elongin C within the HIF-E3 ligase complex (46, 47), is the likely target for *S*-nitrosylation. Additional work will be required to determine which mechanisms are the most important determinants of the hypoxia-mimetic cellular effects of SNOAC in our *in vivo* model.

Specific pulmonary effect of SNOAC. Oral administration of GSNO, an endogenous *S*-nitrosothiol (35) formed during erythrocyte deoxygenation (3), did not cause PAH, though GSNO has hypoxia-mimetic effects *in vitro* (5, 13, 14). This suggests that GSNO toxicity is prevented by mechanisms that may be bypassed by SNOAC. GGT cleaves GSNO to *S*-nitrosocysteinyl glycine and glutamate, serving as a gatekeeper in certain cells to regulate intracellular GSNO effects (3). SNOAC can bypass this regulation. However, pulmonary vascular endothelial cells express functional GGT (5). Therefore, we propose that the pulmonary vasculature is protected from oral GSNO, in part, by gastrointestinal GSNO metabolism (6). Additionally, NAC and SNOAC did not affect the kidney or liver; systemic vascular beds may be insensitive to SNOAC.

Alternatively, slow transnitrosation kinetics (Figure 3) may cause SNOAC to be formed only gradually as hypoxic systemic blood returns to the right heart, favoring an effect of SNOAC on the pulmonary vascular bed, where it is consumed before returning to the systemic circulation. However, mice fed SNOAC for 3 weeks at a dose that caused PAH had no change in portal histology. Therefore, we speculate that the pulmonary vascular bed is selectively sensitive to SNOAC, perhaps reflecting differential pulmonary expression of *S*-nitrosothiol metabolic enzymes (6). In this regard, the pulmonary vascular bed is susceptible to remodeling in the face of increased flow, chronic inflammation, and chronic hypoxia (7); each of these conditions could lead to increased *S*-nitrosothiol delivery to the lung. A fuller understanding of regional *S*-nitrosothiol metabolism, perhaps in animals in which long-term intra-arterial *S*-nitrosothiols can be delivered, will likely prove to be important.

The role of eNOS in this model of PAH. eNOS has been reported to have opposing roles in PAH (18–21, 26–29). An increase in pulmonary eNOS expression, described in certain species early in the course of PAH, may have a compensatory pulmonary vasodilator role. Consistent with this paradigm, we observed a transient increase in eNOS mRNA as well as a later increase in eNOS protein in PAH. On the other hand, the upregulation of eNOS protein could also represent a feed-forward mechanism by which SNOAC worsens pulmonary vascular remodeling, since eNOS^{-/-} mice were protected from NAC-induced PAH.

The role of eNOS in chronic PAH certainly involves effects in addition to an eNOS-associated increase in *S*-nitrosothiol deliv-



Table 1
Primers used for PCR experiments

Gene	Primers
HIMF (51)	Forward: 5'-GGTCCCAGTGCATATGGATGAGACCATAGA-3' Reverse: 5'-CACCTCTTCACTCGAGGGACAGTTGGCAGC-3'
VEGF-A (52)	Forward: 5'-CTCTACCTCCACCATGCCAAG-3' Reverse: 5'-GGTACTCCTGGAGGATGTCCACC-3'
Glut-1 (53)	Forward: 5'-GGTGTGCAGCAGCCTGTGTA-3' Reverse: 5'-AAATGAGGTGCAGGGTCCGT-3'
eNOS	Forward: 5'-AAGACAAGGCAGCGGTGGAA-3' Reverse: 5'-GCAGGGGGACAGGAAATAGTT-3'

ery to the pulmonary vascular bed: eNOS^{-/-} mice have increased PA pressure at baseline, suggesting a role of eNOS on pulmonary vascular smooth muscle tone. These potential opposing roles for eNOS in regulating pulmonary vascular gene expression and smooth muscle tone might help to explain paradoxical observations regarding pulmonary vascular eNOS expression and activity in the setting of PAH.

Conclusions. Chronic exposure to NAC and to SNOAC causes murine PAH. We propose that these observations may be understood according to the following pathway. In normoxic, NAC-treated animals, oxyhemoglobin desaturation in erythrocytes leads to SNOAC formation in systemic blood returning to the lungs. These reactions require the presence of endogenous SNO_{hbc} formed, in part, by eNOS. Formation of SNOAC — like that of GSNO, S-nitrosothiol-AE1, and other S-nitrosothiols during erythrocyte deoxygenation — is dependent on transnitrosation reactions. In these reactions, an NO⁺ equivalent, protected from heme autocapture, is transferred from one thiolate moiety to another as Hb changes conformation during deoxygenation (1, 3, 4, 11, 12). The demonstration that SNOAC is formed during blood deoxygenation in vitro is complemented by the direct demonstration that it is present in hypoxic, but not normoxic, blood in vivo. While the cellular effects of GSNO and other S-nitrosothiols are regulated (1, 3, 5, 6, 14), delivery of NO to the pulmonary endothelium by SNOAC appears to bypass this regulation, causing hypoxia-mimetic effects. These observations may help to explain hypoxia-mimetic effects of systemic NAC therapy observed in humans in vivo (48).

The effect of chronic NAC exposure to cause pulmonary vascular pathology may be species dependent. It is reassuring that the NAC dose that caused PAH in mice was higher than the hypoxia-mimetic dose used in humans (48). However, PAH can be subclinical, even presenting as a terminal event (7, 8). In this context, it is noteworthy that NAC treatment may fail to decrease mortality in human clinical trials, despite beneficial antiinflammatory and antioxidant effects (30): PAH has not previously been considered as a NAC toxicity. Surveillance for this toxicity may be appropriate for long-term human trials with NAC.

In summary, these data: (a) provide the first in vivo measurements to our knowledge suggesting that NO can signal erythrocytic oxygen desaturation through S-nitrosothiol formation; (b) introduce a novel murine model of PAH, one in which transgenic animals are informative; (c) provide one explanation for previously reported, hypoxia-mimetic effects of NAC; and (d) suggest that PAH may be an unappreciated risk of systemic therapy with the pharmaceutical antiinflammatory and antioxidant agent NAC.

Methods

Animal protocols. C57BL/6/129SvEv, C57BL/6, and eNOS^{-/-} mice (10–12 weeks old) were treated in normoxia (21% O₂) or hypoxia (10% O₂, normobaric) as described (27) with or without 10 mg/ml NAC in the drinking water for 3 weeks (achieving serum NAC levels of 16.2 ± 4.3 μM as measured by liquid chromatography/MS). The plasma NAC level at this dose was similar to the target peak level in the human study of the hypoxia-mimetic effects of NAC (48), though the dose per weight was approximately 40-fold higher and the exposure continuous. Additional mice were treated for 3 weeks with 1 mM SNOAC in the drinking water (achieving venous plasma SNOAC levels of 350 ± 34 nM). The eNOS^{-/-} mice used in these studies were on a C57BL/6 background, maintained by our group and backcrossed for 10 generations (27). Protocols were approved by the University of Virginia Animal Care and Use Committee.

RV pressure measurements. A Millar Mikro Tip catheter/transducer (1.4 F) was inserted through the external jugular vein of sedated (5 mg/ml pentobarbital) mice and threaded into the RV. RV pressure was determined from the average of 10–12 measurements (PulmoDyne; Hugo Sachs Elektronik) at a stable baseline (Figure 1C).

Immunohistochemistry, vessel morphometry, and ventricular weight ratio measurements. Inflated lungs fixed in 10% formaldehyde were assessed for endothelium and smooth muscle using antibodies for von Willebrand factor and α-SMA (A0082 and M0851; Dako). Vessel morphometry was performed (>50 vessels per animal) by an investigator blinded to the treatment group. Muscularization of small (<80-μm) vessels was classified as nonmuscular, partly muscular, or muscular based on α-SMA staining. Immunostaining for 3-nitrotyrosine was performed using anti-nitrotyrosine antibody (Upstate; Supplemental Data). Cardiac tissue was dissected free from the great vessels immediately post mortem and washed with PBS. RV tissue was dissected from the septum and LV; RV weight was expressed as the ratio RV/LV+S.

NO transfer from intact erythrocytes during deoxygenation. Oxygenated, heparinized blood in a septated glass tonometer was treated with NAC (100 μM) and deoxygenated with 95% argon/5% CO₂. Serial samples underwent (a) co-oximetry; (b) plasma separation for SNOAC measurement by MS (see below); and (c) SNO_{hbc} assay by chemiluminescence following reduction in a CuCl-saturated solution of 1 mM cysteine purged with blended argon and CO, as previously described (11).

Primary cell cultures and other cell lines. Murine lungs were harvested in PBS containing heparin (10 U/ml) and 1% penicillin/streptomycin (Invitrogen; Millipore), minced, digested in 0.3% collagenase (PBS; 37°C; 30–95 minutes), and resuspended in DMEM with D-valine (Chemicon International; Millipore) containing 20% FCS, 10 μM HEPES, 2 mM glutamine, 2 mM sodium pyruvate, 1% nonessential amino acids, 90 μg/ml heparin, 100 μg/ml endothelial growth cell factor, 1% ITS reagent, 1% penicillin/streptomycin, 50 μM 3-isobutyl-1-methylxanthine, 50 μM N-6-O-dibutyryl cAMP and 1 μg/ml hydrocortisone acetate. After 3 days' incubation (37°C), cells were sorted for Dil-A_c-LDL uptake (Biomedical Technologies Inc.). Positive cells were cultured for 9–12 passages. BPAECs were isolated as previously described (5). COS cells were grown to confluence in DMEM/high glucose with 10% FCS. 786-O cells (ATCC) and 780-O pVHL (gift from W. Kaelin, Dana Farber Cancer Institute, Harvard University, Boston, Massachusetts, USA) were grown in RPMI.

Immunoblotting. Immunoblot analysis on proteins isolated from lung homogenates, whole-cell extracts, and nuclear extracts was performed using antibodies against HIF1α (Novus Biologicals), Sp3, neuronal NOS, VEGF-A, MAPK (Santa Cruz Biotechnology Inc.), HIMF (gift from Dechun Li, Saint Louis University, St. Louis, Missouri, USA), fibronectin (Abcam Inc.), eNOS, iNOS (BD Biosciences), and endothelin-1 (Research Diagnostics Inc.) as described previously (5, 14).



Biotin substitution of S-nitrosothiol bonds. This was performed according to the method of Jaffrey et al. (49).

EMSA. EMSAs were performed on nuclear extracts using oligonucleotides and antibodies (for supershift) as described previously (5).

Real-time PCR. Messenger RNA was isolated from whole-lung homogenates by an RNA Easy kit (QIAGEN) as per the manufacturer's instructions. Expression of *eNOS*, *VEGF*, *HIMF*, *fibronectin*, and *Glut-1* mRNA was assessed by real-time PCR using the primers (Integrated DNA Technologies Inc.) noted in Table 1. The RT reaction was performed using 200 ng RNA under the following conditions: 25°C for 10 minutes, 48°C for 30 minutes, and 95°C for 5 minutes using the Reverse Transcriptase Kit (Applied Biosystems), as described by the manufacturer, in the presence of SYBR Green Supermix (Bio-Rad). PCR cycles for HIMF were: 95°C for 3 minutes, 95°C for 30 seconds, 63°C, 72°C for 30 seconds; for VEGF: 95°C for 3 minutes, 95°C for 30 seconds, 60°C for 1 minute, 72°C for 1 minute; for eNOS: 95°C for 3 minutes, 95°C for 30 seconds, 58°C for 1 minute, 72°C for 1 minute; for fibronectin: 95°C for 3 minutes, 95°C for 30 seconds, 55.6°C for 1 minute, 72°C for 1 minute; for Glut-1: the same conditions as for VEGF, each for 50 cycles. Relative gene expression was determined according to Livak and Schmittgen (50).

Coinmunoprecipitation. COS cells were transiently transfected with HA-HIF-1 α and FLAG-pVHL using Lipofectamine 2000 (Invitrogen) according to the manufacturer's instructions. Following S-nitrosothiol treatment, cells were lysed in lysis buffer (20 mM Tris pH 7.6, 150 mM NaCl, 10% glycerol, 2 mM EDTA 1% Triton X-100, 1 mM Na₂VO₄, 1 μ g/ml leupeptin, 1 mM PMSF). Lysates were incubated with Flag M2 affinity gel (Sigma-Aldrich) (2 hours; 4°C). The gel was washed 4 times in lysis buffer. Samples were eluted with 50 μ l 2 \times SDS buffer, heated (100°C; 3 minutes), and separated by 8% SDS-PAGE. HIF 1 α was identified by immunoblot (5).

Nickel column isolation. BPAECs were transfected with HA-HIF-1 α and pCW-8, a His-6-Myc-tagged ubiquitin containing the K48R mutation (gift from R. Kopito, Stanford University, Palo Alto, California, USA), using Lipofectamine 2000. Untransfected and transfected cells were grown in the absence or presence of S-nitrosothiol (21% O₂) or in 10% O₂. Cells were lysed in the absence of EDTA, and lysates were passed over a ProBond Resin nickel column (Invitrogen) to isolate monoubiquitin-containing complexes. Complexes were eluted with imidazole and separated on 8% SDS-PAGE. HIF 1 α protein was detected by immunoblot.

Site-directed mutagenesis of pVHL. pVHL was mutated using the Quick-Change Site-Directed Mutagenesis Kit (Stratagene) according to the manufacturer's instructions using the following primers: pVHL C77S primer 1, 5'-CCCTCCCAGGTTCATCTTCTCTAATCGCAGTCCG-3'; primer 2, 5'-CGGACTGCGATTAGAGAAGATGACCTGGGAGGG-3'; pVHL C162S primer 1, 5'-CTGAAAGAGCGATCGCTCCAGTTGTCCGGAGC-3'; primer 2, 5'-GCTCCGGACAACCTGGAGCGATCGCTCTTTTCAG-3'.

MS. Plasma (100 μ l) spiked with ¹⁵N-labeled SNOAC was applied to a Phenomenex Strata XC 33 μ M SPE cartridge (60 mg, 3 ml), preequilibrated (and washed following loading) with methanol/0.02% trifluoroacetic acid in water. Analytes were eluted with methanol and concentrated under reduced pressure (0°C). Partially purified samples were reconstituted in methanol, separated on a C8 column (5 mm, 2.1 \times 150 mm) (Waters 2695 HPLC) with a gradient of 0.1% formic acid in water and methanol, and analyzed by electrospray ionization MS using a Finnigan LCQ system. (Finnigan Corp.) SNOAC cations were monitored at a mass to charge ratio of 192.5–193.5.

Statistics. Multiple comparisons were made using ANOVA followed by pairwise analysis. Individual comparisons were made by Student's *t* test if normally distributed; or otherwise by Mann-Whitney rank-sum test (using SigmaStat; Jandel). Relative gene expression by RT-PCR was quantitated as above (50). Except where noted, data are presented as mean \pm SD. *P* < 0.05 was considered significant.

Acknowledgments

We thank Dechun Li for the gift of HIMF antibody; Kimberly DeRonde, Kathleen Brown-Steinke, Jaclyn Kline, Edward Henderson, and Joseph Doherty for technical assistance; and Brian Duling for his thoughtful comments on the manuscript. This work was supported by NIH grants HL068173 (to L.A. Palmer), HL059337 (to B. Gaston), and 1KO8GM069977 (to A. Doctor).

Received for publication June 20, 2006, and accepted in revised form May 24, 2007.

Address correspondence to: Benjamin Gaston, Pediatric Respiratory Medicine University of Virginia Health System, Box 800386, Charlottesville, Virginia 22908, USA. Phone: (434) 924-1820; Fax: (434) 924-8388; E-mail: bmg3g@virginia.edu.

- Gaston, B., Doctor, A., Singel, D., and Stamler, J.S. 2006. S-Nitrosothiol signaling in respiratory biology. *Am. J. Respir. Crit. Care Med.* **173**:1186–1193.
- Kim, S.F., Huri, D.A., and Snyder, S.H. 2005. Inducible nitric oxide synthase binds, S-nitrosylates and activates cyclooxygenase-2. *Science*. **310**:1966.
- Lipton, A.J., et al. 2001. S-Nitrosothiols signal the ventilatory response to hypoxia. *Nature*. **413**:171–174.
- Jia, L., Bonaventura, C., Bonaventura, J., and Stamler, J.S. 1996. S-Nitrosohaemoglobin: a dynamic activity of blood involved in vascular control. *Nature*. **380**:221–226.
- Palmer, L.A., Gaston, B., and Johns, R.A. 2000. Normoxic stabilization of hypoxia-inducible factor-1 expression and activity: redox-dependent effect of nitrogen oxides. *Mol. Pharmacol.* **58**:1197–1203.
- Liu, L., et al. 2004. Essential roles of S-nitrosothiols in vascular homeostasis and endotoxic shock. *Cell*. **116**:617–628.
- Farber, H.W., and Loscalzo, J. 2004. Pulmonary arterial hypertension. *N. Engl. J. Med.* **351**:1655–1665.
- Blaise, G., Langleben, D., and Hubert, B. 2003. Pulmonary arterial hypertension: pathophysiology and anesthetic approach. *Anesthesiology*. **99**:1415–1432.
- Semenza, G.L. 2004. O₂-regulated gene expression: transcriptional control of cardiorespiratory physiology by HIF-1. *J. Appl. Physiol.* **96**:1173–1177.
- Jiang, B.H., Semenza, G.L., Bauer, C., and Marti, H. 1996. Hypoxia-inducible factor 1 levels vary exponentially over a physiologically relevant range of O₂ tension. *Am. J. Physiol.* **271**:C1172–C1180.
- Doctor, A., et al. 2005. Hemoglobin conformation couples erythrocyte S-nitrosothiol content to O₂ gradients. *Proc. Natl. Acad. Sci. U. S. A.* **102**:5709–5714.
- Pawloski, J.R., Hess, D.T., and Stamler, J.S. 2001. Export by red blood cells of nitric oxide bioactivity. *Nature*. **409**:622–626.
- Sandau, K.B., Faus, H.G., and Brune, B. 2000. Induction of hypoxia-inducible-factor 1 by nitric oxide is mediated via the PI 3K pathway. *Biochem. Biophys. Res. Com.* **278**:263–267.
- Zaman, K., Palmer, L.A., Doctor, A., Hunt, J.F., and Gaston, B. 2004. Concentration-dependent effects of endogenous S-nitrosoglutathione on gene regulation by specificity proteins Sp3 and Sp1. *Biochem. J.* **380**:67–74.
- Ricardo, K., Shishido, S., de Oliveira, M., and Krieger, M. 2002. Characterization of the hypotensive effect of S-nitroso-N-acetylcysteine in normotensive and hypertensive conscious rats. *Nitric Oxide*. **7**:57–66.
- Teng, X., Li, D., Champion, H.C., and Johns, R.A. 2003. FIZZ1/RELMalpha, a novel hypoxia-induced mitogenic factor in lung with vasoconstrictive and angiogenic properties. *Circ. Res.* **92**:1065–1067.
- Vyas-Somani, A.C., et al. 1996. Temporal alterations in basement membrane components in the pulmonary vasculature of the chronically hypoxic rat: impact of hypoxia and recovery. *Am. J. Med. Sci.* **312**:54–67.
- Le Cras, T.D., et al. 1999. Effects of chronic hypoxia and altered hemodynamics on endothelial nitric oxide synthase expression in the adult rat lung. *J. Clin. Invest.* **101**:795–801.
- Lam, C.-F., Peterson, T.E., Croatt, A.J., Nath, K.A., and Katusic, Z.S. 2005. Functional adaptation and remodeling of pulmonary artery in flow-induced pulmonary hypertension. *Am. J. Physiol. Heart Circ. Physiol.* **289**:H2334–H2341.
- Xue, C., and Johns, R.A. 1996. Upregulation of nitric oxide synthase correlates temporally with onset of pulmonary vascular remodeling in the hypoxic rat. *Hypertension*. **28**:743–753.
- Tyler, R.C., et al. 1999. Variable expression of endothelial NO synthase in three forms of rat pulmonary hypertension. *Am. J. Physiol.* **276**:L297–L303.
- Kanazawa, F., et al. 2005. Expression of endothelin-1 in the brain and lung of rats exposed to permanent hypobaric hypoxia. *Brain Res.* **1036**:145–154.
- Grover, T.R., et al. 2003. Intrauterine hypertension decreases lung VEGF expression and VEGF inhibition causes pulmonary hypertension in the



- ovine fetus. *Am. J. Physiol. Lung Cell Mol. Physiol.* **284**:L508–L517.
24. Zhao, Y.D., et al. 2006. Microvascular regeneration in established pulmonary hypertension by angiogenic gene transfer. *Am. J. Respir. Cell Mol. Biol.* **35**:182–189.
25. Li, Q., and Dai, A. 2004. Hypoxia-inducible factor-1 alpha regulates the role of vascular endothelial growth factor on pulmonary arteries of rats with hypoxia-induced pulmonary hypertension. *Chin. Med. J.* **117**:1023–1028.
26. Hoehn, T., et al. 2003. Endothelial nitric oxide synthase (NOS) is upregulated in rapid progressive pulmonary hypertension of the newborn. *Intensive Care Med.* **29**:1757–1762.
27. Shesely, E.G., et al. 1996. Elevated blood pressures in mice lacking endothelial nitric oxide synthase. *Proc. Natl. Acad. Sci. U. S. A.* **93**:13176–13181.
28. Steudel, W., et al. 1998. Sustained pulmonary hypertension and right ventricular hypertrophy after chronic hypoxia in mice with congenital deficiency of nitric oxide synthase 3. *J. Clin. Invest.* **101**:2468–2477.
29. Fagan, K.A., et al. 1999. The pulmonary circulation of homozygous or heterozygous eNOS-null mice is hyperresponsive to mild hypoxia. *J. Clin. Invest.* **103**:291–299.
30. Hunninghake, G.W. 2005. Antioxidant therapy for idiopathic pulmonary fibrosis. *N. Engl. J. Med.* **353**:2285–2287.
31. Springer, J., and Fischer, A. 2003. Substance P-induced pulmonary vascular remodelling in precision cut lung slices. *Eur. Respir. J.* **22**:596–601.
32. Shatrov, V.A., Sumbayev, V.V., Zhou, J., and Brüne, B. 2003. Oxidized low-density lipoprotein (oxLDL) triggers hypoxia-inducible factor 1 α (HIF-1 α) accumulation via redox-dependent mechanisms. *Blood.* **101**:4847–4849.
33. Scharfstein, J.S., et al. 1994. In vivo transfer of nitric oxide between a plasma protein-bound reservoir and low molecular weight thiols. *J. Clin. Invest.* **94**:1432–1439.
34. McMahon, T.J., et al. 2005. A nitric oxide processing defect of red blood cells created by hypoxia: deficiency of S-nitrosohemoglobin in pulmonary hypertension. *Proc. Natl. Acad. Sci. U. S. A.* **102**:14801–14806.
35. Gaston, B., et al. 1993. Endogenous nitrogen oxides and bronchodilator S-nitrosothiols in human airways. *Proc. Natl. Acad. Sci. U. S. A.* **90**:10957–10961.
36. Wada, T., Shimba, S., and Tezuka, M. 2006. Transcriptional regulation of the hypoxia inducible factor 2alpha (HIF-2alpha) gene during adipose differentiation in 3T3-L1 cells. *Biol. Pharm. Bull.* **29**:49–54.
37. Sumbayev, V.V., Budde, A., Zhou, J., and Brüne, B. 2003. HIF-1 alpha protein as a target for S-nitrosation. 2003. *FEBS Lett.* **535**:106–112.
38. Zhou, J., and Brüne, B. 2005. NO and transcriptional regulation: from signaling to death. *Toxicology.* **208**:223–233.
39. Metzen, E., Zhou, J., Jelkmann, W., Fandrey, J., and Brüne, B. 2003. Nitric oxide impairs normoxic degradation of HIF-1 α by inhibition of prolyl hydroxylases. *Mol. Biol. Cell.* **14**:3470–3481.
40. Kohl, R., Zhou, J., and Brüne, B. 2006. Reactive oxygen species attenuate nitric-oxide-mediated hypoxia-inducible factor-1alpha stabilization. *Free Radic. Biol. Med.* **40**:1430–1442.
41. Jeffers, A., et al. 2005. Hemoglobin mediated nitrite activation of soluble guanylyl cyclase. *Comp. Biochem. Physiol. A Mol. Integr. Physiol.* **142**:130–135.
42. Masson, N., Willam, C., Maxwell, P.H., Pugh, C.W., and Ratcliffe, P.J. 2001. Independent function of two destruction domains in hypoxia-inducible factor-alpha chains activated by prolyl hydroxylation. *EMBO J.* **20**:5197–5206.
43. Ivan, M., et al. 2001. HIF α targeted for VHL-mediated destruction by proline hydroxylation: implications for O₂ sensing. *Science.* **292**:464–468.
44. Yao, D., et al. 2004. Nitrosative stress linked to sporadic Parkinson's disease: S-nitrosylation of Parkin regulates its E3 ligase activity. *Proc. Natl. Acad. Sci. U. S. A.* **101**:10810–10814.
45. Lonergan, K.M., et al. 1998. Regulation of hypoxia-inducible mRNAs by the von Hippel-Lindau tumor suppressor protein requires binding to complexes containing elongins B/C and Cul2. *Mol. Cell. Biol.* **18**:732–741.
46. Ohh, M., et al. 2000. Ubiquitination of hypoxia-inducible factor requires direct binding to the beta-domain of the von Hippel-Lindau protein. *Nat. Cell Biol.* **2**:423–427.
47. Stebbins, C.E., Kaelin, W.G., Jr., and Pavletich, N.P. 1999. Structure of the VHL-ElonginC-ElonginB complex: implications for VHL tumor suppressor function. *Science.* **284**:455–461.
48. Hildebrandt, W., Alexander, S., Bartsch, P., and Droge, W. 2002. Effect of N-acetyl-cysteine on the hypoxic ventilatory response and erythropoietin production: linkage between plasma thiol redox state and O(2) chemosensitivity. *Blood.* **99**:1552–1555.
49. Jaffrey, S.R., Erdjument-Bromage, H., Ferris, C.D., Tempst, P., and Snyder, S.H. 2001. Protein S-nitrosylation: a physiological signal for neuronal nitric oxide. *Nat. Cell Biol.* **3**:193–197.
50. Livak, K.J., and Schmittgen, T.D. 2001. Analysis of relative gene expression data using real-time quantitative PCR and the 2^{- $\Delta\Delta C_T$} method. *Methods.* **25**:402–408.
51. Loke, P., Nair, M.G., Parkinson, J., Guiliano, D., and Allen, M.E. 2002. IL4-dependent alternatively-activated macrophages have distinctive in vivo gene expression phenotype. *BMC Immunol.* **3**:7.
52. Chintalgattu, V., Nair, D.M., and Katwa, L.C. 2003. Cardiac myofibroblasts: a novel source of vascular endothelial growth factor (VEGF) and its receptors Flt-1 and KDR. *J. Mol. Cell. Cardiol.* **35**:277–286.
53. Tang, Y., et al. 2006. Effect of hypoxic preconditioning on brain genomic response before and following ischemia in the adult mouse: identification of potential neuroprotective candidates for stroke. *Neurobiol. Dis.* **21**:18–28.

Gender Differences in S-Nitrosogluthione Reductase Activity in the Lung

Kathleen Brown-Steinke, Kimberly deRonde, Sean Yemen, Lisa A. Palmer*

Department of Pediatrics, University of Virginia Health System, Charlottesville, Virginia, United States of America

Abstract

S-nitrosothiols have been implicated in the etiology of various pulmonary diseases. Many of these diseases display gender preferences in presentation or altered severity that occurs with puberty, the mechanism by which is unknown. Estrogen has been shown to influence the expression and activity of endothelial nitric oxide synthase (eNOS) which is associated with increased S-nitrosothiol production. The effects of gender hormones on the expression and activity of the de-nitrosylating enzyme S-nitrosogluthione reductase (GSNO-R) are undefined. This report evaluates the effects of gender hormones on the activity and expression of GSNO-R and its relationship to N-acetyl cysteine (NAC)-induced pulmonary hypertension (PH). GSNO-R activity was elevated in lung homogenates from female compared to male mice. Increased activity was not due to changes in GSNO-R expression, but correlated with GSNO-R S-nitrosylation: females were greater than males. The ability of GSNO-R to be activated by S-nitrosylation was confirmed by: 1) the ability of S-nitrosogluthione (GSNO) to increase the activity of GSNO-R in murine pulmonary endothelial cells and 2) reduced activity of GSNO-R in lung homogenates from eNOS^{-/-} mice. Gender differences in GSNO-R activity appear to explain the difference in the ability of NAC to induce PH: female and castrated male animals are protected from NAC-induced PH. Castration results in elevated GSNO-R activity that is similar to that seen in female animals. The data suggest that GSNO-R activity is modulated by both estrogens and androgens in conjunction with hormonal regulation of eNOS to maintain S-nitrosothiol homeostasis. Moreover, disruption of this eNOS-GSNO-R axis contributes to the development of PH.

Citation: Brown Steinke K, deRonde K, Yemen S, Palmer LA (2010) Gender Differences in S Nitrosogluthione Reductase Activity in the Lung. PLoS ONE 5(11): e14007. doi:10.1371/journal.pone.0014007

Editor: Amit Gaggar, University of Alabama Birmingham, United States of America

Received: May 13, 2010; **Accepted:** October 20, 2010; **Published:** November 16, 2010

Copyright: © 2010 Brown Steinke et al. This is an open access article distributed under the terms of the Creative Commons Attribution License, which permits unrestricted use, distribution, and reproduction in any medium, provided the original author and source are credited.

Funding: Work for this project has been supported by the Peer Reviewed Medical Research Program through the Department of Defense, Award Number W81XWH 07 1 0134 to LAP. The funders had no role in study design, data collection and analysis, decision to publish or preparation of the manuscript.

Competing Interests: The authors have declared that no competing interests exist.

* E mail: lap5w@virginia.edu

Introduction

S nitrosylation, a redox based modification of a cysteine thiol by nitric oxide, is a post translational modification that can alter a protein's function. Mechanisms that control the addition and/or removal of the NO group from cysteine thiols are essential in determining the net effect of this modification. Formation of endogenous S nitrosothiols can be mediated through: 1) the activity of any one of the nitric oxide synthase (NOS) isoforms, 2) oxidative reactions generating nitrosative species (for example, Fe⁺³NO, N₂O₃), or 3) transnitrosative reactions (NO⁺ transfer) [1–3]. The production of S nitrosothiols is opposed by mechanisms mediating de nitrosylation which can: 1) occur non enzymatically via homolytic or heterolytic cleavage, 2) be catalyzed by transition metal ions and reactive oxygen species, or 3) occur through enzymatic degradation [1,4]. One specific enzyme that regulates S nitrosothiol catabolism is S nitrosogluthione reductase (GSNO R), a ubiquitously expressed NADH dependent enzyme [2]. GSNO R is responsible for the breakdown of S nitrosogluthione (GSNO) to oxidized glutathione and ammonia [5,6]. Although the primary substrate for GSNO R is GSNO [5,6], the levels of other S nitrosylated proteins are affected indirectly through altered transnitrosation equilibria with GSNO.

S nitrosothiols have been implicated in pulmonary diseases such as cystic fibrosis [3,7–9], pulmonary hypertension [3,7,10,11] and asthma [3,7,12,13]. All of these pulmonary diseases display distinct

gender preferences in presentation or a change in disease severity that occurs at puberty, the cause of which is unknown [14–17]. Gender differences in the activity and/or expression of GSNO R have been suggested. Gastric activity of GSNO R may be a component of the enhanced vulnerability of women to develop alcohol related diseases [18]. Likewise, gender differences seen in the lipopolysaccharide (LPS) model of septic shock are eliminated in GSNO R knockout mice [6]. To date, the influence of de nitrosylation on the gender predilection of these lung diseases has not been addressed. The current studies evaluate the relationship between gender and the activity and/or expression of GSNO R in the lung. The data demonstrate that GSNO R activity is elevated in the female mouse lung when compared to the male. This increased activity does not reflect differences in GSNO R protein expression, but rather, reflects differences both in endothelial nitric oxide synthase (eNOS) dependent GSNO R S nitrosylation and androgen exposure. Indeed, mice deficient in eNOS have reduced GSNO R activity, and S nitrosylation increases GSNO R activity, suggesting that estrogen dependent increases in eNOS lead to increased GSNO R activity in the female lung, protecting against excessive S nitrosylation. Lastly, this gender discordance in the eNOS/GSNO R axis is relevant to pulmonary biology. Female mice are protected from the physiological effects mediated by the conversion of N acetyl cysteine (NAC) to S nitroso N acetyl cysteine (SNOAC) in vivo, despite increased eNOS expression. However, they develop hypoxia mimetic pulmonary hypertension

(PH) in response to chronic SNOAC exposure like their male littermates. This observation may have implications for human disease. For example, increased eNOS expression in females could predispose them to PH if the counter regulatory GSNO R response is abnormal.

Results

GSNO-R activity, not protein expression, is greater in lung homogenates of female than male mice

Initial studies evaluated the activity and expression of GSNO R in lung homogenates in male and female mice. GSNO R activity was evaluated using liquid chromatography/mass spectroscopy (LC/MS). GSNO R activity measured by LC/MS was significantly higher in adult (10–12 w) female animals compared to their corresponding adult male counterparts (Figure 1A). Similar gender specific differences (2–3 fold) were detected when GSNO R activity was measured by GSNO dependent NADH consumption or modified Saville Assay (Tables 1,2,3). In contrast, no significant differences in GSNO R activity were seen in the lungs of young (4 w) male and female animals (Figure 1B). To determine if this gender difference was specific for the lung, GSNO R activity was measured in the liver and the kidney. Unlike the lung, no gender specific differences in GSNO R activity were seen in either tissue (Tables 1 and 2). To determine if the differences in GSNO R activity in the adult murine lung were due to changes in protein expression, Western blot analysis was performed (Figure 1C). No significant differences in GSNO R protein expression were seen in the lung homogenates of adult male and female animals.

GSNO-R S-nitrosylation is greater in female than male mice

The detected difference in GSNO R activity present in the lung homogenates of male and female animals could be explained by differences in S nitrosylation. To examine if GSNO R is an S nitrosylated protein, lung homogenates obtained from male and female animals were subjected to biotin switch followed by Western blot analysis (Figure 1D). GSNO R was found to be S nitrosylated in both male and female lung homogenates. The level of S nitrosylation was greater in lung homogenates of female mice as compared to lung homogenates from male animals. S nitrosylation was confirmed by the ability of mercuric chloride to significantly reduce the appearance of S nitrosylated GSNO R.

S-nitrosoglutathione activates GSNO-R

Post translational modifications by S nitrosylation often results in a change in a protein's activity. Previous data demonstrate lung homogenates obtained from female animals have greater GSNO R activity and elevated GSNO R S nitrosylation compared to male animals, suggesting that S nitrosylation and activity are related. To define the impact of S nitrosylation on the activity of GSNO R, murine pulmonary endothelial cells were treated with and without 10 μ M GSNO for 5 min. GSNO R activity was measured in cell homogenates obtained from the untreated and treated cells. Treatment of murine lung endothelial cells with GSNO resulted in a significant increase in GSNO R activity (Figure 2A). To determine if GSNO R can be directly S nitrosylated, cell lysates from murine pulmonary endothelial cells were treated with or without 5 μ M L SNO cysteine (L SNO Cys) for 5 minutes and GSNO R activity measured using alterations in NADH consumption. L SNO Cys was found to significantly increase NADH consumption approximately 2 fold (Figure 2B). This increase in NADH consumption with L SNO Cys was independent of gender.

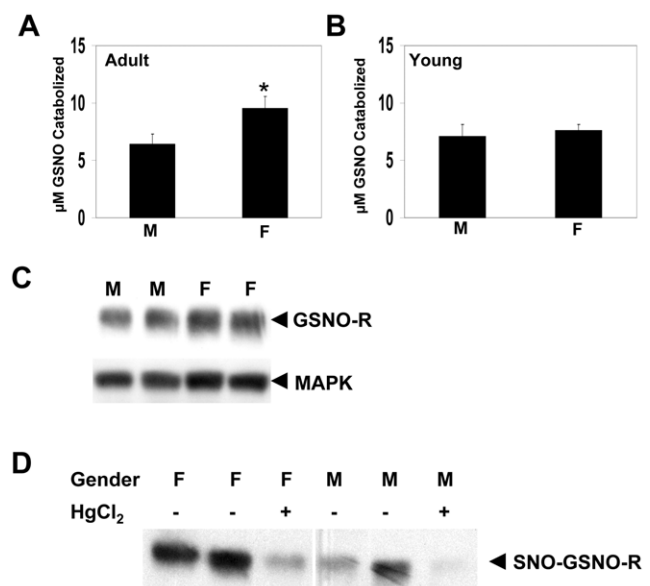


Figure 1. GSNO R activity and S nitrosylation is elevated in the female mouse lung. (A) GSNO R activity was measured in lung homogenates from male and female C57Bl6/129SvEv mice using LC/MS. GSNO R activity is expressed as the amount of GSNO catabolized after 5 min. Activity present in female mouse lung homogenates was approximately two times that seen in the males ($n=20$, $p<0.003$). (B) GSNO R activity was measured by LC/MS in lung homogenates from young (4 w) C57Bl6/129SvEv sexually immature male and female mice. Gender differences in GSNO R activity were not seen in the young animals ($n=5$). (C) GSNO R protein expression was determined in adult C57Bl6/129SvEv male and female lung homogenates. Protein expression was not significantly different between genders. (D) Lung homogenates from C57Bl6/129SvEv male and female mice were subjected to biotin switch to determine if GSNO R was S nitrosylated in vivo. Lung homogenates from both male and female animals demonstrate the presence of GSNO R S nitrosylation. However, the extent of S nitrosylation was greater in the female animals. Incubation of the lung homogenates with mercuric chloride reduced the abundance of S nitrosylated GSNO R. doi:10.1371/journal.pone.0014007.g001

Endothelial nitric oxide synthase increases GSNO-R Activity

eNOS is the prominent isoform present in the pulmonary vascular endothelium. Estrogen increases the expression and

Table 1. GSNO-R Activity determined by GSNO-dependent NADH Consumption is greater in lung homogenates obtained from female mice.

	GSNO-dependent NADH Consumption (μ M NADH/min/mg protein)		
	Male	Female	Female: Male Ratio
Lung	5.51+/- 2.9	10.58+/- 3.6	1.92
Liver	28.1+/- 3.77	19.46+/- 5.75	0.70
Kidney	39.96+/- 8.68	34.32+/- 9.11	0.85

GSNO R activity was measured in lung, liver, and kidney homogenates obtained from adult (10–12 w) male and female mice using a GSNO dependent NADH Consumption assay. NADH consumption was evaluated in homogenates (0.3 μ g) in the absence or presence of 100 μ M GSNO. Gender specific differences were seen in the lung homogenates ($n=4$). No gender specific differences were seen with either the liver or the kidney homogenates ($n=2-4$). doi:10.1371/journal.pone.0014007.t001

Table 2. GSNO-R activity measured by modified Saville Assay is greater in lung homogenates obtained from female mice.

	NADH-Dependent GSNO-R Activity (μM GSNO/min/mg protein)				
	Male		Female		Female: Male Ratio
Lung	2.56+/ 0.20		5.32+/ 1.06		2.07
Liver	6.24+/ 1.96		6.14+/ 0.25		0.98
Kidney	5.68+/ 0.69		6.06+/ 1.1		1.10

GSNO R activity was determined in homogenates from the lung, liver and kidney of adult male and female mice. GSNO R activity was measured in homogenates (250 μg) in the presence of 100 μM GSNO in the presence or absence of NADH at 37°C for 5 min. GSNO R activity was significantly higher in lung homogenates obtained from female mice compared to male mice ($n=4$). No gender specific differences were seen in either the liver or kidney homogenates ($n=2-4$).

doi:10.1371/journal.pone.0014007.t002

activity of eNOS [19,20]. Consistent with this observation, lung homogenates from female mice contained greater eNOS protein expression when compared to lung homogenates from male mice (Figure 3A). Increases in NOS activity are associated with increased formation of S-nitrosothiols. To determine if the increase in GSNO R activity in the lungs of female animals is due to estrogen induced increases in eNOS activity, murine pulmonary endothelial cells isolated from female mice were treated with 10 nM estrogen in the absence or presence of L-NAME. Estrogen increased the level of S-nitrosylated GSNO R compared to control cells (Figure 3B). This increase was abrogated in the presence of L-NAME. To further confirm the effects of eNOS on the activity of GSNO R, GSNO R activity was examined in lung homogenates of eNOS deficient (eNOS^{-/-}) mice using the modified Saville Assay (Figure 4A). Consistent with a role for eNOS in regulating the activity of GSNO R, GSNO R

Table 3. Comparison of Methods used to Measure NADH-Dependent GSNO-R Activity.

Gender	[GSNO] μM	GSNO-R activity $\mu\text{M}/\text{min}/\text{mg}$ protein		Protein precipitation	Female:Male ratio
		$\mu\text{M}/\text{min}/\text{mg}$	protein		
Female	28	5.01+/ 1.51	N		
Male	28	2.37+/ 0.35	N		2.11
Female	28	3.94+/ 1.52	Y		
Male	28	1.16+/ 0.33	Y		3.40
Female	100	8.41+/ 2.69	N		
Male	100	3.06+/ 0.52	N		2.75
Female	100	5.32+/ 1.06	Y		
Male	100	2.56+/ 0.20	Y		2.07

Lungs were harvested from adult (10-12 w) C57Bl6/129SeEv mice. Lung homogenates were subjected to NADH dependent GSNO R activity. The assay was performed as described in Methods. The effect of altering the concentration of GSNO in the assay and the precipitation of protein prior to measurement were compared in the same samples ($n=4$). Note that higher activity was obtained in the absence of protein precipitation for both GSNO concentrations. Highest GSNO R activity was obtained in the presence of 100 μM GSNO. GSNO R activity was found to be 2-3 fold higher in the lung homogenates from female animals regardless of the method used to measure activity.

doi:10.1371/journal.pone.0014007.t003

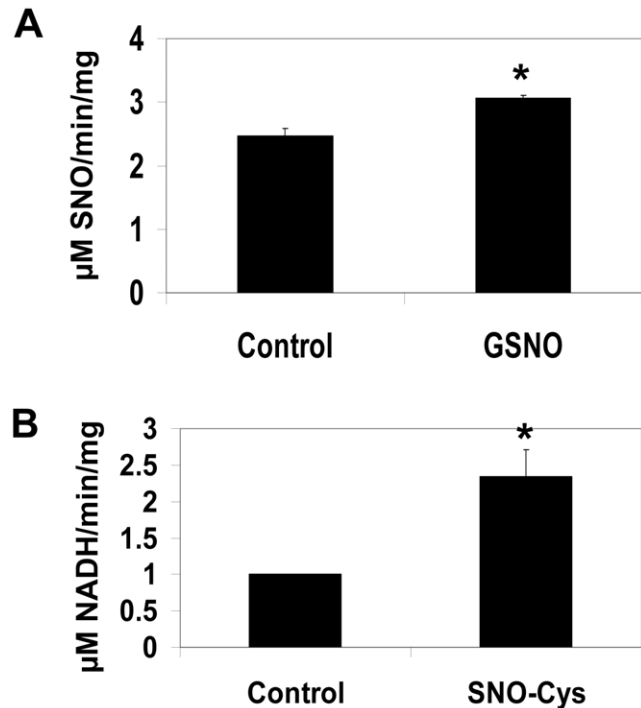


Figure 2. S-nitrosoglutathione activates GSNO R. (A) Primary mouse lung endothelial cells were treated with 10 μM GSNO for 5 min and the activity of GSNO R determined using a modified Saville Assay using 28 μM GSNO. GSNO R activity was significantly increased after treatment of GSNO. ($n=3$, $p<0.011$). (B) Cell lysates obtained from mouse lung endothelial cells were treated with or without 5 μM L-SNO cysteine for 5 min. GSNO R activity was measured by L-SNO cysteine dependent NADH consumption. L-SNO Cysteine resulted in a 2 fold increase in NADH consumption ($n=4$, $p<0.011$).

doi:10.1371/journal.pone.0014007.g002

activity was found to be reduced by approximately 50% in eNOS^{-/-} animals compared to wild type control animals. The reduction in GSNO R activity was not mediated by a decrease in GSNO R expression (Figure 4B).

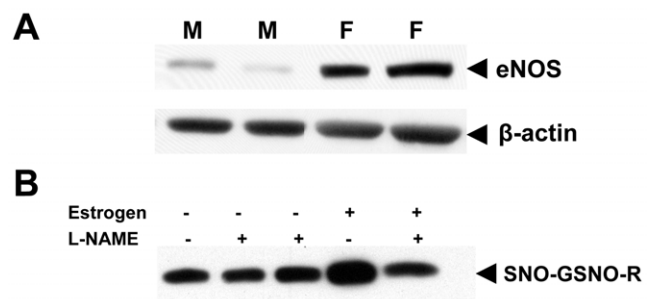


Figure 3. Estrogen Activation of GSNO R is eNOS dependent. (A) Abundance of eNOS present in lung homogenates from male and female C57Bl6/129SeEv mice was determined by Western blot analysis using antibodies directed against eNOS and β -actin. eNOS protein levels were greater in lung homogenates of female animals. (B) Mouse lung endothelial cells isolated from female mouse lungs were treated with or without 10 μM estrogen in the presence or absence of 100 μM L-NAME for 4 h. Estrogen resulted in an increase in GSNO R S-nitrosylation. The increased in GSNO R S-nitrosylation was abrogated by pretreatment with L-NAME.

doi:10.1371/journal.pone.0014007.g003

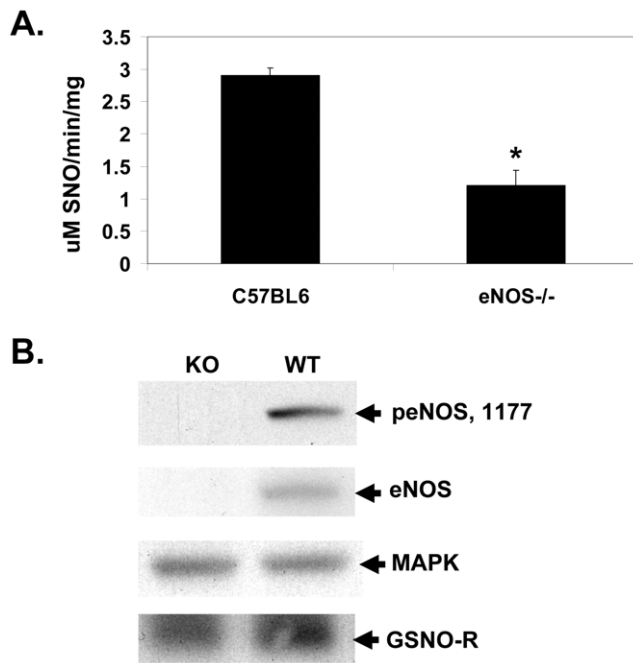


Figure 4. eNOS is required for GSNO R activity. (A) GSNO R activity was measured in the lung homogenates obtained from eNOS^{-/-} and wild type (C57BL6) mice using a modified Saville Assay using 28 μ M GSNO with no protein precipitation. GSNO R activity was reduced by 50% in the eNOS^{-/-} lung homogenate compared to that seen in the wild type mice (n = 5–6, p < 0.002). (B) Western blot analysis of GSNO R protein present in wild type (C57BL6) and eNOS^{-/-} mouse lungs. No significant differences were detected in GSNO R protein levels (n = 3). doi:10.1371/journal.pone.0014007.g004

Female mice are protected from increases in right ventricular weight and right ventricular pressure with NAC

NAC was found to increase right ventricular pressure and right ventricular weight in C57BL6/129SEV male mice in a manner that was indistinguishable from that induced by hypoxia [11]. Published data indicate that female gender is less susceptible to hypoxia induced PH [21–23]. To determine if the female gender is less susceptible to NAC induced PH, C57BL6/129SvEv mice were subjected to normoxia, 10 mg/ml NAC, 1 mg/ml SNOAC, or hypoxia for a period of three weeks [11]. In contrast to the male animals [11], the female animals responded with increases in right heart weight and right ventricular pressure only after treatment with SNOAC and hypoxia (Figure 5A, B).

Serum SNOAC levels are greater in male mice

NAC is S-nitrosylated forming SNOAC in the plasma [11]. To examine the relative levels of SNOAC present in the plasma in male and female animals, blood was harvested from the right ventricle of NAC treated mice and SNOAC levels determined by mass spectroscopy. The level of SNOAC found in the plasma of NAC treated female animals was significantly less than SNOAC levels found in the plasma obtained from NAC treated male animals (Figure 6). None the less, exogenous administration of SNOAC still resulted in increases in right ventricular pressure and right ventricular weight characteristic of PH (Figure 5). In contrast, analysis of the total amount of endogenously produced S-nitrosothiols in whole blood taken from the left ventricle of untreated male and female mice demonstrate no significant differences in the levels of S-nitrosothiols (Table 4).

Castration increases GSNO-R activity and protects males from NAC-induced pathology

Male animals develop PH when exposed to chronic systemic administration of NAC [11]. To determine if sex hormones influence the ability of NAC to induce changes in right ventricular weight and right ventricular pressure in mice, the pulmonary effects of NAC were examined in castrated mice (Figure 7A, B). Analysis of right ventricular weight and right ventricular pressure in the castrated animals show no significant difference between in gonad intact and castrated animals under untreated conditions. However, castrated animals were protected from the increases in right ventricular weight and right ventricular pressure in response to NAC. Castration was accompanied by an increase in GSNO R activity compared to the gonad intact animals as measured by LC/MS (Figure 8A). The increase in GSNO R activity was not mediated by increases in GSNO R protein expression (Figure 8B), but to changes in GSNO R S-nitrosylation (Figure 8C). Moreover, GSNO R activity in the castrated animals was comparable to that seen in female animals. It should be noted that eNOS phosphorylation at serine 1177 in castrated animals was elevated compared to gonad intact animals (Figure 8B). To further evaluate the role of androgens in the activation of GSNO R, eNOS^{-/-} animals were castrated and the activity of GSNO R was evaluated using a modified Saville Assay. Surprisingly, GSNO R activity in eNOS^{-/-} castrated animals was significantly increased compared to eNOS^{-/-} gonad intact animals (Figure 9) suggesting the presence of an eNOS independent androgen mediated effect on GSNO R activity.

Discussion

Cysteine S-nitrosylation/de-nitrosylation is a regulated process in normal physiology which has parallels to the protein kinase/phosphatase system [1]. All NOS isoforms as well as other proteins have been shown to cause formation of S-nitrosothiol bonds on specific cysteine residues in co-localized proteins and/or cellular peptides. Likewise, specific enzymes and other proteins are responsible for de-nitrosylating these cysteine residues, particularly downstream of transnitrosation reactions between S-nitrosylated proteins and glutathione. One de-nitrosylating enzyme is S-nitrosogluthathione reductase (GSNO R), a ubiquitously expressed NADH dependent enzyme. GSNO R has been shown to be necessary for a variety of effects ranging from the nitrosylation of G protein coupled receptor kinases to cellular protection from pathological nitrosative stress [1]. GSNO R activity in this manuscript was measured by LC/MS, GSNO dependent NADH consumption, and modified Saville Assay (Tables 1,2,3). Regardless of the method used to measure GSNO R activity, GSNO R activity was found to be approximately 2–3 fold higher in the lung homogenates obtained from female animals. In contrast, lung homogenates obtained from sexually immature mice did not demonstrate any gender specific differences in GSNO R activity. Moreover, the gender dependent effects on GSNO R activity appear to be specific for the lung as GSNO R activity in kidney and the liver homogenates were not seen. The data, taken together, strongly suggests gender, most likely through the influence gonadal steroids, influences the activity of GSNO R in the lung.

High dose, long term systemic treatment with NAC causes PH in male mice by conversion to SNOAC resulting in the upregulation of hypoxia regulated genes [11]. This effect is eNOS dependent as eNOS^{-/-} mice are completely protected [11]. In this report, we demonstrate: 1) NAC treatment results in lower plasma SNOAC levels in female mice than in male mice,

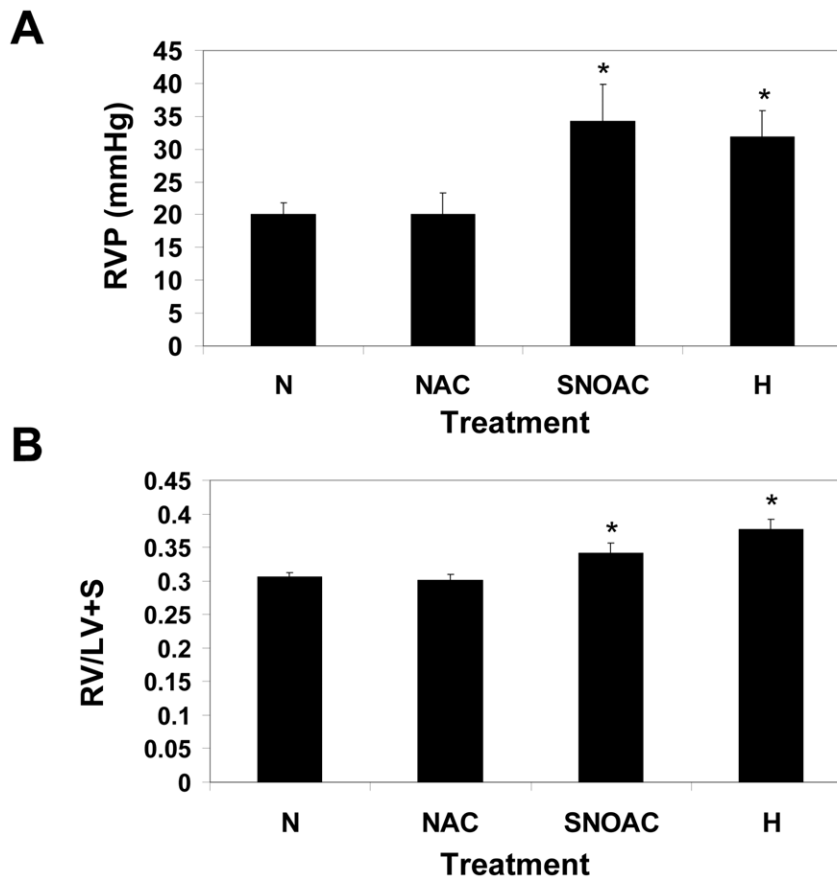


Figure 5. Female C57BL6/129SvEv mice do not develop PH with chronic, systemic administration of N acetyl cysteine. C57BL/129SvEv mice were untreated (N) or treated with 10 mg/ml NAC (NAC), 52 mM SNOAC (SNOAC) or hypoxia (H) for a period of 3 weeks. (A) Right ventricular pressure (RVP) and (B) right heart weight (expressed as right ventricular weight/left ventricular weight + septum weight (RV/LV+S)) were determined. Female mice responded to only to SNOAC and hypoxia. * ($n = 19-25$, $p < 0.05$). doi:10.1371/journal.pone.0014007.g005

despite increased eNOS expression and 2) female mice exposed to long term NAC treatment do not develop PH in contrast to male mice. We hypothesize that in vivo, females might be protected against eNOS dependent nitrosative stress through the actions of GSNO R. This GSNO R based protection can be overwhelmed by chronic high dose systemic SNOAC treatment or by chronic hypoxia.

Female rats [21,22] and swine [23] have been shown to develop less severe PAH in response to chronic hypoxia compared to males. Sex hormones may be involved in mediating this gender dependent difference. Estrogen receptors are present in the rat [24] and human lung [25]. Female animals produce more estrogen which is known to enhance the vascular expression and activity of eNOS [22,25]. This increase in eNOS protein/activity levels is thought to be responsible for the protective effects on the vasculature. In support of this concept, estrogens have been shown to attenuate the severity of PH in rats [22], although the mechanism by which this occurs does not appear to be associated with alterations in eNOS expression [22]. Theoretically, increased eNOS levels produce an increase in S nitrosylated proteins. Thus, GSNO R might protect against nitrosative stress, which would be anticipated to be greater in female mice than in males because of the estrogen mediated increase in eNOS activity. In this report, GSNO R activity is, indeed, higher in the female mouse lung when compared to the male. Surprisingly, this difference was not

driven by a difference in protein expression, but rather by a difference in activity.

Analysis of S nitrosothiol levels in the serum of untreated normal male and female mice indicate no significant differences in S nitrosothiol levels, suggesting that the formation and catabolism of S nitrosothiols is balanced in healthy untreated animals. Because eNOS activity is elevated in the female mouse lung, it is possible that GSNO R opposes protein S nitrosylation by eNOS through its de nitrosylating activity. Thus, the increased eNOS activity present in the female mouse lung might lead to the increased GSNO R activity as a counter regulatory mechanism to minimize nitrosative stress. Indeed, in vitro treatment of endothelial cells with GSNO increases GSNO R activity through S nitrosylation. This appears to be confirmed in vivo as eNOS⁷ mice (reduced S nitrosothiol formation) have decreased GSNO R activity which is not due to decreased expression. Moreover, in other maladies, there is evidence for gender discordance in GSNO R expression and/or activity. For instance, gastric activity of GSNO R may be a component of the enhanced vulnerability of women to develop alcohol related diseases [8]. Likewise, gender differences seen in the LPS model of septic shock are eliminated in GSNO R knockout mice [4]. However, the gender dependent differences in GSNO R activity in the pulmonary vasculature and the influence this may have on the gender predilection of pulmonary diseases, such as PH have not been examined.

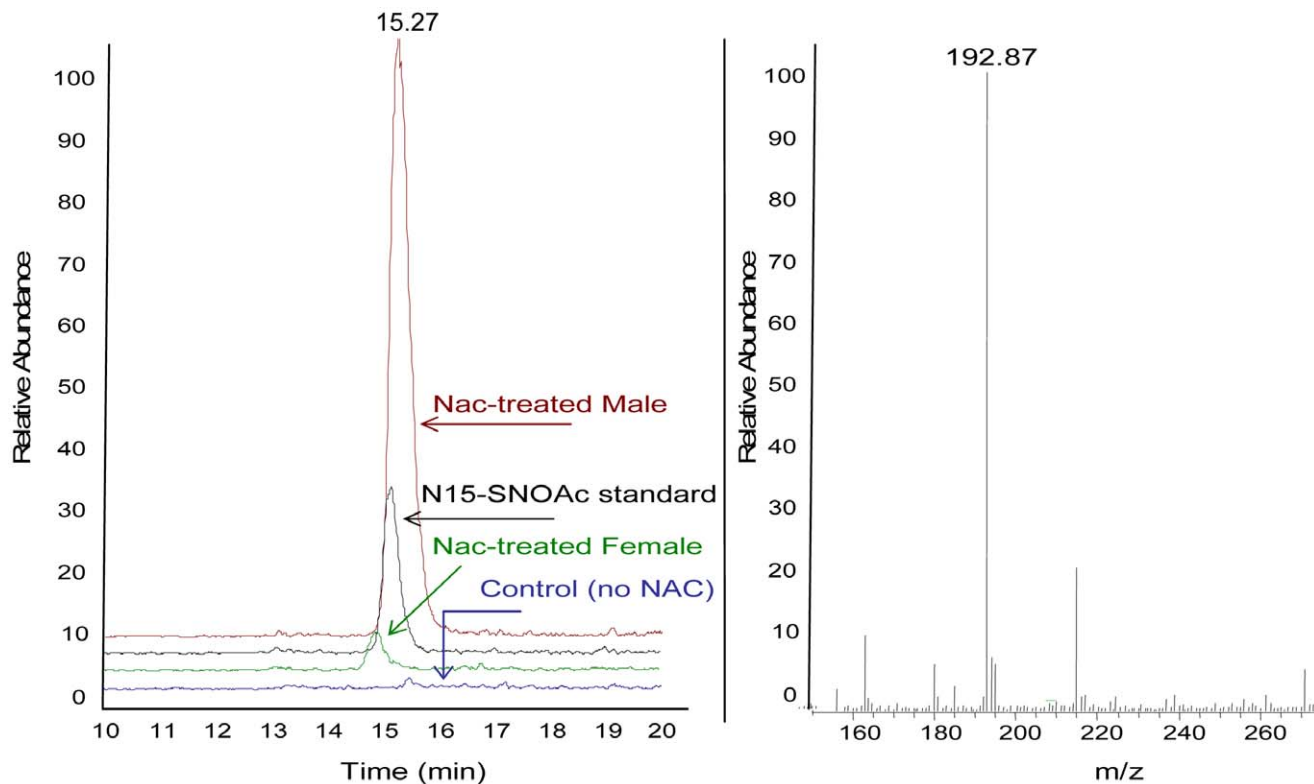


Figure 6. Serum SNOAC levels are lower in female mice. Serum SNOAC was measured by mass spectrometry (MS) in C57BL6/129SvEv male and female mice treated with NAC. Left panel = LC chromatogram; Right panel = MS spectrum. Serum from NAC treated male (red) and female (green) mice had a SNOAC peak (m/z 193) that co migrated with the ^{15}N SNOAC standard (black). No signal was seen in non treated mice (blue). The amount of SNOAC was less in the female mice. doi:10.1371/journal.pone.0014007.g006

The data suggest that androgens may also have a role in regulating the activity of GSNO R. Specifically, castration increases GSNO R activity to a level similar to that seen in female mice. This increase does not appear to be due to increases in protein expression but again reflects increases in GSNO R S nitrosylation. Moreover, the resulting increase in GSNO R activity correlates with protection from NAC induced PH. The mechanism by which androgens activate GSNO R is not yet known. The data indicate, on one level, castration increases the expression and activity of eNOS, consistent with the observation that eNOS^{-/-} mice have reduced GSNO R activity. It also suggests that androgens decrease the expression and activity of eNOS within the pulmonary vasculature. However, the effects of androgens on eNOS expression and activity are in contrast to published data. For instance, in the aorta, androgens have been reported to activate eNOS through a non genomic pathway mediated by cSrc, PI3K and Akt [26,27]. Moreover, male androgen receptor knockout mice show decreased aortic eNOS expression and phosphorylated eNOS compared to wild type mice [28]. Lastly, neither androgen receptors nor nitric oxide are involved in the vasodilatory actions in the pulmonary vasculature in response to acute administration of testosterone, a major androgen produced in the testes [29]. The reasons for these discrepancies are unclear, but may be due to the vascular bed studied, or differences mediated by chronic versus acute effects of androgens. On a second level, studies examining the activity of GSNO R in castrated eNOS^{-/-} mice demonstrate an increase in GSNO R activity with castration in the absence of eNOS, suggesting that androgens have a separate eNOS independent mechanism by which they alter GSNO R activity. Thus, it is possible that the net effect in females in GSNO R activity

is increased, in part, through S nitrosylation by eNOS as well as by the absence of what appears to be a distinct, androgen dependent effect.

In the pulmonary vascular bed, evidence has emerged for the following paradigm: increased delivery of nitrosothiols to the pulmonary vascular bed results in the activation of hypoxia related gene regulatory proteins including specificity proteins and hypoxia inducible factor 1 through S nitrosylation reactions [11]. Down stream, this effect results in the upregulation of hypoxia regulated genes, leading to cellular and morphologic changes characteristic of PH. Thus, excessive S nitrosothiol delivery in the pulmonary vasculature recapitulates hypoxia. To some extent, this paradigm can provide insight into PH of diverse causes: 1) hypoxia results in transnitrosation from deoxyhemoglobin to glutathione and other thiols in the systemic periphery which then return in erythrocytes and plasma and are dumped into the pulmonary vascular bed

Table 4. SNO/Hb levels are similar in untreated Male and Female C57BL6/129SvEv Mice.

Gender	SNO/Hb
Male	$7.75 \times 10^{-5} \pm 2.49 \times 10^{-5}$
Female	$8.75 \times 10^{-5} \pm 1.50 \times 10^{-5}$

Left ventricular blood was collected from male (n=4) and female (n=4) mice and subjected to reductive chemiluminescence in the presence of carbon monoxide (3C assay). SNO values were normalized to hemoglobin content. doi:10.1371/journal.pone.0014007.t004

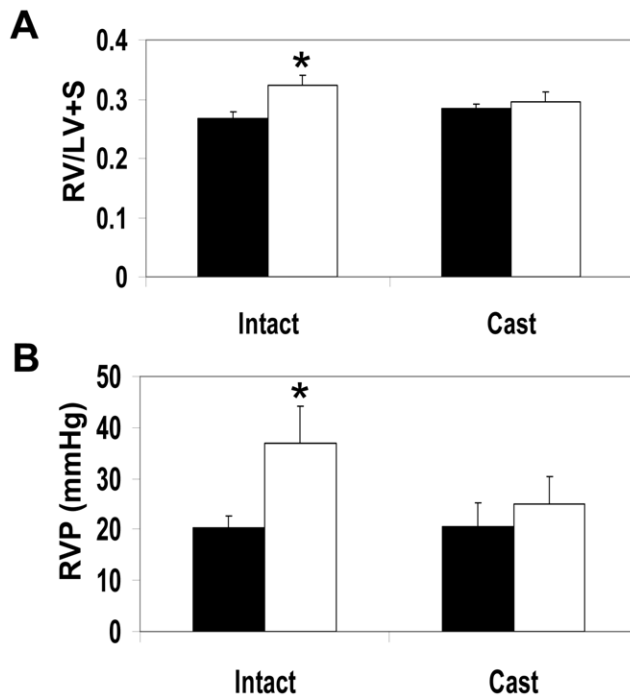


Figure 7. Castration increases GSNO R activity, protecting against NAC induced increases in right heart weight and ventricular pressure. Male C57BL6/129SvEv mice with either intact gonads or castrated were treated with (white bars) or without NAC (black bars) for 3 weeks. (A) RVW and (B) RVP were measured. Castration eliminated the increase in both RVW and RVP (N=11 intact, N=10 castrated, $p < 0.001$). doi:10.1371/journal.pone.0014007.g007

causing PH by activating hypoxia responsive genes; 2) to the extent that normal levels of deoxygenation increase systemic vascular S nitrosothiols, a tripling of venous return in high flow states triples the burden of S nitrosothiols returning to the lung, perhaps explaining high flow state induced PH; 3) systemic inflammation can increase erythrocytic S nitrosothiol load, contributing to the risk of PH seen in systemic inflammation. Note the paradox: S nitrosothiols delivered acutely to the pulmonary vascular bed are vasodilators and will reverse PH; whereas, chronic exposure of the pulmonary vascular bed to S nitrosothiols gradually causes pulmonary vascular remodeling and chronic pulmonary hypertension. If increased GSNO R activity in female mice can protect against the adverse affects of nitrosative stress associated with eNOS activation, chronic inflammation, chronic hypoxemia and high flow states, why are female humans at higher risk for the development of PH from a variety of causes than are males? The answer may lie in GSNO R itself. In the absence of androgens and in the presence of eNOS activation, increased GSNO R activity is protective. However, this system leaves females particularly vulnerable to GSNO R dysfunction. For example, if there is decreased GSNO R activation by eNOS or an androgen mimetic effect to decrease GSNO R activity in the female pulmonary vascular endothelium, by virtue of increased eNOS activity and the resulting chronic nitrosative stress, females will be at increased risk for hypoxia mimetic pulmonary vascular remodeling. Indeed, there are single nucleotide polymorphisms resulting in increased or decreased GSNO R activity that appear to be associated with both increased and decreased asthma risk respectively [30]. These data suggest that future studies regarding

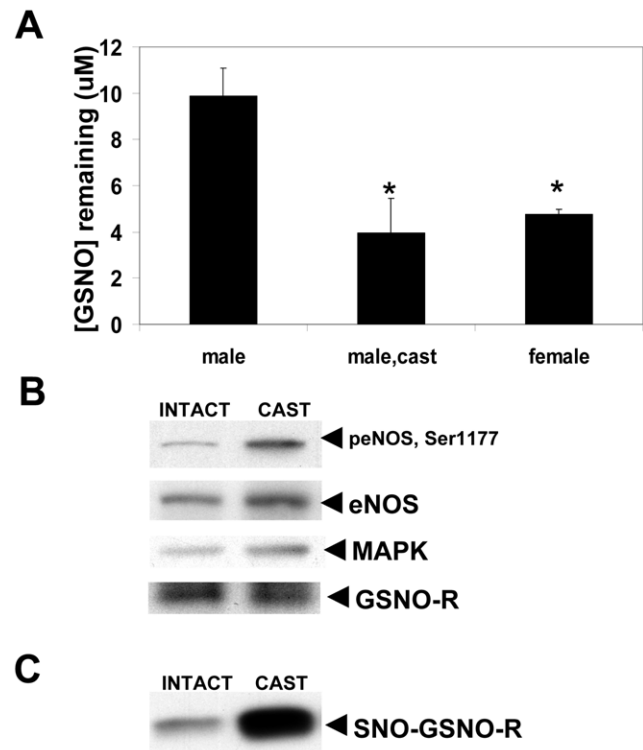


Figure 8. Castration increases GSNO R S nitrosylation and activity. (A) Castrated mice show an increase in GSNO R activity compared to the male gonad intact animals. It should be noted that the levels of GSNO R activity seen in the castrated mice is similar to that seen in the female mice. The data are presented as the amount of GSNO remaining after 5 min as determined by LC/MS. (B) GSNO R protein expression in gonad intact and castrated animals was determined by western blot. No differences in GSNO R protein expression were seen in the intact or castrated animals. (C) S nitrosylated GSNO R (SNO GSNO R) was determined by biotin switch followed by western blot analysis using anti GSNO R antibodies. S nitrosylated GSNO R levels were elevated in the castrated animals. doi:10.1371/journal.pone.0014007.g008

GSNO R expression, genetics and activity in the lungs of women with PH may be worthwhile.

In summary, GSNO R activity is increased post translationally in the female murine lung. This observation is important because

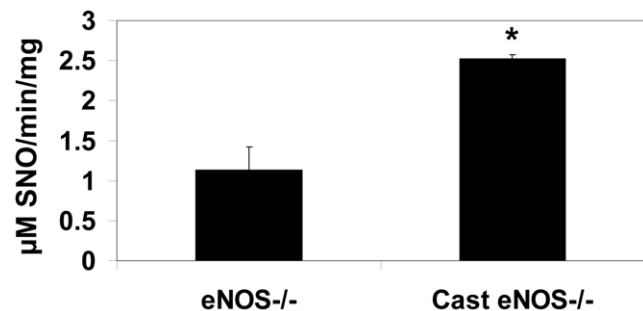


Figure 9. Androgen mediated increases in GSNO R activity are eNOS independent. GSNO R activity was measured in lung homogenates obtained from gonad intact and castrated eNOS^{-/-} mice. Castration resulted in a significant increase in GSNO R activity as measured by modified Saville Assay using 28 μ M GSNO with no protein precipitation. (n=6 intact, n=4 castrated, $p < 0.038$). doi:10.1371/journal.pone.0014007.g009

it suggests that GSNO R can protect against chronic nitrosative stress associated with increased eNOS expression in female mice. This may be particularly important in protecting against the high flow state and chronic eNOS upregulation associated with mammalian pregnancy [31,32]. In addition, it may also help to explain why females, in general, are more tolerant of high altitude living than males [33,34]. However, an extension of these murine results to human studies has not yet been undertaken.

Materials and Methods

Materials

All chemical reagents used in the studies were obtained from Sigma Chemical Company (St. Louis, MO) unless otherwise stated.

Animals

All procedures in the treatment and care of the animals used in this study were approved by the Animal Care and Use Committee at the University of Virginia. Female C57BL6/129SvEv mice (10–12 w) were exposed to normoxia, 52 mM N acetyl cysteine, 1 mM S nitrosylated N acetyl cysteine, or 10% oxygen for 3 weeks as previously described [11]. Castrations were performed when animals reached 3 w of age. All animals were anesthetized using interperitoneal injection of ketamine/xylazine (60/80/5–10 mg/kg) prior to the procedure. In addition, the surgical site was made aseptic using betadine solution and 70% ethyl alcohol. Local anesthesia at the incision site was by infiltration of 0.1 ml 0.25% bipivacaine. For castration, a small incision was made at the tip of the scrotum. The tunic opened and the testis, cauda epididymis, vas deferens and the spermatic blood vessels exteriorized. The blood vessels and the vas deferens were cauterized and the testis and epididymis removed. The remaining tissue was returned into the sac and the procedure repeated for the other testis. The skin incision was closed with Nexaband. Mice are kept warm after surgery until they are responsive to stimuli and monitored until they can completely right themselves on their own. Right ventricular pressure was measured in anesthetized mice using a 1.4 F Millar catheter/transducer as previously described [11]. Right heart hypertrophy was measured as a ratio of the weight of the right ventricle/weight of the left ventricle + septum.

Measurement of S-nitrosogluthathione reductase activity

LC/MS: Lung homogenate (0.25–0.5 µg) in homogenation buffer was incubated with GSNO (28 µM) and 2 mM GSH in the presence or absence of 300 µM NADH at 37°C for 5 minutes. Protein was precipitated from the reaction using 8% trichloroacetic acid. HPLC analysis was performed on a Waters 2695 separation module using a Waters Symmetry C8 (2.1×150 mm) column. GSNO analytes were eluted using an isocratic method of 95% formic acid (0.1%) in water and 5% methanol. Mass spectrometry was performed using a Finnigan LCQ ion trap mass spectrometer equipped with an electrospray ionization source. Data were collected in positive ion mode with selective ion monitoring at *m/z* 336.5–337.5 and quantified against GS¹⁵NO cations *m/z* 337.5–338.5. Integrated peak areas were determined using Xcalibur software. GSNO dependent NADH Consumption [35]: Cell lysate (0.3 µg/ml) was incubated with 75 µM NADH in reaction buffer (20 mM Tris HCL pH 8.0 and 0.5 mM EDTA containing 0 or 100 µM GSNO at room temperature. NADH fluorescence (absorption at 340 nm and emission at 455 nm) was measured over time in a FLUOstar Omega (BMG Labtech, Offenburg, Germany). Concentration of

NADH was determined from a standard curve. Modified Saville Assay: GSNO R activity was measured by modified Saville Assay. Briefly, 250 µg of cell lysate or lung homogenate was incubated in the absence or presence of 300 µM NADH, in the presence of 2 mM GSH and 28 µM or 100 µM GSNO. Assay was performed with and without protein precipitation (Table 3). Two aliquots of 75 µl were placed into a 96 well plate at 1 min intervals for a total of 5 min. One aliquot was placed with 75 µl of (+) reagent (58 mM Sulfanilamide +7.36 mM HgCl₂ in 1 N HCl) while the second aliquot was placed with () reagent (58 mM Sulfanilamide in 1 N HCl). Samples were incubated 5 min in the dark. At the end of this incubation, 75 µl of (N) reagent (0.77 M n(1 naphthyl) ethylene diamine dihydrochloride) was added. Samples were incubated 5–10 min for color to develop. Absorbance was read at 540 nm. Amount of GSNO remaining in the reaction was determined from a GSNO standard curve. Activity was obtained from the slope of the time course divided by the amount of protein in the reaction.

Measurement of S-nitroso-N-acetyl cysteine (SNOAC)

The abundance of SNOAC was determined by liquid chromatography/mass spectroscopy as previously described [11].

Immunoprecipitation

Cell lysate or lung homogenate (100–300 µg) prepared in lysis buffer (20 mM Tris pH 7.6, 150 mM NaCl, 2 mM EDTA, 10% glycerol 1% Triton X 100 +1X proteinase inhibitors) were immunoprecipitated using 4 µg anti eNOS antibody (BD Biosciences, San Diego) overnight at 4°C on a rotator. Samples were incubated with 100 µl protein A agarose beads (Roche Diagnostics, Mannheim, Germany) for 2–4 hours at 4°C. At the end of the incubation, the agarose beads were spun at 3000×g for 1 min and washed three times with lysis buffer. Protein was eluted from the protein A agarose beads by incubation with 50 µl SDS loading buffer.

Biotin-Switch

The biotin switch procedure for the identification of S nitrosothiols was performed to identify S nitrosylated proteins [36]. Briefly, cell lysate or lung homogenate (100–300 µg) were precipitated using acetone and resuspended in 100 µl HEN Buffer (250 mM HEPES pH 7.7, 1 mM EDTA, 0.1 mM neocuproine). Samples were mixed with 4 volumes Blocking Buffer (9 vol HEN+1 vol 25%SDS containing 20 mM MMTS) and incubated at 50°C for 20 min with shaking. Protein was precipitated by acetone, resuspended in HEN Buffer containing 1 mM Biotin HPDP (Pierce) and 1 mM ascorbate and incubated for 1 h at room temperature. Biotin HPDP was removed by precipitation with acetone and pellet resuspended in 100 µl HEN buffer. Resuspended sample was neutralized using Neutralization Buffer (20 mM HEPES pH 7.7, 10 mM NaCl, 1 mM EDTA, 0.5% Triton X 100.) Biotinylated proteins were isolated by incubation with Streptavidin agarose for 1 h at room temperature. Resin was washed 5 times with Neutralization Buffer containing 600 mM NaCl and biotinylated protein eluted with 50 µl 2X SDS PAGE Loading Buffer.

Western Blot analysis

Proteins were separated on a 10% polyacrylamide gel as previously described [11]. Proteins were transferred to Immobilon P transfer membranes (Billerica, MA) and signal detected using SuperSignal West Pico Chemiluminescent Substrate (Thermo Scientific, Rockford, IL).

Statistics

All data will be expressed as the mean \pm SEM. All statistical analysis was performed using Sigma Stat software. Data comparing 2 groups were analyzed using a paired T test, with $p < 0.05$ considered significant. Data comparing more than one group will be analyzed by one way ANOVA. Significance was determined using the Holm Sidak post hoc test with $p < 0.05$ considered significant.

References

1. Benhar M, Forrester MT, Stamler JS (2009) Protein denitrosylation: enzymatic mechanisms and cellular functions. *Nature Reviews* 10: 721–732.
2. Angelo M, Singel DJ, Stamler JS (2006) An S-nitrosothiol (SNO) synthase function of hemoglobin that utilizes nitrite as a substrate. *Proc Natl Acad Sci USA* 103: 8366–8371.
3. Gaston B, Singel D, Doctor A, Stamler JS (2006) S-nitrosothiol signaling in respiratory biology. *Am J Respir Crit Care Med* 173: 1186–93.
4. Haqqani AS, Do SK, Birnboim HC (2003) The role of a formaldehyde dehydrogenase-glutathione pathway in protein S-nitrosylation in mammalian cells. *Nitric Oxide* 9: 172–181.
5. Liu L, Hausladen A, Zeng M, Que L, Heitman J, et al. (2001) A metabolic enzyme for S-nitrosothiol conserved from bacteria to humans. *Nature* 410: 490–494.
6. Liu L, Yan Y, Zeng M, Zhang J, Hanes MA, et al. (2004) Essential role of S-nitrosothiols in vascular homeostasis and endotoxic shock. *Cell* 116: 617–628.
7. Foster MW, Hess DT, Stamler JS (2009) Protein S-nitrosylation in health and disease: a current perspective. *Trends in Molecular Medicine* 15: 391–404.
8. Zaman K, McPherson M, Vaughn J, Hunt J, Mendes F, et al. (2001) S-nitrosoglutathione increases cystic fibrosis transmembrane regulator maturation. *Biochemical and Biophysical Res Communication* 284: 65–70.
9. Zaman K, Carraro S, Doherty J, Henderson EM, Lendermon E, et al. (2006) A novel class of compounds that increase CFTR expression and maturation in epithelial cells. *Mol Pharm* 70: 1435–42.
10. McMahon TJ, Ahearn GS, Moya MP, Gow AJ, Huang YC, et al. (2005) A nitric oxide processing defect of red blood cells created by hypoxia: deficiency of S-nitrosohemoglobin in pulmonary hypertension. *Proc Natl Acad Sci USA* 102: 14801–6.
11. Palmer LA, Doctor A, Chhabra P, Sheram ML, Laubach VE, et al. (2007) S-nitrosothiols signal hypoxia-mimetic vascular pathology. *J Clin Invest* 117: 2592–601.
12. Que LC, Liu L, Yan Y, Whitehead GS, Gavel T, et al. (2005) Protection from experimental asthma by an endogenous bronchodilator. *Science* 308: 1618–1621.
13. Que LG, Yang Z, Stamler JS, Lugogo NL, Kraft M (2009) S-nitrosoglutathione reductase: an important regulator in human asthma. *Am J Respir Crit Care Med* 180: 226–31.
14. Carey MA, Card JW, Voltz JW, Arbes SJ, Jr., Germolec DR, et al. (2007) It's all about sex: gender, lung development and lung disease. *Trends in Endocrinology and Metabolism* 18: 308–313.
15. Skobeloff EM, Spivey WH, St. Clair SS, Schoffstall JM (1992) The influence of age and sex on asthma admissions. *JAMA* 268: 3437–40.
16. Bonner JR (1984) The epidemiology and natural history of asthma. *Clin Chest Med* 5: 557–65.
17. Martin AJ, McLennan LA, Landau LI, Phelan PD (1980) The natural history of childhood asthma to adult life. *Br Med J* 280: 1397–400.
18. Baraona E, Abittan CS, Dohmen K, Moretti M, Pozzato G, et al. (2001) Gender differences in pharmacokinetics of alcohol. *Alcohol Clin Exp Res* 25: 502–7.
19. Goetz RM, Thatte HS, Prabhakar P, Cho MR, Michel T, et al. (1999) Estradiol induces the calcium-dependent translocation of endothelial nitric oxide synthase. *Proc Natl Acad Sci USA* 96: 2788–2793.
20. Chambliss KL, Shaul PW (2002) Estrogen modulation of endothelial nitric oxide synthase. *Endocrine Reviews* 23: 665–686.
21. Rabinovitch M, Gamble WJ, Miettinen OS, Reid L (1981) Age and sex influence on pulmonary hypertension of chronic hypoxia and on recovery. *Am J Physiol* 240: 62–72.
22. Resta TC, Kanagy NL, Walker BR (2001) Estradiol-induced attenuation of pulmonary hypertension is not associated with altered eNOS expression. *Am J Physiol* 280: 88–97.
23. McMurtry IF, Frith CH, Will DH (1973) Cardiopulmonary responses of male and female swine to simulated high altitude. *J Appl Physiol* 45: 459–462.
24. Morishige WK, Uctake CA (1978) Receptors for androgen and estrogen in the rat lung. *Endocrinology* 102: 1827–37.
25. Chen Z, Yuhanna IS, Galcheva-Bargova Z, Karas RH, Mendelsohn ME, et al. (1999) Estrogen receptor alpha mediates nongenomic activation of eNOS by estrogen. *J Clin Invest* 103: 401–6.
26. Baron S, Manin M, Beaudoin C, Leotoing L, Communal Y, et al. (2004) Androgen receptor mediates non-genomic activation of phosphatidylinositol-3-OH kinase in androgen sensitive epithelial cells. *J Biol Chem* 279: 14579–14586.
27. Bai CX, Kurokawa J, Tamagawa M, Makaya H, Furukawa T (2005) Nontranscriptional regulation of cardiac repolarization current by testosterone. *Circulation* 112: 1701–1710.
28. Ikeda Y, Akhara K-I, Yoshida S, Sato T, Yagi S, et al. (2009) Androgen-androgen receptor system protects against angiotensin II induced vascular remodeling. *Endocrinology* 150: 2857–2864.
29. Smith AM, Jones RD, Channer KS (2006) The influence of sex hormones on pulmonary vascular reactivity: possible vasodilator therapies for the treatment of pulmonary hypertension. *Current Vascular Pharmacology* 4: 9–15.
30. Wu H, Romieu I, Siemra-Monge J-J, del Rio-Nararro BE, Anderson DM, et al. (2007) Genetic variation in S-nitrosoglutathione reductase (GSNOR) in childhood asthma. *J Allergy Clin Immunol* 120: 322–8.
31. Gaston B, Fry E, Sears S, Heroman WM, Ignarro L, Stamler JS (1998) Umbilical arterial S-nitrosothiols in stressed newborns: Role in perinatal circulatory transition. *Biochemical and Biophysical Research Communications* 253: 899–901.
32. Funai EF, Davidson A, Seligman SP, Finley TH (1997) S-nitrosohemoglobin in the fetal circulation may represent a cycle for blood pressure regulation. *Biochemical and Biophysical Research Communications* 239: 875–877.
33. Beall CM, Song K, Elston RC, Goldstein MC (2004) Higher offspring survival among Tibetan women with high oxygen saturation genotypes residing at 4,000 m [Multicenter Study]. *Proc Natl Acad Sci USA* 101: 14300–14304.
34. Beall CM, Decker MJ, Brittenham GM, Kushner I, Gebremedhin A, et al. (2002) An Ethiopian pattern of human adaptation to high-altitude hypoxia. *Proc Natl Acad Sci USA* 99: 17215–17218.
35. Wei W, Li B, Hanes MA, Kadar S, Chen X, Liu L (2010) S-nitrosylation from GSNOR deficiency impairs DNA repair and promotes hepatocarcinogenesis. *Sci Transl Med* 2: 19ra13.
36. Jaffrey SR, Erdjument-Bromage H, Ferris CD, Tempst P, Snyder SH (2001) Protein S-nitrosylation: a physiological signal for neuronal nitric oxide. *Nature Cell Biol* 3: 193–97.

Acknowledgments

We would like to thank Dr. Ben Gaston and Dr. Steve Lewis for comments and critical review of the manuscript and Dr. Loretta Que for providing the initial GSNO R antibody used in the initiation of these studies.

Author Contributions

Performed the experiments: KBS KdR SY LAP. Analyzed the data: KBS KdR SY LAP. Wrote the paper: KBS LAP. Involved in revising the paper: KdR SY.

Arteriosclerosis, Thrombosis, and Vascular Biology

JOURNAL OF THE AMERICAN HEART ASSOCIATION

American Heart
Association®



Learn and Live SM

Compartmentalized Connexin 43 S-Nitrosylation/Denitrosylation Regulates Heterocellular Communication in the Vessel Wall

Adam C. Straub, Marie Billaud, Scott R. Johnstone, Angela K. Best, Sean Yemen,
Scott T. Dwyer, Robin Looft-Wilson, Jeffery J. Lysiak, Ben Gaston, Lisa Palmer and
Brant E. Isakson

Arterioscler Thromb Vasc Biol published online Nov 11, 2010;

DOI: 10.1161/ATVBAHA.110.215939

Arteriosclerosis, Thrombosis, and Vascular Biology is published by the American Heart Association,
7272 Greenville Avenue, Dallas, TX 75214

Copyright © 2010 American Heart Association. All rights reserved. Print ISSN: 1079-5642. Online
ISSN: 1524-4636

The online version of this article, along with updated information and services, is
located on the World Wide Web at:

<http://atvb.ahajournals.org>

Data Supplement (unedited) at:

<http://atvb.ahajournals.org/cgi/content/full/ATVBAHA.110.215939/DC2>

Subscriptions: Information about subscribing to Arteriosclerosis, Thrombosis, and Vascular
Biology is online at

<http://atvb.ahajournals.org/subscriptions/>

Permissions: Permissions & Rights Desk, Lippincott Williams & Wilkins, a division of Wolters
Kluwer Health, 351 West Camden Street, Baltimore, MD 21202-2436. Phone: 410-528-4050. Fax:
410-528-8550. E-mail:

journalpermissions@lww.com

Reprints: Information about reprints can be found online at

<http://www.lww.com/reprints>

Compartmentalized Connexin 43 S-Nitrosylation/Denitrosylation Regulates Heterocellular Communication in the Vessel Wall

Adam C. Straub, Marie Billaud, Scott R. Johnstone, Angela K. Best, Sean Yemen, Scott T. Dwyer, Robin Looft-Wilson, Jeffery J. Lysiak, Ben Gaston, Lisa Palmer, Brant E. Isakson

Objective—To determine whether S-nitrosylation of connexins (Cx) modulates gap junction communication between endothelium and smooth muscle.

Methods and Results—Heterocellular communication is essential for endothelium control of smooth muscle constriction; however, the exact mechanism governing this action remains unknown. Cxs and NO have been implicated in regulating heterocellular communication in the vessel wall. The myoendothelial junction serves as a conduit to facilitate gap junction communication between endothelial cells and vascular smooth muscle cells within the resistance vasculature. By using isolated vessels and a vascular cell coculture, we found that Cx43 is constitutively S-nitrosylated on cysteine 271 because of active endothelial NO synthase compartmentalized at the myoendothelial junction. Conversely, we found that stimulation of smooth muscle cells with the constrictor phenylephrine caused Cx43 to become denitrosylated because of compartmentalized S-nitrosoglutathione reductase, which attenuated channel permeability. We measured S-nitrosoglutathione breakdown and NO_x concentrations at the myoendothelial junction and found S-nitrosoglutathione reductase activity to precede NO release.

Conclusion—This study provides evidence for compartmentalized S-nitrosylation/denitrosylation in the regulation of smooth muscle cell to endothelial cell communication. (*Arterioscler Thromb Vasc Biol.* 2011;31:00-00.)

Key Words: NO ■ GSNO-R ■ connexin ■ myoendothelial junction ■ nitrosylation

Within the vessel wall of resistance arteries, coordinated vascular smooth muscle cell (SMC) and endothelial cell (EC) function is integrated by complex intercellular signaling to regulate the constriction and dilation of the artery. The anatomic structures that facilitate direct SMC and EC communication within the resistance artery are myoendothelial junctions (MEJs), which are cellular extensions from ECs or SMCs that project through the internal elastic lamina¹⁻³ and link the plasma membranes of the 2 different cell types together. The gap junctions (GJs) at the MEJ provide a conduit for second messenger and electric signaling between the 2 cell types.^{2,4,5} For example, phenylephrine (PE) stimulation of SMCs induces inositol 1,4,5-triphosphate (IP₃) generation and an increase in [Ca²⁺]_i concentrations, constricting the artery. It is thought that the IP₃ progresses to the adjacent EC through GJs at the MEJ, initiating an increase in [Ca²⁺]_i and the release of NO to modulate the magnitude of vasoconstriction, thereby regulating the tone of the artery.⁶⁻⁸ Elucidation of the mechanisms regulating this process could

provide novel insight into blood pressure regulation; however, the process remains uncharacterized.

GJs are intracellular signaling channels formed by 2 hexameric hemichannels, with each adjacent cell contributing 1 hemichannel. Connexin (Cx) proteins compose the channels, of which 4 different Cxs have been identified in the vasculature, with multiple studies demonstrating a potentially important role for Cx43 at the MEJ.⁹ Recent studies have demonstrated that GJ communication and trafficking of Cx43 are modulated by caveolae¹⁰⁻¹² and caveolin-1,¹³ supporting the observation that caveolin-1 could regulate Cx43 trafficking to the MEJ.¹⁴ In addition to regulating Cx43, caveolin-1 also regulates, mobilizes, and organizes several proteins, including endothelial NO synthase (eNOS).¹⁴⁻¹⁷ Although eNOS has not been shown at the MEJ, it is possible that it resides in this location because of the caveolae-rich environment.

NO participates in a plethora of physiological functions within the vessel wall, including vasodilation¹⁸ and posttrans-

Received on: September 6, 2010; final version accepted on: October 25, 2010.

From the Robert M. Berne Cardiovascular Research Center (A.C.S., M.B., S.R.J., A.K.B., and B.E.I.), University of Virginia School of Medicine, Charlottesville; the Department of Pediatrics (S.Y., S.T.D., B.G., and L.P.), University of Virginia School of Medicine, Charlottesville; the Department of Kinesiology and Health Sciences (R.L.-W.), College of William and Mary, Williamsburg, Va; the Department of Urology (J.J.L.), University of Virginia School of Medicine, Charlottesville; and the Department of Molecular Physiology and Biological Physics (B.E.I.), University of Virginia School of Medicine, Charlottesville.

Correspondence to Brant Isakson, Department of Molecular Physiology and Biological Physics, University of Virginia School of Medicine, PO Box 801394, Charlottesville, VA 22908. E-mail beifn@virginia.edu

© 2010 American Heart Association, Inc.

Arterioscler Thromb Vasc Biol is available at <http://atvb.ahajournals.org>

DOI: 10.1161/ATVBAHA.110.215939

lational protein *S*-nitrosylation.¹⁹ *S*-nitrosylation has emerged as a key mechanism by which NO may influence the function of a wide array of cellular proteins by covalently modifying sulfhydryl groups on cysteine residues both in vivo and in vitro.^{20,21} Despite its high ability to diffuse, growing evidence^{22,23} supports the concept that NO is generated locally; however, more important, this occurs in a concentration-dependent manner to elicit specific protein *S*-nitrosylation. Indeed, maintaining a critical balance between normal physiological protein *S*-nitrosylation and protein denitrosylation is essential.²⁴ One enzyme involved in regulating the balance between protein *S*-nitrosylation/denitrosylation is *S*-nitrosoglutathione reductase (GSNOR).²⁴ GSNOR indirectly regulates the levels of *S*-nitrosylated proteins by reducing GSNO, thereby providing equilibrium between *S*-nitrosylated proteins and GSNO.^{25,26} Indeed, mice deficient in GSNOR and in vitro studies have confirmed that GSNOR mediates multiple cardiovascular functions.^{24,27,28}

In this study, we provide evidence of an eNOS/GSNOR axis that regulates compartmentalized *S*-nitrosylation/denitrosylation of Cx43 permeability at the MEJ, thereby altering the constriction and dilatory response of a resistance artery. We propose that the specific cellular localization of proteins capable of dynamic *S*-nitrosylation/denitrosylation may be a template for heterocellular communication in general.

Methods

The supplemental materials (available online at <http://atvb.ahajournals.org>) provide expanded descriptions.

Mice

Wild-type mice, strain C57Bl/6 (Taconic), GSNOR^{-/+}, and GSNOR^{-/-} (originally described by Liu et al²⁴), were all males aged approximately 8 to 10 weeks and were used according to the University of Virginia Animal Care and Use Committee guidelines.

Vessel Cannulation

Mice were euthanized with an intraperitoneal injection of pentobarbital (60 to 90 mg/kg). First-order thoracodorsal (TD) arteries, a pair of resistance arteries (diameter, approximately 245 μ m) with extensive MEJs and endothelium-dependant hyperpolarization that supplies blood to spinotrapezius muscle (supplemental Figure I), were isolated for cannulation.²⁹

Immunolabeling on TEM Sections

TD arteries and cremaster, coronary, and mesentery vessels were isolated and processed for immunogold labeling and quantified as previously described.³¹

Cell Culture, Isolation of In Vitro MEJ Fractions, and Biotin Switch Assay

The vascular cell coculture (VCCC) was constructed as previously described.⁴

In vitro MEJ fractions were isolated from the VCCC as previously described.³¹

Isolated EC, MEJ, and SMC fractions were subjected to the biotin switch assay as previously described.³²

Immunoblots, Immunostaining, and Antibodies

Proteins were resolved using 4% to 12% bis-Tris gels, transferred to nitrocellulose, and visualized and analyzed using an imager (Li-Cor Odyssey Imager), as previously described.³⁴

Immunostaining on frozen sections of VCCC and HeLa cells was performed as previously described.⁴ All images were captured using a confocal microscope (Fluoview 1000).

Data on antibody source, application, concentration, and company of purchase are found in supplemental Table I.

Statistics

Statistics were performed using computer software (Origin Pro 6.0). All experiments were analyzed using 1- or 2-way ANOVA, followed by the Bonferroni posttest for differences between treatments where indicated. $P < 0.05$ was considered significant.

Results

NO and GJs Regulate Heterocellular Communication

As demonstrated in Figure 1A, the stimulation of a control TD artery with PE induces an initial constriction, followed by a redilation to bring the vessel back to near resting tone. We believe that this response is because of heterocellular communication between the SMCs and the ECs, specifically the generation of a second messenger by PE in SMCs (eg, IP₃ or constriction), which traverses GJs at the MEJ to activate eNOS in the ECs (redilation). For this reason, we initially tested a GJ inhibitor (carbenoxylone, Figure 1A) and an NOS inhibitor (L-NAME, Figure 1B) and found them both capable of significantly enhancing the constriction and inhibiting the redilation response. Because these data indicated that both Cxs and eNOS might be important regulators for intercellular communication between SMCs and ECs, we used TEM and quantified the amount of Cx43 and eNOS present in the TD artery (Figure 1C and 1D). Cx43 was the only Cx enriched at MEJs (supplemental Figure IIA), indicating that it is likely a major contributor of GJ heterocellular communication from SMCs to ECs. This observation was also seen at the in vitro MEJ.³¹ The presence of eNOS was also localized to the MEJ (Figure 1D), a trend we found throughout vascular beds (supplemental Figure IIB). Normal rabbit serum confirmed the specificity of our gold bead staining (supplemental Figure IIC). By using the VCCC, we also identified localized eNOS to the in vitro MEJ (Figure 1E and 1F). In contrast, neuronal NO synthase expression in TD MEJs (supplemental Figure IID through IIF), inducible NO synthase (supplemental Figure IIG through III), or another vasodilatory enzyme (cystathionine, supplemental Figure III through IIII) was not detected. Last, we observed caveolin-1, a protein capable of trafficking both eNOS and Cx43,^{10–17} as being localized at the MEJ in TD arteries and in the VCCC (supplemental Figure IIIA through IIIE).

Although eNOS was identified at the MEJ in vivo and in vitro, this was not indicative of its activity. Therefore, we applied L-NAME to vessels, measured resting tone in the absence of an agonist, and found a significant constriction (Figure 2A). These data coincided with the localization of phosphorylated S1177 eNOS at the MEJ in vivo and in vitro (Figure 2B and 2C) in the absence of any agonist. Phosphorylated S633 eNOS (active) was also observed at MEJs in vitro; however, phosphorylated T495 eNOS (inactive) was not observed (Figure 2D and 2E).

S-Nitrosylation of Cx43 on C271 Regulates GJ Communication

Because our ex vivo and in vitro evidence demonstrated basally active eNOS and the presence of Cx43 at the MEJ, the capacity

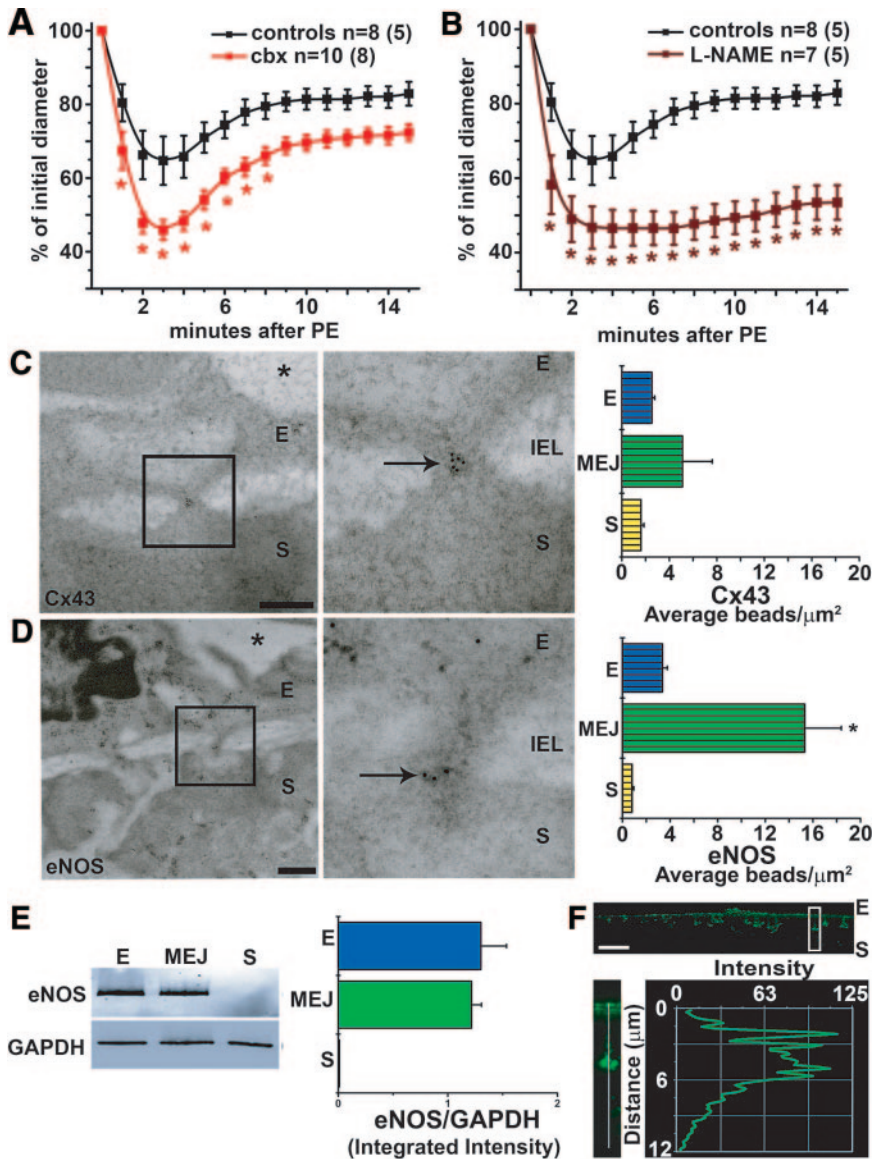


Figure 1. Vasoreactivity is altered by inhibition of GJ communication and NO correlating with Cx43 and eNOS expression at the MEJ. Mouse TD arteries were cannulated, pressurized, and stimulated with 50- $\mu\text{mol/L}$ PE. A and B, Application of carbenoxolone (50 $\mu\text{mol/L}$, A) and L-NAME (100 $\mu\text{mol/L}$, B) significantly enhanced PE-induced vasoconstriction in the TD arteries. C and D, Immunocytochemistry analysis of Cx43 (C) and eNOS (D) localization labeled with 10-nm gold beads (arrows) at MEJs from the TD arteries quantified the number of beads per micrometer squared. E, Isolated EC, MEJ, and SMC protein fractions from the VCCC blotted for eNOS and normalized to GAPDH. F, Immunocytochemistry of transverse sections from a VCCC were labeled for eNOS (green). The white box illustrates an enlarged MEJ with a line scan measuring fluorescence down the pore. Data are represented as the mean \pm SE. (C, n=8; D, n=6; E, n=4). Significant differences ($*P < 0.05$) were analyzed using a 2-way ANOVA (A and B) or a 1-way ANOVA (C-E). In A and B, n is the number of vessels and the value in parentheses is the number of mice. E indicates endothelial cell; IEL, internal elastic lamina; S, smooth muscle cell; *, lumen. The scale bar in C and D is 0.5 μm ; and F, 10 μm . In C through E, the open bars indicate in vitro measurements; and bars with horizontal lines, in vivo measurements.

of Cx43 to be *S*-nitrosylated was tested. Initial studies confirmed Cx43 to be constitutively *S*-nitrosylated in isolated TD arteries and at the in vitro MEJ (Figure 3A), whereas Cx40, a Cx found at the MEJ in some instances, was not *S*-nitrosylated (supplemental Figure IVA). To identify which cysteines may be responsible for *S*-nitrosylation, we used HeLa cells (which do not express Cxs or eNOS) and transfected in either Cx43 or Cx43 with all of the cysteines in the C-terminal mutated to alanines (Cx43^{C260/271/298A}). After treatment of transfected HeLa cells with GSNO, *S*-nitrosylated Cx43 was only detected in the nonmutated sample (Figure 3B). This was repeated on purified Cx43 C-terminal and Cx43^{C260/271/298A} C-terminal peptides, which produced identical results to Cx43 proteins expressed in HeLa cells (Figure 3C). Thus, to identify whether *S*-nitrosylation was site specific, we generated Cx43 containing only 1 C-terminal cysteine. After GSNO treatment, only Cx43^{C260/298A} was *S*-nitrosylated, indicating that C271 in the Cx43 C-terminal was the target for *S*-nitrosylation of Cx43 (Figure 3D). Functional changes as a result of *S*-nitrosylation were then tested in HeLa cells transfected with cysteine mutants by measuring the

extent of Ca^{2+} wave propagation after uncaging of NPE-IP₃. Calcium propagation rates were increased in response to GSNO for both Cx43 and Cx43^{C260/298A} cells but unchanged in Cx43^{C260/271A-}, Cx43^{C271/298A-}, and Cx43^{C260/271/298A-} expressing cells (Figure 3E). HeLa cells transfected without Cx43 did not propagate Ca^{2+} waves after pseudouncaging (supplemental Figure IVB). The differences in calcium wave propagation did not result from trafficking defects of the Cx43 mutations because all were effectively localized to the plasma membrane (supplemental Figure IVC through IVH). These data indicate that Cx43 and its GJ function are capable of being regulated by *S*-nitrosylation at C271.

Compartmentalized Denitrosylation of Cx43 at the MEJ

Because our previous results had demonstrated that Cx43 was extensively expressed at the MEJ and had the capacity to be *S*-nitrosylated, we tested whether PE stimulation could alter Cx43 *S*-nitrosylation. By using isolated TD arteries, we found a reduction in *S*-nitrosylation of Cx43 3 minutes after PE

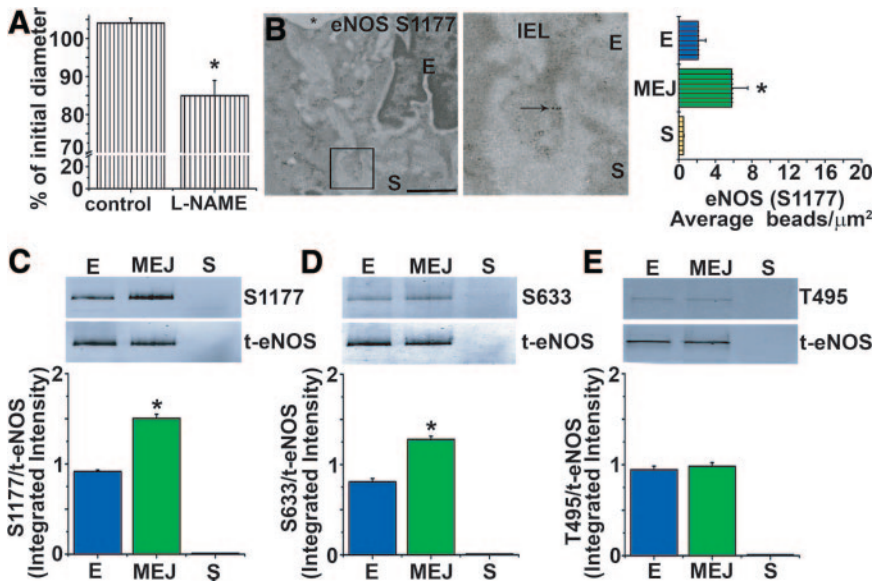


Figure 2. eNOS is differentially phosphorylated at the MEJ. Mouse TD arteries were cannulated and pressurized. A, The basal vascular tone was attenuated in the presence of L-NAME (100 $\mu\text{mol/L}$). B, Phosphorylated eNOS S1177 localization using 10-nm gold beads (arrow) in TD arteries using immuno-TEM and quantified as the number of beads per micrometer squared. C through E, Isolated EC, MEJ, and SMC fractions from the VCCC blotted for phosphorylated eNOS at sites S1177, S633, and T495 in EC, MEJ, and SMC fractions. Data are represented as the mean \pm SE. (A, n=5; B-E, n=4). Significant differences (* P <0.05) were analyzed using a 1-way ANOVA (A-D). E, endothelial cell; IEL, internal elastic lamina; S, smooth muscle cell; *, lumen. The scale bar is 0.5 μm (B). In A through E, open bars indicate in vitro measurements; and bars with horizontal lines, in vivo measurements.

stimulation, which returned to baseline after 10 minutes (Figure 4A). This result indicated that, in vivo, Cx43 at the MEJ is likely S-nitrosylated. Concurrent with this result, denitrosylation of Cx43 was only observed at the MEJ, and not the EC or SMC monolayer (Figure 4B), indicating a highly localized denitrosylation response (an effect identical to that seen on silver-stained gels of total S-nitrosylated proteins after PE stimulation) (supplemental Figure VA through VC). Neither application of 18GA (supplemental

Figure VD) nor the UV used for uncaging (supplemental Figure VE) altered Cx43 S-nitrosylation. To test whether denitrosylation of Cx43 correlated with changes in channel permeability, we stimulated SMCs on the VCCC with PE and then temporally uncaged NPE-IP₃ (Figure 4C). Under control conditions, uncaging of NPE-IP₃ in the SMCs elicited a robust increase in EC [Ca²⁺]_i, which was significantly inhibited by the GJ blocker (18GA, Figure 4D). At 1 minute after PE stimulation, there was a significant reduction in EC

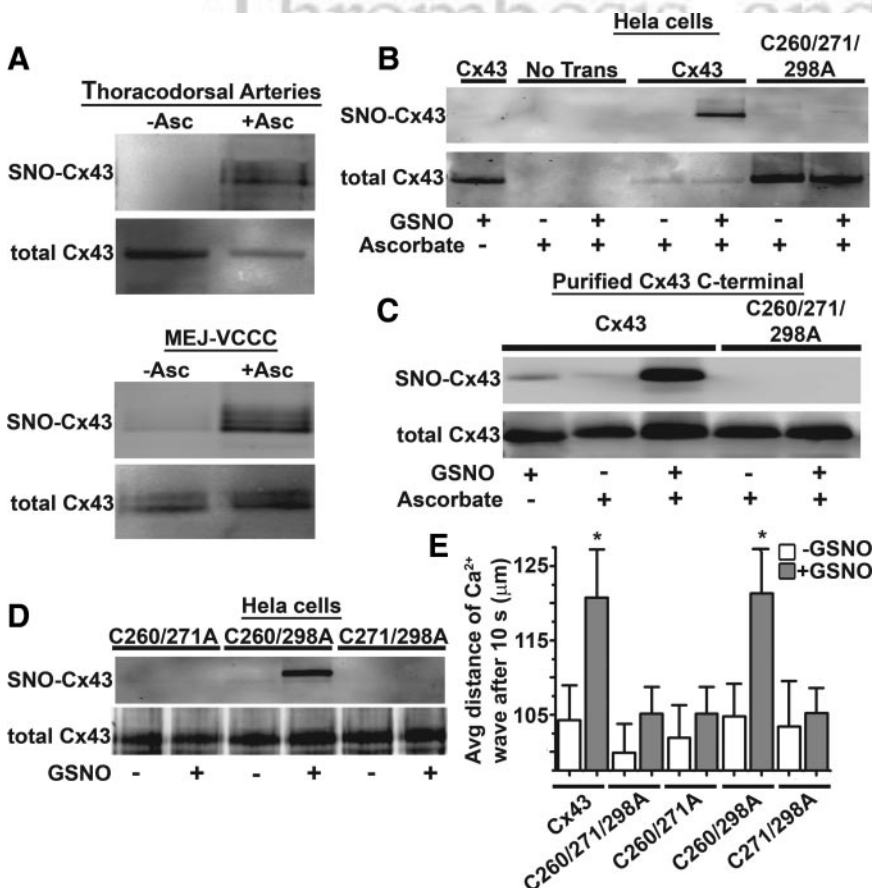


Figure 3. Cx43 is S-nitrosylated on cysteine 271. A, Unstimulated TD arteries or MEJ fractions analyzed by the biotin switch assay for Cx43, in which ascorbate-dependent labeling demonstrates the presence of an S-nitrosylated cysteine residue(s). B, Nontransfected and transfected HeLa cells with Cx43 or Cx43^{C260/271/298A} were treated with or without 100- $\mu\text{mol/L}$ GSNO for 1 hour. C, Biotin switch assay of purified Cx43 C-terminal or Cx43^{C260/271/298A} C-terminal peptides treated with or without 100- $\mu\text{mol/L}$ GSNO for 1 hour. D, HeLa cells transfected with Cx43^{C260/271A}, Cx43^{C260/298A}, or Cx43^{C271/298A} and treated with 100- $\mu\text{mol/L}$ GSNO for 1 hour were lysed and subjected to the biotin switch assay. E, Uncaging of NPE-IP₃ and analysis of calcium wave propagation and transfected HeLa cells with Cx43, Cx43^{C260/271/298A}, Cx43^{C260/271A}, Cx43^{C260/298A}, and Cx43^{C271/298A}. Data are represented as the mean \pm SE (n=6 to 8). Significant differences (* P <0.05) were analyzed using a 1-way ANOVA.

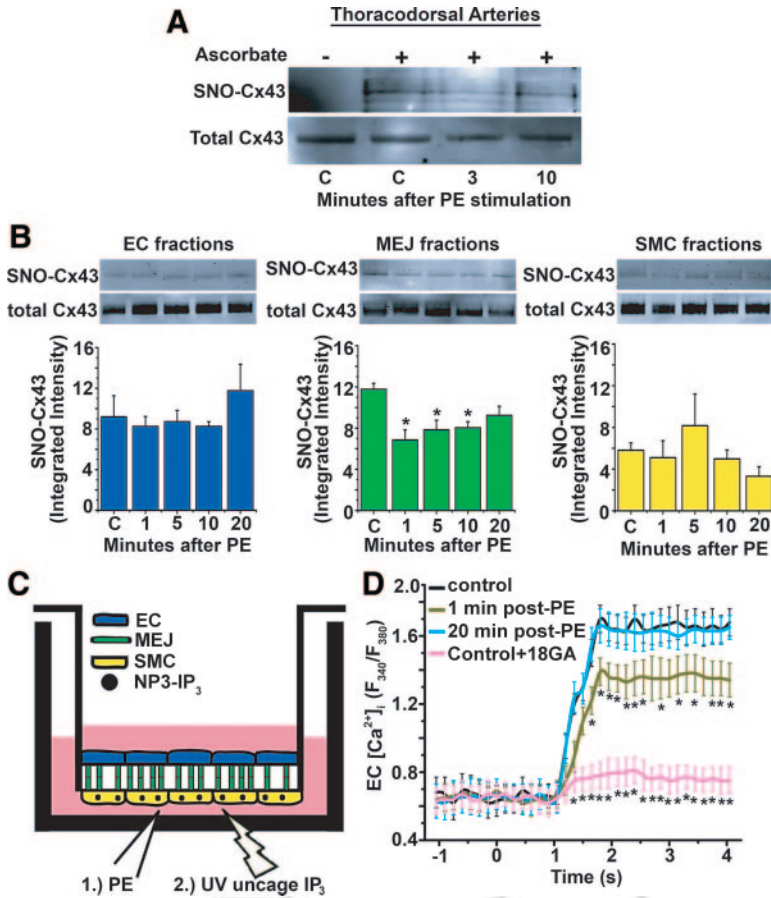


Figure 4. PE promotes denitrosylation of Cx43 and alters channel permeability. A and B, Immunoblots of isolated TD arteries or EC, MEJ, and SMC fractions identifying S-nitrosylated Cx43 using the biotin switch assay from VCCCs stimulated with PE. C, Schematic illustration of the experimental protocol used for measuring EC [Ca²⁺]_i using an initial stimulus of PE, followed by uncaging of NPE-IP₃ in SMCs using UV flash at specific points after PE stimulation. D, The maximum values of EC [Ca²⁺]_i were measured at control, 0, 1, and 20 minutes after PE stimulation or with the addition of 18GA. Data are represented as the mean ± SE (n=3). Significant differences (*P<0.05) were analyzed using a 1-way ANOVA. Open bars in B indicate in vitro experiments.



[Ca²⁺]_i, which returned to control levels at 20 minutes after PE stimulation. This suggested that the permeability of the GJ channel immediately after PE stimulation was decreased, which was likely because of a loss of Cx43 S-nitrosylation.

GSNOR Denitrosylates Cx43 at the MEJ

Because of the rapid denitrosylation of Cx43 at the MEJ on PE stimulation, we hypothesized that an enzyme capable of denitrosylating proteins may also be localized to the MEJ. Probing for GSNOR, we found the enzyme to be enriched in MEJ fractions both in vitro and in vivo (Figure 5A through 5C). In contrast, other enzymes known to denitrosylate proteins, thioredoxin-1,³⁷ and carboxyl reductase³⁸ were not present at the MEJ (supplemental Figure VIA through VIC). Next, we tested the activity of GSNOR after PE stimulation specifically in MEJ fractions and found increased activity at 1 minute, which returned to baseline after 20 minutes (Figure 5D). From the same MEJ lysates, we also measured total NO_x and found a significant increase at 20 minutes compared with control and 1 minute (Figure 5E), suggesting that GSNOR activity precedes NO release. To test the effect of GSNOR activity on Cx43 denitrosylation and GJ permeability at the MEJ, we used the GSNOR inhibitor that was identified in a high-throughput screen for GSNOR inhibitors and thereby arbitrarily named C3.²⁸ We found a complete lack of Cx43 denitrosylation after PE stimulation (Figure 5F), a result that was similar to the result obtained using GSNOR small-interfering RNA (supplemental Figure VIIA and VIIB).

Consistent with lack of denitrosylation after inhibiting GSNOR, application of C3 did not alter GJ permeability of IP₃ from SMCs to ECs when compared with control (Figure 5G). TD arteries treated with C3 had an attenuated constriction after application of PE (Figure 5H). The C3 did not alter baseline artery diameter during equilibration (supplemental Figure VIIC). The GSNOR^{+/+} mice were also less responsive to PE (Figure 5I), which was dependent on NOS activity and not S-nitrosothiols (supplemental Figure VIID). Last, the GSNOR^{-/-} mice were not different from controls (supplemental Figure VIIE), a result that is due to compensatory increases in carboxyl reductase in the TD arteries (supplemental Figure VIIF).

Discussion

Highly coordinated EC and SMC cross talk regulates vessel diameter and, by extension, the blood flow rate and blood pressure. GJs positioned at the MEJ between ECs and SMCs in resistance arteries allow for signals (eg, IP₃) originating from 1 cell type (eg, SMCs) to rapidly diffuse to adjacent cells (eg, ECs). Although GJs have been identified at the MEJ, the specific mechanisms that regulate GJ communication at the MEJ remain largely unknown. We define a pivotal posttranslational mechanism that ECs and SMCs use to regulate heterocellular communication before, during, and after SMC constriction. Our mechanism consists of compartmentalized S-nitrosylation/denitrosylation of Cx43 at the MEJ to regulate the magnitude of vasoconstriction (Figure 6).

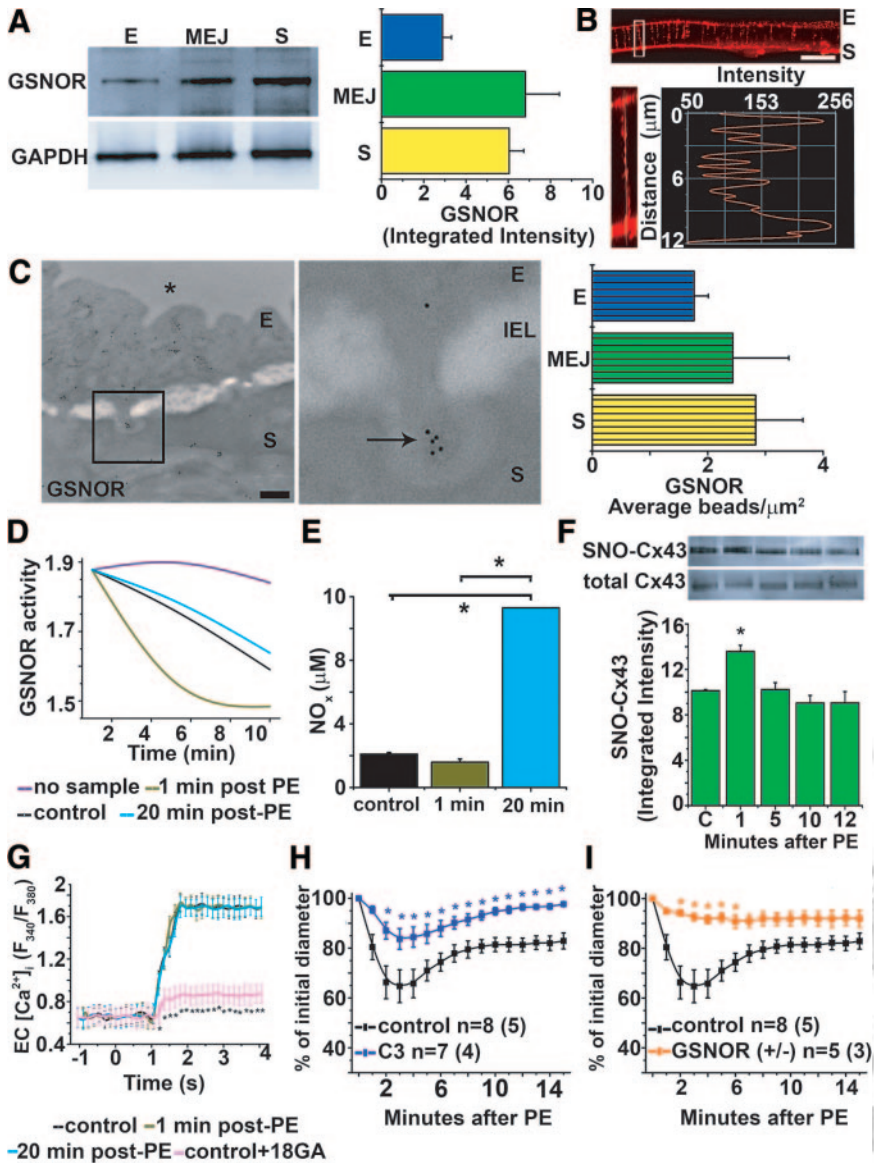


Figure 5. GSNOR regulates heterocellular communication. **A**, Quantitative Western blot analysis of GSNOR expression in isolated EC, MEJ, and SMC protein fractions from the VCCC normalized to GAPDH. Immunocytochemistry of transverse sections of a VCCC labeled for GSNOR (red). **B**, The white box illustrates an enlarged MEJ with a line scan measuring fluorescence down the pore. **C**, Immuno-TEM analysis of GSNOR expression labeled with 10-nm gold beads (arrows) at MEJs from the TD arteries and quantified as the number of beads per micrometer squared. **D**, Measurement of GSNOR activity by breakdown of GSNO in MEJ fractions at 1 and 20 minutes after PE stimulation. **E**, Identification of total NO_x in MEJ fractions at 1 and 20 minutes after PE stimulation. **F**, Immunoblot of S-nitrosylated Cx43 from in vitro MEJ fractions pretreated with C3 inhibitor and then stimulated with PE for 0, 1, 5, 10, and 20 minutes. **G**, Measurement of maximum values of EC [Ca²⁺]_i after UV uncaging is plotted at 0, 1, and 20 minutes after PE stimulation from the VCCCs pretreated with C3. **H** and **I**, Vasoconstriction response measuring percentage change of initial diameter to PE in TD arteries pretreated with C3 in wild-type mice (**H**) and GSNOR^{-/+} mice (**I**). Data are represented as the mean \pm SE. (**A**, n=5; **C**, n=5; **E**, n=2; and **F**, n=3). In **H** and **I**, n is the number of vessels and the value in parentheses is the number of mice. Significant differences (**P*<0.05) were analyzed using a 1-way (**E**-**G**) or a 2-way (**H**-**I**) ANOVA. The scale bar in **B** is 10 μm ; and in **C**, 0.5 μm . **E** indicates endothelial cell; **IEL**, internal elastic lamina; **S**, smooth muscle cell; *, lumen. Open bars indicate in vitro measurements (**A**, **E**, and **F**); and bars with horizontal lines, in vivo measurements (**C**).

Several compelling observations support this discovery: (1) eNOS is enriched and active at the MEJ, (2) Cx43 S-nitrosylation on cysteine 271 regulates more permeable GJ channels, and (3) compartmentalized GSNOR denitrosylates Cx43, promoting less permeable GJs at the MEJ to modulate the movement of IP₃ (and potentially other factors). The cellular, pharmacological, and genetic results presented herein imply that oxidation-reduction-based protein modifications on site-specific cysteine residues are regulated in specific regions of cells to coordinate heterocellular communication.

SMC relaxation after PE-induced constriction is thought to be due to IP₃ movement from SMCs, through GJs at the MEJ, to ECs.⁷ There is evidence to indicate that the IP₃ activates IP₃ receptor 1 localized to the MEJ³⁵ and induces an elevation of EC [Ca²⁺]_i, thereby activating eNOS and releasing NO to induce subsequent vasodilation.^{6,7,39} Our observation of Cx43 and active eNOS being localized to the MEJ provides the proteins necessary for a regulatable mechanism. This is supported by the observation that caveolae and caveolin-1

localize to the MEJ, thereby providing an optimal microsignaling domain whereby binding partners, including Cx43, eNOS, and many other proteins, could cluster.^{10-17,35,40} Indeed, spatial partitioning of proteins within a cell provides an important level of control to ensure fidelity of cell signaling. Accumulating evidence from monolayers of cultured cells has suggested that localized eNOS could allow for NO to be generated in a specific cellular region.^{22,23} It is reasonable to speculate that the active pool of eNOS we observe at the MEJ is regulating basal vascular tone and blood pressure because we show, with L-NAME, induced constriction in Figure 2. This would provide an energy-efficient mechanism to minimize NO diffusion distance to the SMCs. Thus, our identification of a pool of compartmentalized active eNOS uniquely at the MEJ throughout different vascular beds places these initial descriptive observations into a physiological context.

Our data go beyond the possibility of paracrine release of NO at the MEJ mediating the magnitude of vasoconstriction and suggest another function for the pool of localized eNOS

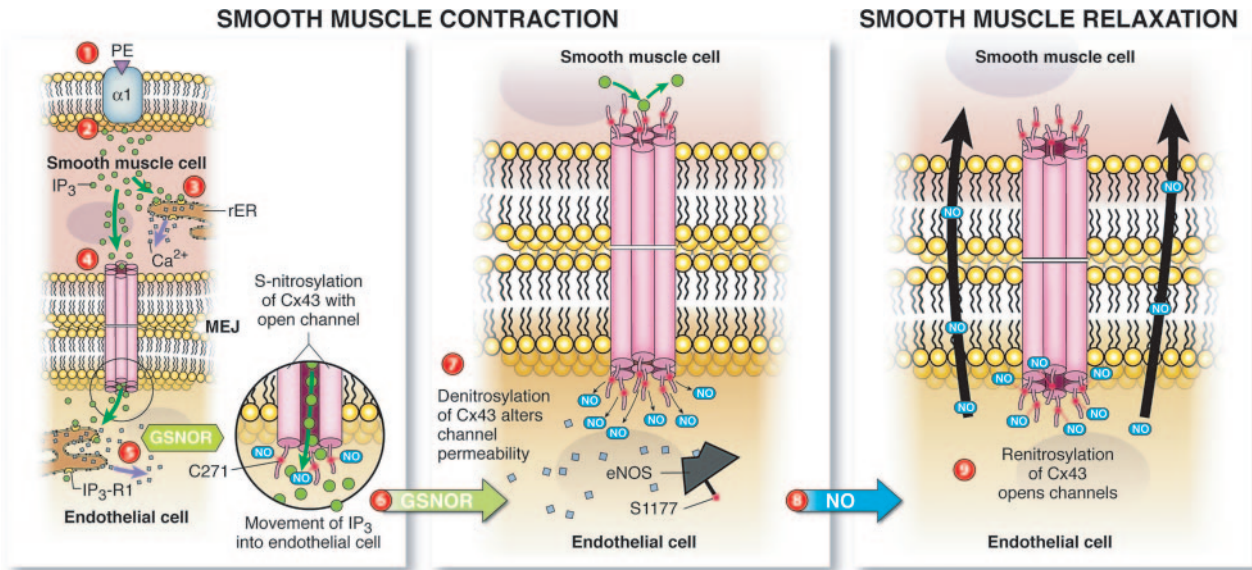


Figure 6. Schematic summary of Cx43 S-nitrosylation/denitrosylation regulating heterocellular communication in the vessel wall. Application of PE stimulates the $\alpha 1$ receptor (1), followed by the induction of IP₃ release in SMCs (2). The release of IP₃ activates intracellular calcium stores in endoplasmic reticulum promoting SMC contraction (3). In addition, IP₃ traverses S-nitrosylated Cx43 GJ channels at the MEJ to stimulate IP₃ receptors in ECs, inducing calcium release (5). GSNOR activity increases (6), which promotes denitrosylation of Cx43, altering channel permeability (7). Calcium and phosphorylation activate eNOS, resulting in released NO (8) to promote SMC relaxation and renitrosylation of Cx43 to open GJ channels (9).

at the MEJ (ie, regulation of GJ-mediate intracellular communication by NO). There are sporadic reports that NO could alter the function of GJ channels. For example, NO reduced Cx37 permeability and electric coupling in microvascular cells,^{41,42} whereas other reports^{43,44} suggest that NO enhances Cx43 electric current. However, this study used NO donors and did not explore how NOS-derived NO may posttranslationally modify the channel. It is becoming increasingly clear that S-nitrosylation is a critical posttranslational modification that regulates protein function.^{20,21} Our study demonstrates that NO derived from eNOS at the MEJ constitutively S-nitrosylates Cx43 in unstimulated conditions in TD arteries and in the VCCC, thereby maintaining a more permeable GJ channel. These data correlate with recent reports^{43,44} that NO acts on Cx43 hemichannels (not intact GJs) via S-nitrosylation to induce a more permeable state. Although the exact cysteines were not identified, these reports did show that the cysteines were more likely intracellular than extracellular. Therefore, we created several point mutations on the C-terminal of Cx43 and identified C271 as the critical site that significantly enhanced calcium wave propagation after IP₃ uncaging. The sum of these data indicates that Cx43 S-nitrosylation on C271 enhances permeability of the GJ channel; this can occur in a discreet cellular compartment.

Although the aggregate of our work indicated that S-nitrosylation maintained a more permeable GJ channel, it was reasonable to propose that denitrosylation of Cx43 modulated a less permeable GJ channel. Remarkably, we observed that denitrosylation after PE stimulation was confined to the MEJ rather than the EC or SMC monolayer. Of the multiple enzymes that have regulated denitrosylation, including GSNOR/GSNO,^{24,45} thioredoxin-1 reductase/

thioredoxin-1,³⁷ and carboxyl reductase,³⁸ we found that GSNOR was the dominant enzyme localized at the MEJ. This was evident because GSNOR activity specifically at the MEJ increased immediately after PE stimulation, which returned to baseline after 20 minutes. Conversely, we found that NO_x was increased only at the 20-minute point, supporting the idea that GSNOR activity precedes eNOS activity. It is unknown how GSNOR activity is regulated, although one likely possibility is through a Ca²⁺-dependent signaling pathway based on the rapid IP₃-induced increase in EC [Ca²⁺]_i and the immediacy of the effect. The pharmacological and genetic approaches in this study also support that GSNOR regulates denitrosylation at the MEJ. In cannulated vessels, C3 and GSNOR^{-/+} mice both had severely attenuated constriction. It is not clear how this occurs, but based on the data from the VCCC, we believe this is due to the enhanced GJ permeability, allowing for greater IP₃ transfer from SMCs to ECs enhancing eNOS-derived NO. Previous studies^{24,28} have demonstrated that inhibition of GSNOR increases S-nitrosothiols, thereby promoting SMC relaxation. However, our model system does not support this because L-NAME increased the magnitude of the constriction in cannulated vessels. Rather, these data confirm that NOS activity is a critical modulator of SMC constriction. These observations underpin the central role that compartmentalized GSNOR plays in regulating heterocellular communication in the artery wall.

In summary, results from this study emphasize the critical role that S-nitrosylation/denitrosylation contributes to heterocellular communication. Specifically, the evidence provided herein supports multiple roles for eNOS at the MEJ, including the following: (1) basal release of NO for regulating vasomotor tone and blood pressure, (2) local S-nitrosylation of

Cx43 to regulate more permeable channels, and (3) local production of NO for immediate feedback on SMCs. The presence of GSNOR provides a check on this system by inducing Cx43 denitrosylation on constriction and inducing a less permeable GJ. The results provide an investigational framework for future endeavors focusing on the eNOS/GSNOR axis as a potential therapeutic target for treating vascular pathological features, such as hypertension.

Acknowledgments

We thank Mark Yeager, Brian Duling, Michael Koval, and Aaron Barchowsky for critical reading and discussion of the manuscript; John Hunt for use of the NO analyzer; the University of Virginia Histology Core for sectioning of VCCCs; and Jan Redick and Stacey Guillot at the Advanced Microscopy Core.

Sources of Funding

This study was supported by a postdoctoral fellowship from the NRSA (Dr Straub); postdoctoral fellowships from the American Heart Association (Drs Billaud and Johnstone); grants HL082647 (Dr Looft-Wilson), HL59337 and HL69170 (Dr Gaston), and HL088554 (Dr Isakson) from the National Institutes of Health; DOD W81VWH-07-1 to 0134 (Dr Palmer); and American Heart Association SDG (Dr Isakson).

Disclosures

None.

References

- Rhodin JA. The ultrastructure of mammalian arterioles and precapillary sphincters. *J Ultrastruct Res*. 1967;18:181–223.
- Sandow SL, Hill CE. Incidence of myoendothelial gap junctions in the proximal and distal mesenteric arteries of the rat is suggestive of a role in endothelium-derived hyperpolarizing factor-mediated responses. *Circ Res*. 2000;86:341–346.
- Taugner R, Kirchheim H, Forssmann WG. Myoendothelial contacts in glomerular arterioles and in renal interlobular arteries of rat, mouse and Tupaia belangeri. *Cell Tissue Res*. 1984;235:319–325.
- Isakson BE, Duling BR. Heterocellular contact at the myoendothelial junction influences gap junction organization. *Circ Res*. 2005;97:44–51.
- Yashiro Y, Duling BR. Participation of intracellular Ca²⁺ stores in arteriolar conducted responses. *Am J Physiol Heart Circ Physiol*. 2003;285:H65–H73.
- Dora KA, Doyle MP, Duling BR. Elevation of intracellular calcium in smooth muscle causes endothelial cell generation of NO in arterioles. *Proc Natl Acad Sci U S A*. 1997;94:6529–6534.
- Isakson BE, Ramos SI, Duling BR. Ca²⁺ and inositol 1,4,5-trisphosphate-mediated signaling across the myoendothelial junction. *Circ Res*. 2007;100:246–254.
- Yashiro Y, Duling BR. Integrated Ca(2+) signaling between smooth muscle and endothelium of resistance vessels. *Circ Res*. 2000;87:1048–1054.
- Heberlein KR, Straub AC, Isakson BE. The myoendothelial junction: breaking through the matrix? *Microcirculation*. 2009;16:307–322.
- Barth K, Gentsch M, Blasche R, Pfüller A, Parshyna I, Koslowski R, Barth G, Kasper M. Distribution of caveolin-1 and connexin43 in normal and injured alveolar epithelial R3/1 cells. *Histochem Cell Biol*. 2005;123:239–247.
- Locke D, Liu J, Harris AL. Lipid rafts prepared by different methods contain different connexin channels, but gap junctions are not lipid rafts. *Biochemistry*. 2005;44:13027–13042.
- Schubert AL, Schubert W, Spray DC, Lisanti MP. Connexin family members target to lipid raft domains and interact with caveolin-1. *Biochemistry*. 2002;41:5754–5764.
- Langlois S, Cowan KN, Shao Q, Cowan BJ, Laird DW. Caveolin-1 and -2 interact with connexin43 and regulate gap junctional intercellular communication in keratinocytes. *Mol Biol Cell*. 2008;19:912–928.
- Garcia-Cardena G, Oh P, Liu J, Schnitzer JE, Sessa WC. Targeting of nitric oxide synthase to endothelial cell caveolae via palmitoylation: implications for nitric oxide signaling. *Proc Natl Acad Sci U S A*. 1996;93:6448–6453.
- Ghosh S, Gachhui R, Crooks C, Wu C, Lisanti MP, Stuehr DJ. Interaction between caveolin-1 and the reductase domain of endothelial nitric-oxide synthase: consequences for catalysis. *J Biol Chem*. 1998;273:22267–22271.
- Ju H, Zou R, Venema VJ, Venema RC. Direct interaction of endothelial nitric-oxide synthase and caveolin-1 inhibits synthase activity. *J Biol Chem*. 1997;272:18522–18525.
- Shaul PW, Smart EJ, Robinson LJ, German Z, Yuhanna IS, Ying Y, Anderson RG, Michel T. Acylation targets endothelial nitric-oxide synthase to plasmalemmal caveolae. *J Biol Chem*. 1996;271:6518–6522.
- Palmer RM, Ferrige AG, Moncada S. Nitric oxide release accounts for the biological activity of endothelium-derived relaxing factor. *Nature*. 1987;327:524–526.
- Lima B, Forrester MT, Hess DT, Stamler JS. S-nitrosylation in cardiovascular signaling. *Circ Res*. 2010;106:633–646.
- Stamler JS. Redox signaling: nitrosylation and related target interactions of nitric oxide. *Cell*. 1994;78:931–936.
- Stamler JS, Lamas S, Fang FC. Nitrosylation: the prototypic redox-based signaling mechanism. *Cell*. 2001;106:675–683.
- Iwakiri Y, Satoh A, Chatterjee S, Toomre DK, Chalouni CM, Fulton D, Groszmann RJ, Shah VH, Sessa WC. Nitric oxide synthase generates nitric oxide locally to regulate compartmentalized protein S-nitrosylation and protein trafficking. *Proc Natl Acad Sci U S A*. 2006;103:19777–19782.
- Qian J, Zhang Q, Church JE, Stepp DW, Rudic RD, Fulton DJ. Role of local production of endothelium-derived nitric oxide on cGMP signaling and S-nitrosylation. *Am J Physiol Heart Circ Physiol*. 2010;298:H112–H118.
- Liu L, Yan Y, Zeng M, Zhang J, Hanes MA, Ahearn G, McMahon TJ, Dickfeld T, Marshall HE, Que LG, Stamler JS. Essential roles of S-nitrosothiols in vascular homeostasis and endotoxic shock. *Cell*. 2004;116:617–628.
- Jensen DE, Belka GK, Du Bois GC. S-nitrosoglutathione is a substrate for rat alcohol dehydrogenase class III isoenzyme. *Biochem J*. 1998;331(pt 2):659–668.
- Liu L, Hausladen A, Zeng M, Que L, Heitman J, Stamler JS. A metabolic enzyme for S-nitrosothiol conserved from bacteria to humans. *Nature*. 2001;410:490–494.
- Lima B, Lam GK, Xie L, Diesen DL, Villamizar N, Nienaber J, Messina E, Bowles D, Kontos CD, Hare JM, Stamler JS, Rockman HA. Endogenous S-nitrosothiols protect against myocardial injury. *Proc Natl Acad Sci U S A*. 2009;106:6297–6302.
- Sanghani PC, Davis WI, Fears SL, Green SL, Zhai L, Tang Y, Martin E, Bryan NS, Sanghani SP. Kinetic and cellular characterization of novel inhibitors of S-nitrosoglutathione reductase. *J Biol Chem*. 2009;284:24354–24362.
- Billaud M, Marthan R, Savineau JP, Guibert C. Vascular smooth muscle modulates endothelial control of vasoreactivity via reactive oxygen species production through myoendothelial communications. *PLoS One*. 2009;4:e6432.
- Saltzman D, DeLano FA, Schmid-Schonbein GW. The microvasculature in skeletal muscle, VI: adrenergic innervation of arterioles in normotensive and spontaneously hypertensive rats. *Microvasc Res*. 1992;44:263–273.
- Heberlein KR, Straub AC, Best AK, Greyson MA, Looft-Wilson RC, Sharma PR, Meher A, Leitinger N, Isakson BE. Plasminogen activator inhibitor-1 regulates myoendothelial junction formation. *Circ Res*. 2010;106:1092–1102.
- Jaffrey SR, Snyder SH. The biotin switch method for the detection of S-nitrosylated proteins. *SciSTKE*. 2001;2001:L1.
- Wang X, Kettenhofen NJ, Shiva S, Hogg N, Gladwin MT. Copper dependence of the biotin switch assay: modified assay for measuring cellular and blood nitrosated proteins. *Free Radic Biol Med*. 2008;44:1362–1372.
- Johnstone SR, Ross J, Rizzo MJ, Straub AC, Lampe PD, Leitinger N, Isakson BE. Oxidized phospholipid species promote in vivo differential cx43 phosphorylation and vascular smooth muscle cell proliferation. *Am J Pathol*. 2009;175:916–924.
- Isakson BE. Localized expression of an Ins(1,4,5)P3 receptor at the myoendothelial junction selectively regulates heterocellular Ca²⁺ communication. *J Cell Sci*. 2008;121(pt 21):3664–3673.

36. Duffy HS, Sorgen PL, Girvin ME, O'Donnell P, Coombs W, Taffet SM, Delmar M, Spray DC. pH-dependent intramolecular binding and structure involving Cx43 cytoplasmic domains. *J Biol Chem.* 2002;277:36706–36714.
37. Stoyanovsky DA, Tyurina YY, Tyurin VA, Anand D, Mandavia DN, Gius D, Ivanova J, Pitt B, Billiar TR, Kagan VE. Thioredoxin and lipoic acid catalyze the denitrosation of low molecular weight and protein S-nitrosothiols. *J Am Chem Soc.* 2005;127:15815–15823.
38. Bateman RL, Rauh D, Tavshanjian B, Shokat KM. Human carbonyl reductase 1 is an S-nitrosoglutathione reductase. *J Biol Chem.* 2008;283:35756–35762.
39. Lambole M, Pittet P, Koenigsberger M, Sauser R, Beny JL, Meister JJ. Evidence for signaling via gap junctions from smooth muscle to endothelial cells in rat mesenteric arteries: possible implication of a second messenger. *Cell Calcium.* 2005;37:311–320.
40. Sandow SL, Garland CJ. Spatial association of K-Ca and gap junction connexins in rat mesenteric artery. *FASEB J.* 2006;20:A275–A275.
41. Kameritsch P, Khandoga N, Nagel W, Hundhausen C, Lidington D, Pohl U. Nitric oxide specifically reduces the permeability of Cx37-containing gap junctions to small molecules 19. *J Cell Physiol.* 2005;203:233–242.
42. McKinnon RL, Bolon ML, Wang HX, Swarbreck S, Kidder GM, Simon AM, Tyml K. Reduction of electrical coupling between microvascular endothelial cells by NO depends on connexin37. *Am J Physiol Heart Circ Physiol.* 2009;297:H93–H101.
43. Retamal MA, Cortes CJ, Reuss L, Bennett MV, Saez JC. S-nitrosylation and permeation through connexin 43 hemichannels in astrocytes: induction by oxidant stress and reversal by reducing agents. *Proc Natl Acad Sci U S A.* 2006;103:4475–4480.
44. Retamal MA, Yin S, Altenberg GA, Reuss L. Modulation of Cx46 hemichannels by nitric oxide. *Am J Physiol Cell Physiol.* 2009;296:C1356–C1363.
45. Liu L, Hausladen A, Zeng M, Que L, Heitman J, Stamler JS, Steverding D. Nitrosative stress: protection by glutathione-dependent formaldehyde dehydrogenase. *Redox Rep.* 2001;6:209–210.



Arteriosclerosis, Thrombosis, and Vascular Biology

JOURNAL OF THE AMERICAN HEART ASSOCIATION

FIRST PROOF ONLY

Supplemental Figure Legends

Supplemental Figure I. Dose response curve to acetylcholine in TD arteries in presence of L-NAME.

Mouse TD arteries were cannulated, pressurized and stimulated with PE (10^{-5} M) followed by increasing concentrations of acetylcholine in the presence or absence of L-NAME. Significant differences of $p < 0.05$ were analyzed using a 2-way ANOVA and are indicated by *. N = number of vessels, () are the number of mice.

Supplemental Figure II. Localization of Cxs, eNOS, nNOS, iNOS, and CTH at the MEJ.

(A) Connexin localization at the MEJ. Quantification of gold beads for each connexin were quantified using Metamorph. Data are represented as the mean \pm SE (n=6). Scale bar equals 0.5 μ m.

(B) eNOS localization at the MEJ. Isolated cremaster, coronary, mesentery vessels were immuno-labeled for eNOS expression using 10 nm gold beads. Gold beads were quantified for eNOS expression in ECs, MEJs, and SMCs were measured by averaging the number of total eNOS beads per micron squared. Data are represented as the mean \pm SE (n=6).

(C) Negative control for immuno-TEM labeling. A representative image of a TD artery incubated with normal rabbit serum followed by anti-rabbit 10 nm gold beads. Scale bar equals 0.5 μ m.

(D-F) nNOS localization at the MEJ. Immuno gold labeling for nNOS expression at the MEJ and bead quantification in vivo (D-E). Quantitative western blot analysis of nNOS expression normalized to GAPDH in the VCCC (F). Data are represented as the mean \pm SE (E n=6). Scale bar equals 0.5 μ m.

(G-I) iNOS expression at the MEJ. Immuno gold labeling for iNOS localization at the MEJ and bead quantification in vivo (G-H). Quantitative western blot analysis of iNOS expression normalized to GAPDH in the VCCC (I). Data are represented as the mean \pm SE (H n=6). Scale bar equals 0.5 μ m.

(J-L) CTH localization at the MEJ. Immuno-gold labeling for CTH expression at the MEJ and bead quantification in vivo (J-K) and quantitative western blot analysis of CTH expression in the VCCC (L). Data are represented as the mean \pm SE (K n=5; L n=3). Scale bar equals 0.5 μ m.

Supplemental Figure III. Caveolae and caveolin-1 localization to the MEJ.

(A-E) Caveolae and cav-1 localization at the MEJ. A representative TEM image from a TD artery at low magnification highlighting multiple MEJs (A), with a magnified section (black box) indicating a MEJ. The magnified black box in (B) illustrates multiple caveolae-like vesicles identified with black arrows. Immuno-TEM analysis of cav-1 localization using 10 nm gold beads (arrow) at the MEJ in TD arteries and quantified as the number of beads per micrometer squared (C). Quantitative western blot analysis from EC, MEJ, and SMC fractions for cav-1 normalized to GAPDH expression in the VCCC (D). Immunocytochemistry of a transverse section from the VCCC labeled for cav-1 (green) (E). The white box illustrates enlarged MEJ with a line scan measuring fluorescence down the pore. Enlarged picture of pore illustrated at left edge of line scan. Data are represented as the mean \pm SE (C n=7; D n=4). Scale bar equals 0.5 μ m (A-C) and 10 μ m (E). E: endothelial cell, S: smooth muscle cell, IEL: internal elastic lamina, *: lumen.

Supplemental Figure IV. S-nitrosylation of Cx40, Ca²⁺ propagation in untransfected HeLa cells, and trafficking of Cx43 cysteine mutants.

(A) Connexin 40 is not S-nitrosylated at MEJ. Unstimulated MEJ fraction were isolated and subjected to the biotin switch assay and blotted for Cx40.

(B) Ca²⁺ propagation in untransfected HeLa cells. Untransfected HeLa cells were loaded with NPE-IP₃, treated with GSNO for 1hr followed by UV flash to uncage IP₃ to determine Ca²⁺ wave propagation.

Data are represented as the mean \pm SE (n=6-8).

(C-H) Trafficking of Cx43 cysteine mutants. Confocal analysis of immunofluorescent labeling in HeLa cells transfected with Cx43 mutants (green), F-actin (with phalloidin, red) and nuclei (with DAPI, blue). Arrows indicate Cx43 trafficking to the plasma membrane and formation of GJ plaques between two cells. Scale bar equals 10 μm .

Supplemental Figure V. Total protein denitrosylation at the MEJ and unaltered Cx43 S-nitrosylation using the GJI and UV flash.

(A-C) Total denitrosylated proteins at the MEJ after PE stimulation. Silver stain of total S-nitrosylated proteins using the biotin switch assay from EC, MEJ, and SMC protein fractions treated with PE in the VCCC for 0, 1, 5, 10, and 20 minutes. Using Metamorph, a line scan down each well measured grayscale intensity and was plotted for each time point for each of the isolated fractions.

(D) Connexin 43 S-nitrosylation is unchanged with GJI. VCCCs were pretreated with 18GA for 1 hr and stimulated with PE for 0, 1, 5, 10, and 20 minutes. MEJ fractions were isolated and subjected to the biotin switch assay.

(E) UV flash does not alter Cx43 S-nitrosylation. Western blot analysis of VCCC fractions blotted for S-nitrosylated Cx43 after UV flash.

Supplemental Figure VI. Trx-1 and CBR1 expression at the MEJ in the VCCC.

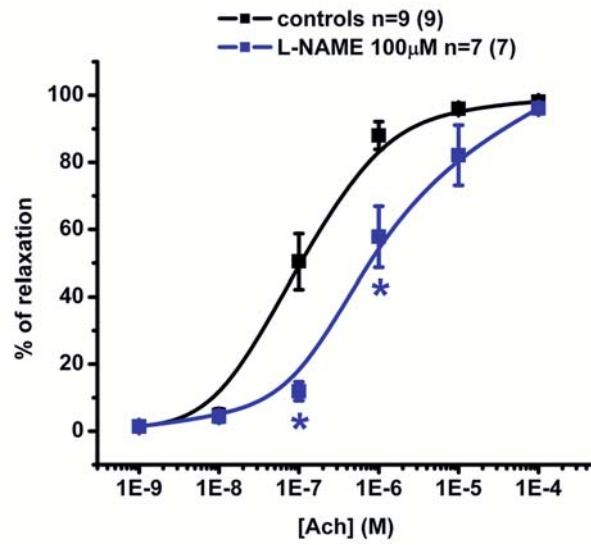
(A-C) Trx-1 and CBR1 expression at the MEJ. Quantitative western blot analysis of Trx-1 and CBR1 expression from EC, MEJ, and SMC fractions normalized to GAPDH.

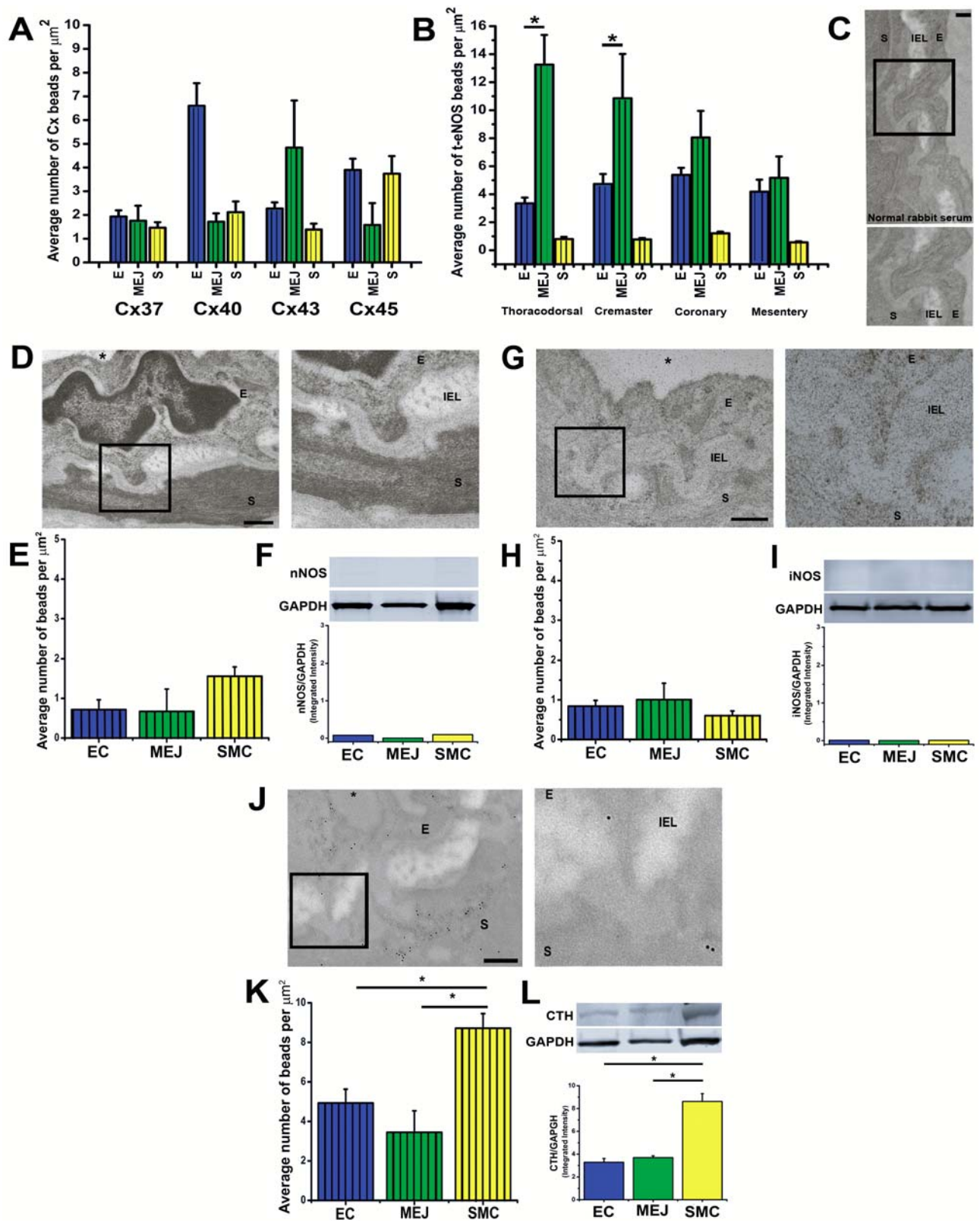
Supplemental Figure VII. GSNOR siRNA treated VCCCs, changes in baseline diameter after with pharmacological inhibitors, vasoreactivity changes in GSNOR^{-/-} mice and up-regulation of CBR1 in TD arteries.

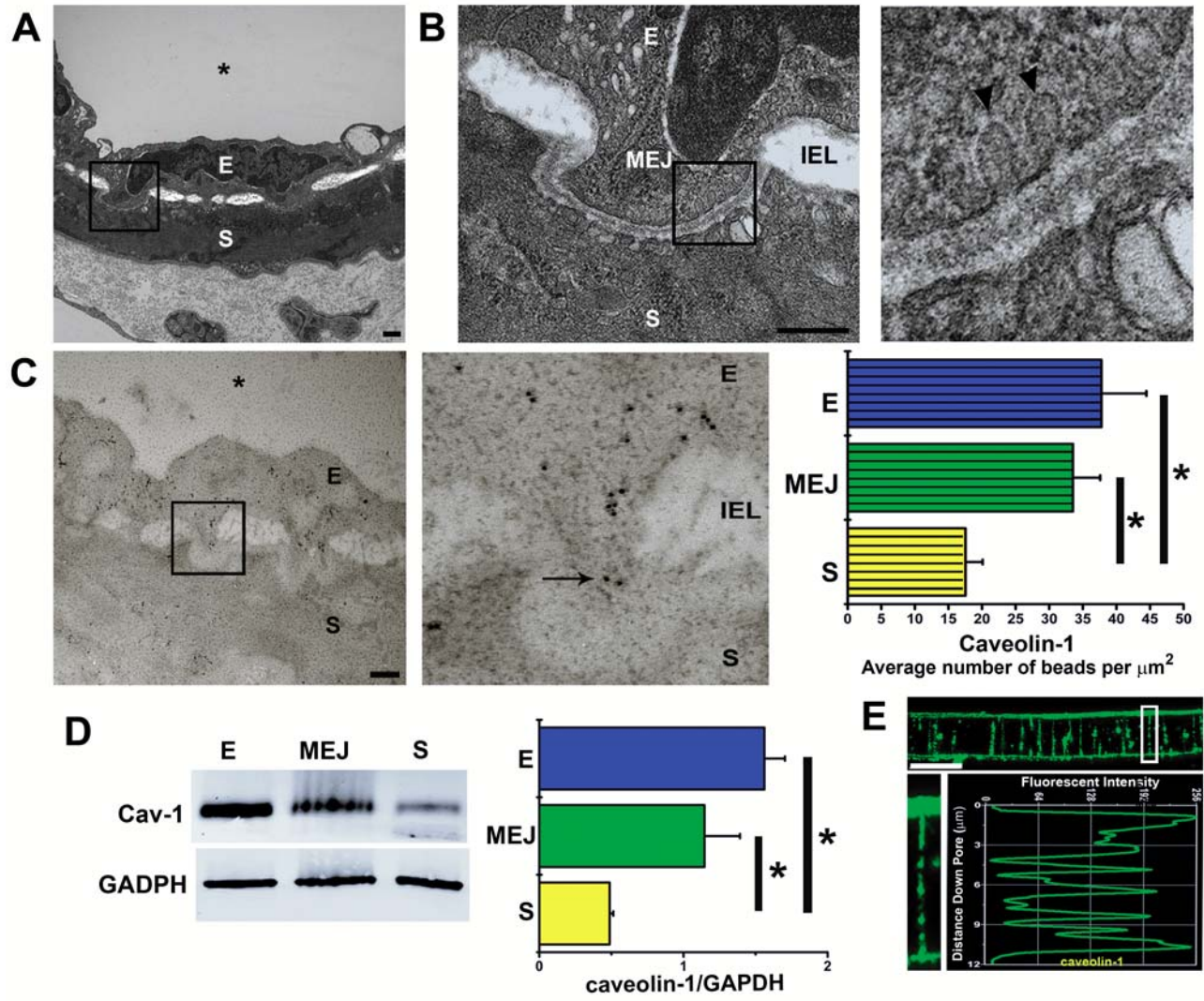
- (A) Knockdown efficiency of GSNOR siRNA. Isolation of MEJ fractions from VCCC treated with or without GSNOR siRNA for 48hrs and subjected to western blot analysis for knockdown of GSNOR protein.
- (B) GSNOR siRNA prevents Cx43 denitrosylation after PE stimulation. Vascular cell co-cultures were pretreated with GSNOR siRNA for 48hrs and stimulated with PE for 0, 1, or 20 min. MEJ fractions were isolated, subjected to the biotin switch assay, and western blotted for Cx43.
- (C) Baseline diameter changes of TD artery in WT treated with pharmacological inhibitors. The percent change is baseline before and after 30 minute equilibration time with CBX and C3. Data are represented as the mean \pm SE (n=5).
- (D) Vascular reactivity changes in GSNOR^{+/-} TD arteries pretreated with L-NAME (100 μ M). Isolated TD arteries from GSNOR^{+/-} mice were cannulated, pretreated with L-NAME and stimulated with PE.
- (E) Vascular reactivity changes in GSNOR^{-/-} mice. Isolated TD arteries from GSNOR^{+/-} mice were cannulated and stimulated with PE (10 μ M). Data are represented as the mean \pm SE (n=8).
- (F) Carboxyl reductase expression from isolated TD arteries from WT, GSNOR^{+/-}, GSNOR^{-/-}. Total protein was isolated from TD arteries and western blotted for CBR1.

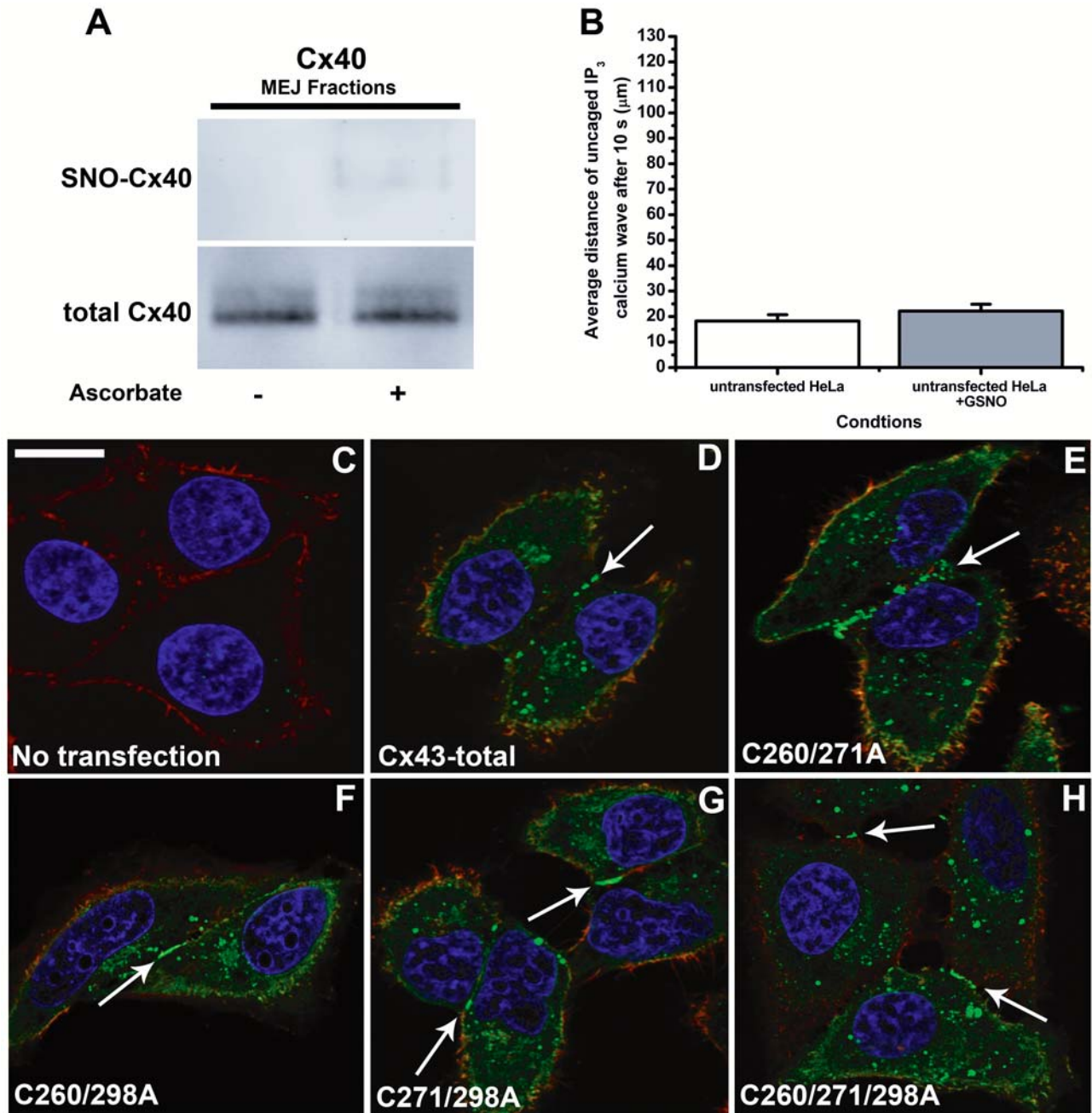
Supplemental Table I

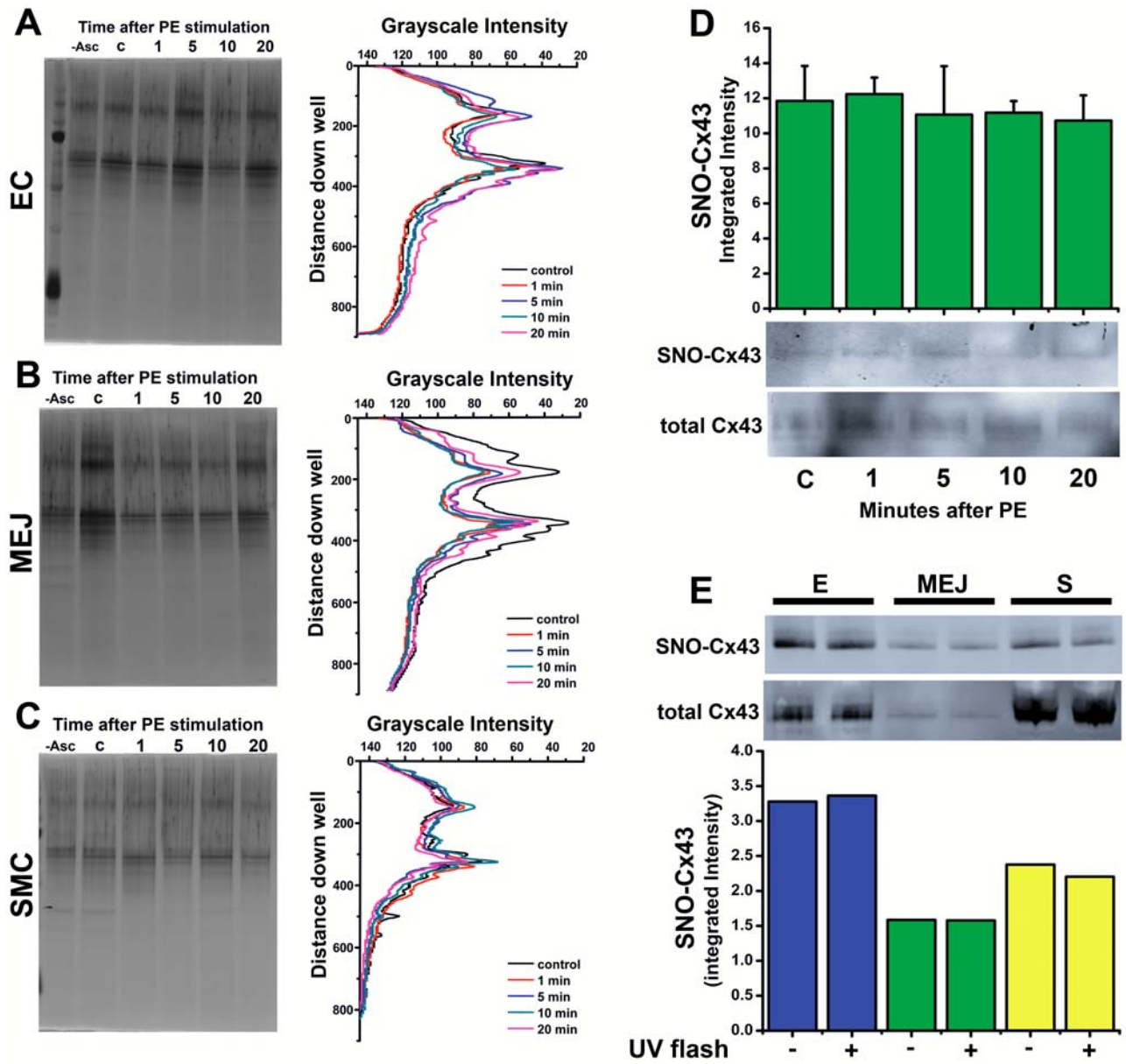
Antibody	Source	Application	Concentration	Company
CBR1	rabbit	WB	1:1000	Abgent
Caveolin-1	rabbit	WB/TEM	1:1000/1:200	BD Biosciences
Connexin 37	rabbit	WB/TEM	1:1000/1:200	Zymed
Connexin40	rabbit	WB/TEM	1:1000/1:200	ADI
Connexin 43	rabbit	WB/TEM	1:2000/1:200	Sigma
Connexin 45	rabbit	WB/TEM	1:1000/1:200	ADI
CTH	rabbit	WB/TEM	1:1000/1:200	Sigma
eNOS	rabbit	WB/TEM	1:1000/1:200	Sigma
eNOS	mouse	WB	1:1000	BD Biosciences
phospho-eNOS T495	mouse	WB	1:1000	BD Biosciences
phospho-eNOS S633	mouse	WB	1:1000	BD Biosciences
phospho-eNOS S1177	mouse	WB	1:1000	BD Biosciences
phospho-eNOS S1177	rabbit	TEM	1:200	Signalway
iNOS	rabbit	WB/TEM	1:1000/1:200	ABCAM
GSNOR	rabbit	WB/TEM	1:1000/1:200	Protein Tech
GAPDH	mouse	WB	1:1000	Invitrogen
Thioredoxin-1	rabbit	WB	1:1000	Cell Signaling
Alexa Fluor 488	mouse	IF	1:500	Invitrogen
Alexa Fluor 594	rabbit	IF	1:500	Invitrogen
IR Dye 680 CW	rabbit/mouse	WB	1:5000	Licor
IR Dye 800 CW	rabbit/mouse	WB	1:5000	Licor
10 nm gold beads	rabbit	TEM	1:20	EM Sciences

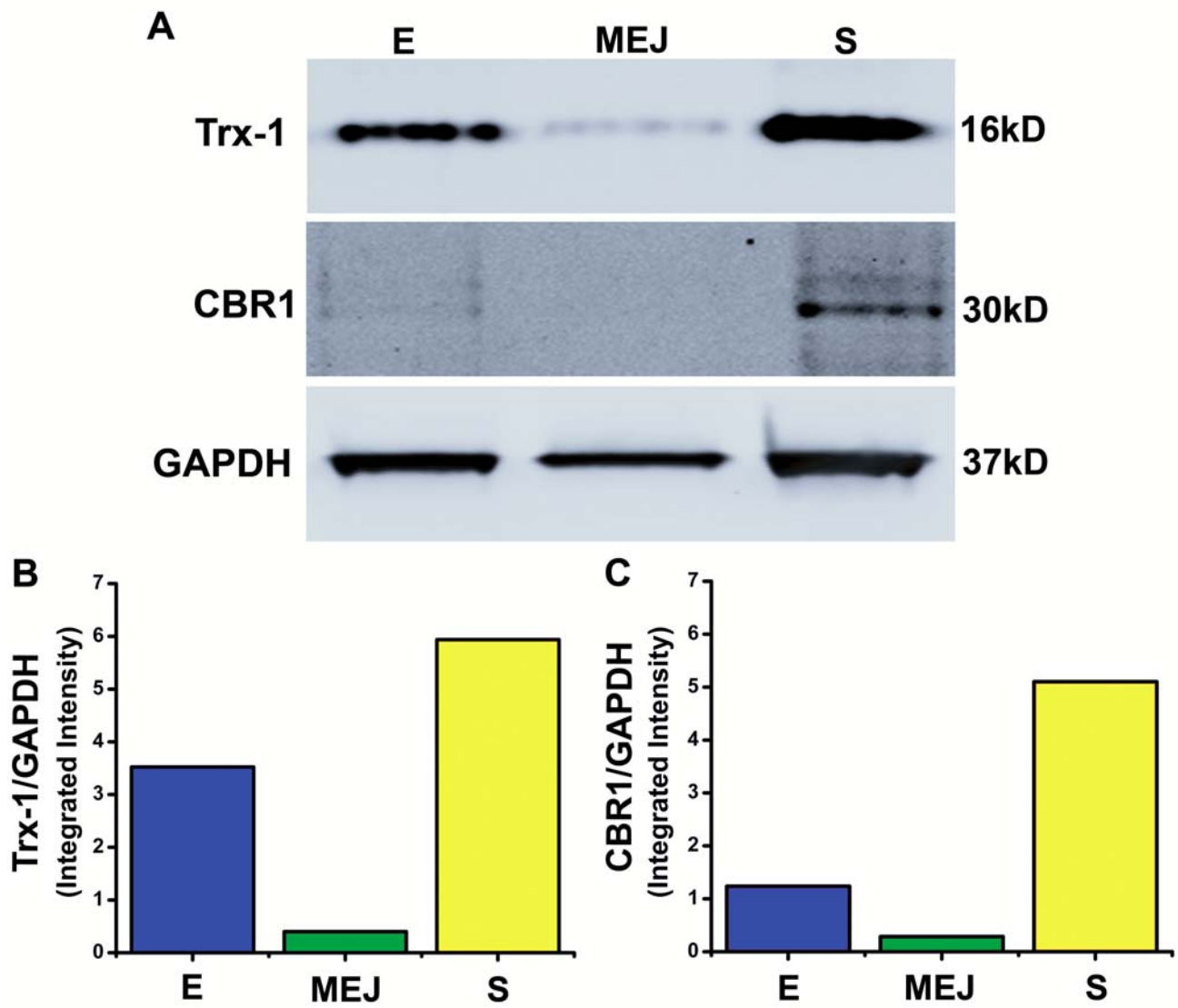


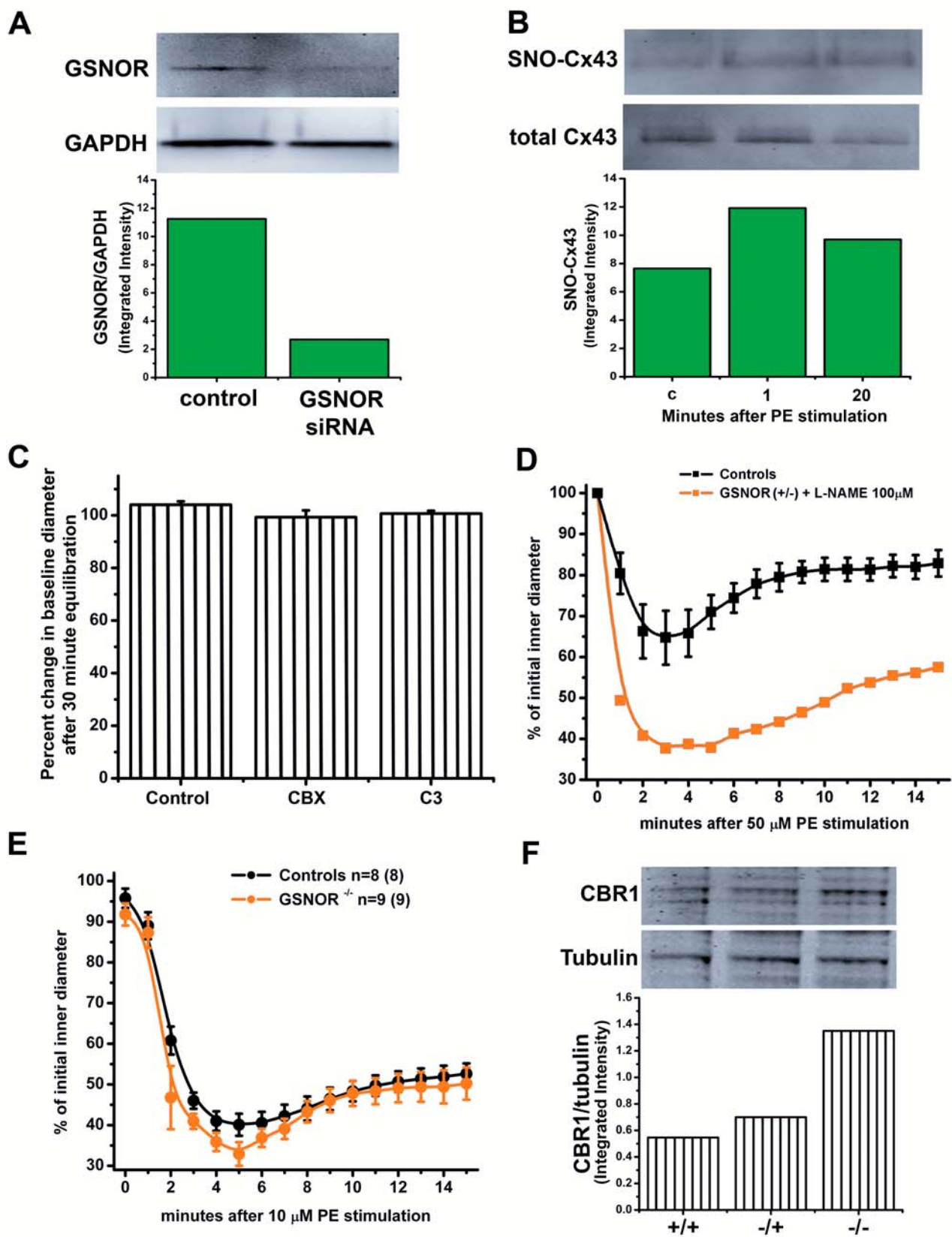












Supplemental Methods:

Cell Culture: Human umbilical vein endothelial and vascular smooth muscle cells were obtained from Cell Applications Inc. and cultured in M199 media supplemented with 10% fetal bovine serum (Gibco), 2mM L-glutamine (Gibco), penicillin (2mM)/streptomycin (50 U/mL) (Gibco). Endothelial cell medium was further supplemented with endothelial growth supplement (5µg/mL, BD Biosciences) and 5µg/mL of sodium heparin (Fisher Scientific). Vascular cell co-culture studies using the pharmacological inhibitors 18α glycyrrhetic acid (18GA) (Sigma) and C3 was performed by pretreating EC and SMC with 50µM for 1 and 3 hours respectively, followed by treatment with PE (50µM). HeLa parental cells (obtained from UVA cell culture core) were maintained in complete DMEM (cDMEM) (Gibco) supplemented with fetal bovine serum (10%), L-glutamine (2 mM), penicillin (50 U/mL), streptomycin (50 (U/mL) and L-glutamine (50 U/mL).

Vessel Cannulation: Mice were sacrificed with an intraperitoneal injection of pentobarbital (60-90 mg/kg) and isolated first order thoracodorsal (TD) arteries were cannulated at both ends with glass micropipettes, secured with 10–0 nylon monofilament suture and placed in a pressure myograph (Danish MyoTechnology). The chamber was superfused and perfused with Kreb's-Hepes solution²⁹, gassed with air, and maintained at 37°C. Vessels were maintained in a no-flow state and held at a constant transmural pressure of 80mm Hg equivalent to the transmural pressure of these vessels in vivo³⁰ Vessels were pretreated with carbenoxolone (CBX) (50µM) (MP Biomedical), L-Nitro-Arginine-Methyl Ester (L-NAME) (100 µM) (Sigma) or C3 (50µM) (Chem Div) described in²⁸ for 30 minutes and baseline diameters were measured after 30 min equilibration using an Olympus Fluoview 1000 confocal microscope. Contractile responses to 10 or 50 µM of PE were measured and recorded every one minute for a total time of 15 minutes and vessel diameter changes were quantified using MetaMorph as described in²⁹. Post PE stimulation, all vessels were tested for functional endothelium by stimulating with 10µM acetylcholine to ensure maximal dilation.

siRNA: Endothelial cells and SMCs were cultured together for 24hrs on Transwells and transfected with pre-designed siRNAs (5nM) for GSNOR (Ambion) using siPORT™ NeoFX™ transfection Agent (Ambion) according to manufactures directions. After 48hrs post transfection of siRNA, MEJ fractions were treated with PE and harvested for knockdown efficiency or subjected to the biotin switch assay. The following siRNA sequences were purchased from Ambion: siRNA ID# s1072-sense 5'AUUUUGUCUAAAUCCUAAAtt 3', antisense 5'UUUAGGAUUUAGACAAAAUtt 3', and siRNA ID#s1070 sense 5'AAAUCAAGCCUUUGAtt 3' and antisense 5'UCAAGGCUUUGUUGAUUUca 3'.

Transfection: Parental HeLa cells were transfected at 70% confluency with Cx43 plasmids described below using a Nucleofector (Lonza) achieving an approximate 70% transfection efficiency. Transfected cells were maintained in cDMEM supplemented with G418 (800 µg/mL) for 48hrs.

Biotin Switch Assay: Briefly, samples were isolated, acetone precipitated, and blocked with 10mM N-ethylmaleimide (ACROS Organics) at 50°C for 30 min. Following an additional acetone precipitation, samples were incubated with biotin-HPDP-N-[6-(biotinamido)hexyl]-3'-(2'-pyridyldithio) propionamide (Peirce) along with 1mM sodium ascorbate with the addition of 10µM copper sulfate for 1hr at RT as described in ³³. Samples were then precipitated and incubated with streptavidin coated agarose beads for 1 hr, washed 5 times, and S-nitrosylated proteins were eluted and subjected to immunoblotting.

Silver Stain: After protein separation, gels were fixed with 50% ethanol and 5% acetic acid overnight followed silver staining according to manufactures instructions (ThermoFisher).

Calcium Signaling after IP₃-uncaging: Both the SMC and HeLa cells were loaded with NPE-IP₃ (300 µM) using the pinocytotic method as previously described ⁴. When using the VCCC, uncaging of the NPE-IP₃ in the SMC was achieved by two synchronized xenon light sources under the control of Slidebook software. The UV-flash was transmitted through a centered 25 µm pinhole at 1, 5, 10 or 20 min post-stimulation of SMC with PE. Simultaneous measurement of changes in EC [Ca²⁺]_i on the VCCC was performed as described ³¹, utilizing a Hamamatsu 9100-13 back-thinned (512x 512) CCD camera. Transfected HeLa cells were initially loaded with P(4(5))-1-(2-nitrophenyl)ethyl-caged IP₃

(NPE-IP₃) and 30 min before imaging they were also loaded with Fluo-4 AM³⁵. Calcium wave propagation occurred radially outward immediately upon uncaging of NPE-IP₃ from the spatially defined UV-flash 25 μm spot (as above). The distance of the calcium wave propagation was measured 10 seconds after UV-flash for each of the Cx43 mutants transfected into HeLa cells.

Generation of Cx43 C-terminal mutant peptides: The Cx43 C-terminal encoding the sequence 236-382 of rCx43 inserted into pGEX-6P-2 plasmid was kindly provided by Dr. Paul Sorgen (University of Nebraska) and was synthesized as described³⁶. Cx43 C-terminal mutations were made via site directed mutagenesis with cysteine to alanine primers designed against the three C-terminal domain cysteines at C25, C36 and C63 in the Cx43 C-terminal sequence corresponding to C260, C271, C298 respectively in the full length Cx43 sequence using primers described above. For mutagenesis reactions the Cx43 C-terminal insert was removed from the pGEX-6P-2 by digest with BAM-H1 and XHO-1 followed by gel extraction of the insert, which was then ligated into pBluescript plasmid. Following mutagenesis, the insert was removed from pBluescript and re-ligated into pGEX-6P-2 plasmid as described above.

Cx43 C-terminal peptide: Proteins were purified as described³⁶ with the following alterations to the protocol. Plasmids containing the Cx43 C-terminal sequence were transformed into BL21 competent bacterial cells. Bacterial clones grown in 2L of LB broth were induced at 0.5 OD with 1mM isopropyl-1-thio-B-D-galactopyranoside (IPTG) for 3 hours. Bacterial pellets were washed in PBS pH 7.4 and re-suspended (1g/5mL) in protein buffer (50mM Tris-HCL (pH7.4), 190mM NaCl, 1mM dithiothreitol (DTT), 0.1mM Pefabloc, 200U of DNase, 1% Glycerol and 1:100 dilution of complete protease inhibitor cocktail (Sigma) then stored at -80°C. Cells were then thawed and disrupted by standard French Pressure 20K then lysates cleared by centrifugation (100,000G, 1 hr, 4°C). Supernatants were incubated with 4mL of glutathione-sepharose beads (Glutathione-sepharose 4 fast flow) for 3 hrs at room temperature. Protein bound beads were washed with 40 column volumes of protein buffer, followed by 20 column volumes of protein buffer without Pefabloc or protease inhibitors and Cx43-GST cleavage performed on the beads with PreScission (80U) at 4°C overnight with rocking. Eluted Cx43 C-terminal peptides were then further purified by incubation with fresh glutathione-sepharose beads for 3 hrs to remove residual

unbound GST, flow through was collected and protein samples were spin concentrated using Amicon centriplus 10 filters. Final Cx43 C-terminal proteins were found to be approximately 80% pure. Cx43 C-terminal were then treated with 100 μ M GSNO at 37°C shaking for 1hr and subjected to the biotin switch assay.

Site-directed Mutagenesis: Mutants were generated using Quikchange (Statagene) site-directed mutagenesis kit according to manufactures directions using Cx43 in a pcDNA 3.1 plasmid (gift from Mike Koval, Emory University). Primers for C260A are as follows: forward 5' ctgagcccatcaaaagacgccggatctccaaaatacgc 3' reverse 5' gcgtatttggagatccggcgtctttgatgggctcag 3'; C271A: 5' gcctacttcaatggcgcctctcaccacggc3', reverse 5' gccgttggtgaggaggcgcattgaagtaggc 3'; and C298A forward 5'gtgacagaaacaattcctcgcccgcaattacaacaagcaag 3', reverse 5' cttgctgttgaattcggggccgaggaattgtttctgtcac 3'. Mutants were sequenced at the UVA DNA sequencing core, confirmed and maxi prepped for transfection studies. The following mutants were generated Cx43^{C260/271/298A}, Cx43^{C260/271A}, Cx43^{C260/298A}, and Cx43^{C271/298A}.

GSNOR activity assay: GSNO-R activity was measured by using a modified Saville Assay. Briefly, 300 μ g of MEJ lysate was incubated with 300 μ M NADH, 2mM GSH and 28 μ M GSNO. Two aliquots of 75 μ l were placed into a 96 well plate at 1 min intervals for a total of 5 min. One aliquot was placed with 75 μ l of (+) reagent (58 mM Sulfanilamide + 7.36 mM HgCl₂ in 1N HCl) while the second aliquot was placed with (-) reagent (58 mM Sulfanilamide in 1N HCl). Samples were incubated 5 min in the dark. At the end of this incubation, 75 μ l of (N) reagent (0.77M n-(1-naphthyl) ethylene-diamine dihydrochloride) was added. Samples were incubated 5-10 min for color to develop. Absorbance was read at 540nm. Amount of GSNO remaining in the reaction was determined from a GSNO standard curve. Activity was obtained from the slope of the time course divided by the amount of protein in the reaction.

Determination of NO metabolites: Total nitrate and nitrite (NO_x) were analyzed according to manufactures instructions (Nitric oxide Analyzer, Sievers). Briefly, 2.5 μ g of MEJ lysate diluted in a final volume of 50 μ L was injected into a purge vessel containing a solution of vanadium (III) chloride

(50 mmol/L) in hydrochloric acid (1 mol/L) at 95°C. A continuously purged stream of nitrogen gas connected to a Sievers 280i NO analyzer measured NO_x.

S-nitrosogluthathione Reductase, Gender, and the Development of Pulmonary Arterial Hypertension

Palmer LA, *Que L, Brown-Steinke K, deRonde K, Gaston B
University of Virginia Health System, Charlottesville VA 22908
*Duke University Medical Center, Durham NC

Nitric oxide bioactivity, mediated through the formation of S-nitrosothiols (SNOs), has a significant influence on vascular tone. Moreover, numerous components that regulate SNO bioavailability in the pulmonary vasculature display gender dependent differences in activity and/or expression. Pulmonary arterial hypertension (PAH) is a condition with known gender disparity. To date, little research has focused on the mechanism(s) mediating this gender discordance. Therefore, we examined the hypothesis that S-nitrosothiol bioavailability, mediated through the actions of S-nitrosogluthathione reductase (GSNO-R), may play a role in the gender predilection seen in this disease. Using a novel mouse model of PAH induced by N-acetyl cysteine (Palmer et al. *J. Clin Invest.* 2007), our data reveal female mice have higher resting right ventricular pressures and right ventricular weights than males, but are protected from the N-acetyl cysteine-induced increases observed in males. Castration eliminated this response. S-nitrosylated N-acetylated cysteine (SNOAC) levels present in the serum of N-acetyl cysteine-treated animals was greater in the male animals, suggesting that differential S-nitrosothiol metabolism may be responsible for these observations. Analysis of the activity and expression of GSNO-R demonstrated: 1) GSNO-R activity was greater in female compared to the male animals with no changes in mRNA or protein expression. 2) Castration elevated GSNO-R activity to levels seen in female animals. 3) GSNO-R is S-nitrosylated. Taken together, the data suggest that changes in GSNO-R activity, possibly mediated by S-nitrosylation, may, in part, contribute to the gender-specific development of PAH induced by the delivery of S-nitrosothiols to the pulmonary vasculature.

S-nitrosylation/denitrosylation coupling and the Regulation of Endothelial Nitric Synthase.

Palmer L. A., Brown-Steinke K, deRonde K, Que L*, and Gaston B

University of Virginia, Charlottesville, Virginia

*Duke University, Durham, North Carolina

The formation of S-nitrosothiols requires nitric oxide synthase (NOS) activation. Endothelial NOS (eNOS) is the primary NOS found in the endothelium. S-nitrosothiol catabolism, in part, requires the action of S-nitrosoglutathione reductase (GSNO-R). Since S-nitrosothiol bioavailability within cells is determined by the balance between S-nitrosothiol formation and catabolism, we examined the relationship between these two proteins. Co-immunoprecipitation studies indicate GSNO-R associated with eNOS in murine pulmonary endothelial cells. Treatment with S-nitrosoglutathione (GSNO), an endogenously produced S-nitrosylating agent, disrupts this interaction. To determine if this interaction alters eNOS activity, murine pulmonary endothelial cells were transfected with GSNO-R in the absence or presence of GSNO. In the absence of GSNO, GSNO-R overexpression decreased the abundance of phosphorylated eNOS at serine 1177, a site associated with eNOS activation whereas, treatment with GSNO reversed the effect. Lastly, the possibility that the interaction between these proteins was regulated by S-nitrosylation was examined using the biotin switch assay. GSNO-R was found to be S-nitrosylated; S-nitrosylation was abrogated by a cysteine to serine mutation at residue 282. Interestingly, eNOS S-nitrosylation was absent in lysates obtained from cells transfected with wild type GSNO-R containing the cysteine to serine mutation. Taken together, the data suggest that the activities and interaction between eNOS and GSNO-R are mediated by S-nitrosylation/denitrosylation coupling and may function to regulate S-nitrosothiols bioavailability within the cells.

Abstract 6982

S-nitrosogluthione reductase and its role in pulmonary arterial hypertension.

Type: Scientific Abstract

Category: S) VASCULAR BIOLOGY/PULMONARY CIRCULATION / 18.19 - Pulmonary Hypertension: Experimental - Animal Models (PC)

Authors: K. Brown-Steinke¹, K. deRonde², S. Sullivan¹, S. Yemen¹, L.A. Palmer¹; ¹Charlottesville, VA/US, ²Charlottesville/US

Abstract Body

RATIONAL: Alterations in S-nitrosothiol bioavailability/abundance have been reported in human and animal models of pulmonary arterial hypertension (PAH). Preliminary data using a novel mouse model of PAH which uses N-acetyl cysteine (NAC) to trace S-nitrosothiol abundance (Palmer et al J. Clin Invest 2007) demonstrate female mice are protected from NAC but not S-nitrosylated-NAC induced increases in right ventricular weight (RVW) and right ventricular pressure (RVP) observed in males. Moreover, S-nitrosylated-NAC levels found in the serum of female mice were significantly less than S-nitrosylated NAC levels detected in male animals. Differential S-nitrosothiol bioavailability may be mediated by the actions of S-nitrosogluthione reductase (GSNO-R) that are gender discrodant. **METHODS:** To test this possibility, the activity and expression of GSNO-R was evaluated in male and female murine lungs. **RESULTS:** 1) GSNO-R acivity was greater in female compared to male animals. 2) Male and female mice demonstrate no differences in GSNO-R protein expression. 3) Castration of male animals elevated GSNO-R activity to levels seen in female animals. Interestingly, castrated animals were protected from NAC-induced increases in RVW and RVP. **CONCLUSIONS:** Endothelial nitric oxide synthase expression is increased in the female murine lung. We speculate that post-translational modification (S-nitrosylation) of GSNO-R modulates GSNO-R activity in female mice which may protect against nitrosylation injury. Thus GSNO-R may protect against high-flow-, hypoxia- and inflammation- induced PAH.

Abstract 6885

Gender differences in the ventilatory responses to hypoxia.

Type: Scientific Abstract

Category: H) INTEGRATIVE PHYSIOLOGY AND PATHOLOGY / 08.05 - Control of Ventilation (SRN)

Authors: S.J. Lewis, W. May, A. Young, S. Yemen, L.A. Palmer; Charlottesville, VA/US

Abstract Body

RATIONAL: Several studies have provided evidence that women have a better capacity to adapt to hypoxia and are less susceptible to hypoxia-associated syndromes than are men. At present, there is little information in mice as to whether sex differences exist with respect to the ventilatory responses that occur during exposure to hypoxia, including the gradual decline referred to as "roll-off", and the enhanced responses associated with re-exposure to room air, known as "facilitation". **METHOD:** We compared the ventilatory effects of acute hypoxia (15 min; 10% O₂ and 90% N₂) in age-matched male (n=8) and female (n=8) C57black 6 (C57Bl6) mice using Buxco plethysmographs. **RESULTS:** Resting Minute Volumes (MV) were similar in male and female mice (58 ± 6 versus 51 ± 5 mls/min, $P < 0.05$). Upon exposure to hypoxia, MV reached similar peak values in male and female mice (112 ± 9 versus 100 ± 7 mls/min, $P > 0.05$). However, MV declined to baseline values (roll off) more rapidly in females than in males (Total response areas in females and males of 180 ± 22 versus 382 ± 29 mls/min per 15 min, $P < 0.05$). Upon re-exposure to room air, MV rose to peak values of 129 ± 10 mls/min in males (facilitation) whereas it only rose to 69 ± 8 mls/min in females ($P < 0.05$). Total response areas in males and females were 521 ± 63 versus 37 ± 8 mls/min per 15 min, $P < 0.05$). **CONCLUSION:** These data clearly demonstrate gender differences in male and female mice with respect to the ventilatory responses during and after exposure to a brief hypoxia.

Therapeutic ultrasound decreases mean right ventricular pressure in hypoxic mice

Yemen S, Marozkina NV, Palmer LA, Gaston B

Ultrasound delivered at the high frequency (~880 kHz) and power settings used for physical therapy converts reduced thiols to S-nitrosothiols (Stepuro II, et al., *Biochem-Russia*. 65:1385, 2000), which relax vascular smooth muscle. We measured acute changes in right ventricular pressure (RVP; Millar transducer; right internal jugular) percutaneously in mice exposed to 10% isocapneic hypoxia before and after systemic exposure to therapeutic ultrasound (TUS) (Koalaty US 1000) providing 1 MHz frequency and maximum intensity 1.5 W/cm². 4 mice (4 male) were studied 9 times. 10% oxygen increased mean RVP from 8.05 +/- 0.88 to 11.97 +/- 0.50 mm Hg pressure ($p < .002$). TUS decreased mean RVP to 8.52 +/- 1.05 mm Hg ($p < .009$ compared to hypoxia) within 5-10 seconds of exposure. TUS directly on the skin created large signal artifacts: an air interface was always maintained. The greater the distance from the skin, the greater the distance in pressure. The effect on diastolic (central venous) pressures was greater than the effect on systolic pressures. These observations suggest that TUS-induced S-nitrosothiol might be of benefit in the setting of acute pulmonary arterial hypertension.

eNOS S-Nitrosylation and Erectile Function

Parviz K. Kavoussi¹, Joseph H. Ellen¹, Janine L. Oliver¹, Robin I. Woodson¹, Raymond A. Costabile¹, William D. Steers¹, Lisa A. Palmer² & Jeffrey J. Lysiak¹
Departments of Urology and Pediatrics, University of Virginia
Charlottesville VA

Introduction and Objective

Endothelial nitric oxide synthase (eNOS) plays a pivotal role in maintenance of penile tumescence. The objective of the current study is to determine if S-nitrosylation is a key post-translational modification of eNOS regulating its activity in the corporal endothelium. S-nitrosylated eNOS is non-functional and does not produce NO. Denitrosylation is controlled, in part, by S-nitrosoglutathione reductase (GSNO-R). Net NO bioavailability, and thus erectile function may be controlled by an S-nitrosylation/denitrosylation regulatory loop and imbalances may lead to ED.

Methods

Biotin-switch assays to identify S-nitrosylated eNOS (sno-eNOS) were performed on murine penile homogenates harvested in the non-erect state and during cavernous nerve electrical stimulation (CNES)-induced tumescence. Penile homogenates from GSNO-R^{-/-}, GSNO-R^{+/-}, and littermate controls were also assayed for sno-eNOS. Intracavernous pressures (ICP) and duration of tumescence during CNES were evaluated in GSNO-R^{-/-}, GSNO-R^{+/-}, and wild type mice. GSNO-R and eNOS were localized in the murine and human penis by immunohistochemistry, immunofluorescence, and western blot. Western blot analyses were performed on erectile response pathway proteins in GSNO-R null mice.

Results

An increase in sno-eNOS was detected in the murine penis over the time course of the erectile response. eNOS and GSNO-R co-localize to the endothelium in both the murine and human corpus cavernosum. Both GSNO-R^{-/-} and GSNO-R^{+/-} mice cannot maintain erections. Erectile response pathway proteins are normal in GSNO-R deficient animals.

Conclusions

Previous studies have shown that eNOS activity is associated with sno-eNOS and that sno-eNOS is inactive suggesting a regulatory loop. We now demonstrate for the first time that eNOS is S-nitrosylated during time of tumescence in the murine penis. We also demonstrate that GSNO-R, an enzyme responsible for the denitrosylation of eNOS, is co-localize with eNOS to the endothelium of the corpus cavernosum. ICP measurements during CNES demonstrate that both GSNO-R^{-/-} and GSNO-R^{+/-} mice can initiate, but cannot maintain tumescence similar to the response demonstrated by eNOS deficient mice. GSNO-R^{+/-} mice have reduced levels of GSNO-R; thus, some minimal amount of GSNO-R protein/activity must exist in the corporal endothelial cells for normal tumescence. Taken together these results suggest that S-nitrosylation is an important mechanism of eNOS activity during tumescence and GSNO-R has an important regulatory role in eNOS activation/inactivation necessary for normal tumescence/detumescence.

Ventilatory responses during and following exposure to hypoxia in conscious mice deficient or null in S-nitrosogluthathione reductase

L.A. Palmer¹, W.J. May^{1,2}, K. deRonde¹, A.P. Young^{1,2}, B. Gaston^{1,2}, S.J. Lewis^{1,2}.

¹Pediatric Respiratory Medicine, University of Virginia School of Medicine, Charlottesville, VA.

²Division of Biology, Galleon Pharmaceuticals, Horsham, PA.

Rationale: Exposure to hypoxia elicits an increase in Minute Ventilation (MV) that diminishes with continued exposure (roll-off). Abrupt termination of the hypoxic challenge is associated with an increase in MV (short-term facilitation - STF). S-nitrosothiols (SNOs) including S-nitrosogluthathione (GSNO) formed during hypoxia contribute to increased ventilatory drive. The NADH-dependent enzyme GSNO reductase (GSNOR) plays a key role in determining SNO homeostasis. Since hypoxia increases intracellular NADH levels, we postulate that ventilatory roll-off during hypoxia may involve a progressive NADH-dependent increase in GSNOR activity.

Methods: Female C57Bl6 (n=12, strain-matched controls), GSNOR+/- (n=9) and GSNOR-/- (n=17) mice were placed in whole-body plethysmography chambers to record ventilatory parameters. After allowing the mice to acclimatize, ventilatory parameters were recorded before and during exposure to a hypoxic challenge (10% O₂, 90% N₂) for 15 min and for 15 min following reintroduction of room air.

Results: In C57Bl6 mice, exposure to hypoxia elicited initial increases Minute Volume (via increases in Frequency and Tidal Volume) and in Peak Inspiratory and Expiratory Flows. These responses were subject to substantial roll-off. In GSNOR+/- and GSNOR-/- mice, exposure to hypoxia elicited similar initial increases in ventilatory parameters as observed in the C57Bl6 mice. In contrast, the ventilatory responses in GSNOR+/- and GSNOR-/- mice did not display roll-off. Upon reintroduction to room air, the C57Bl6 mice displayed STF of approximately 5 min in duration in all ventilatory parameters. This STF was markedly exaggerated in the GSNOR+/- and GSNOR-/- mice.

Conclusions: The absence of roll-off in GSNOR-/- mice suggests that an increase in GSNOR activity during exposure to hypoxia plays a vital role in this phenomenon in C57Bl6. Specifically, the ventilatory stimulatory actions of GSNO formed during hypoxia are overcome by a NADH-dependent increase in GSNOR. The exaggerated expression of STF in GSNOR-/- mice suggests that GSNOR activity plays a vital role in mediating post-hypoxic ventilatory events. Specifically, STF in C57Bl6 mice may occur because reintroduction of room air inhibits GSNOR activity more rapidly than GSNO formation allowing residual GSNO to drive MV. The exaggerated STF in GSNOR-/- mice be due to enhanced levels of GSNO at the point of reintroduction of room air and the absence of GSNOR activity, thereby requiring other (less effective) mechanisms for SNO degradation to remove the SNOs. The finding that GSNOR+/- mice behave similarly to GSNOR-/- mice with respect to roll-off and STF suggests that one gene provides inadequate levels of GSNOR to overcome GSNO formation.

Hemoglobin β -93 cysteine signals increased pulmonary endothelial NOS expression in hypoxia.

Sripriya Sundararajan*, Lisa Palmer, Benjamin Gaston, Department of Pediatrics, Divisions of Respiratory Medicine and Neonatology*, University of Virginia Health System, Charlottesville, Virginia

Rationale: Red blood cells (RBCs) signal oxyhemoglobin (oxyHb) desaturation through transnitrosation - transfer of nitrosonium (NO^+) from one thiol to another - during the Hb transition from R state to T state. Specifically, the Hb β chain 93 cysteine (βC93) thiolate is modified by NO^+ in R state, but this S-NO bond is exposed to transnitrosation to other RBC thiols in T state. Endothelial nitric oxide synthase (eNOS) affects pulmonary vascular tone and remodeling. Expression of specificity proteins (Sp's), transcriptional regulators of eNOS, is modified by transnitrosation signaling (Biochem J 2004;380:67). Therefore, we studied whether eNOS can be upregulated by RBC OxyHb desaturation through an effect of Hb βC93 on Sp expression.

Methods: Wild type C57Bl6 mice (wt) and those expressing either human Hb α and β genes (human knock-in, HKI) or human α and a human β -93 mutant knock-out (H βC93KO) expressing a cysteine (C) to alanine (A) mutation (C-A) (kindly provided by Dr. T. Townes) were each treated (3 wk) with 52 mM N-acetyl cysteine (NAC), 1 mM S-nitroso-N-acetyl cysteine (SNOAC) or 10% oxygen as reported (JCI 2007;117:2592); controls were in normoxia. Lungs underwent immunoblot (IB) for eNOS, Sp1 and Sp3. Three mice were studied in each genotype for each of the four conditions (36 mice total).

Results: Hypoxia increased eNOS expression in HKI, but not H βC93KO mice; and increased S-nitrosylation (SNOAC) and NO^+ transfer (NAC) increased eNOS expression in wt, but not H βC93KO mice. Overall eNOS expression varied linearly with Sp3 expression ($r^2 = 0.71$; $n = 24$), but was unrelated to Sp1 expression. Of note, the HKI were like wt mice except that they tended to have an exaggerated increase in hypoxic eNOS expression.

Conclusions: OxyHb desaturation signals through the Hb β -93 cysteine to increase pulmonary eNOS expression. This effect is recapitulated by S-nitrosothiol loading (SNOAC) and transport (NAC); and increased Sp3 expression - which can be regulated by S-nitrosylation signaling - appears to be a critical intermediate. Therefore, it is likely that the S-nitroso Hb β -93 cysteine signals through transnitrosation signaling during Hb R to T transition. This mechanism makes sense: gene regulation changes more in response to decreased O_2 content than to decreased pO_2 .

THERAPEUTIC APPLICATIONS OF THE EFFECTS OF ANDROGENS ON S-NITROSOTHIOL METABOLISM IN PULMONARY DISEASE

**STATEMENT REGARDING FEDERALLY SPONSORED RESEARCH OR
5 DEVELOPMENT**

This invention was made in part with United States Government support under grants awarded by the National Institutes of Health and the Department of Defense (Army). The United States Government has certain rights in the invention.

10 BACKGROUND

Marked gender discordance has been observed for decades in the incidence, morbidity and mortality associated with human pulmonary diseases. For example, among children, asthma is more common in boys; however, in adults, nearly 2/3 of patients with asthma are women. In the case of cystic fibrosis, overall mortality among
15 women is nearly 1-2 years earlier than that of men, suggesting that female gender is a risk factor for more severe disease. In the case of pulmonary arterial hypertension of most causes, women are overall more susceptible than men. The cause of this gender discordance is not well understood.

20 SUMMARY OF THE INVENTION

The present application provides novel data regarding a previously unrecognized mechanism by which there is gender discordance in lung disease—specifically, androgen-induced inhibition of S-nitrosogluthathione reductase *in vivo*. More specifically, the present application discloses that androgens have a specific effect to inhibit S-nitrosothiol
25 breakdown in the lung; this effect can counterbalance estrogen-induced excess S-nitrosothiol production by endothelial nitric oxide synthase and appears to be protective against asthma and cystic fibrosis. This novel finding introduces a novel set of therapies for asthma, cystic fibrosis and pulmonary arterial hypertension involving nebulation of S-nitrosothiol signaling with the use of androgen inhibitors.

30 There is a balance between cellular S-nitrosothiol breakdown that is co-regulated by androgens and estrogens and appears to be disordered in many patients—particularly women—with pulmonary arterial hypertension. The present invention

encompasses the use of specific agonists and androgen mimetic effects—given by inhalation and/or systemically—for the treatment of asthma, cystic fibrosis, pulmonary arterial hypertension and related lung diseases.

5 The activity of the enzyme, S-nitrosoglutathione (GSNO) reductase, is inhibited in lung homogenates of male mice relative to female mice. Castration of the mice results in an increase in activity; and administration of dihydrotestosterone a decrease in the activity. These are activity effects more than effects on protein expression.

10 GSNO reductase activity regulates cellular levels of S-nitrosoglutathione. GSNO, in turn, is responsible for airway and vascular smooth muscle relaxation, as well as increased expression, maturation and function of mutant and wild-type cystic fibrosis transmembrane regulatory proteins. An increase in S-nitrosoglutathione therefore reverses the adverse effects of many CF-associated mutations, improves airway hydration and relaxes pulmonary vascular smooth muscle. Therefore, the effect of androgens, dihydrotestosterone, that we observed to inhibit GSNO reductase activity will increase GSNO levels in the lung, and will provide a novel treatment option for asthma, cystic fibrosis and key pulmonary arterial hypertension.

15 However, chronic, long-term, unregulated exposure to high levels of S-nitrosothiols can result in upregulation of genes that cause pulmonary remodeling. This is particularly true in the case of pulmonary arterial hypertension. There is a balance between S-nitrosothiol production by endothelial nitric oxide synthase and S-nitrosothiol breakdown by S-nitrosoglutathione reductase. In women, it is known that there is increased endothelial nitric oxide synthase expression in the lung. The same has been observed in female mice. This increased expression is balanced by lack of inhibition of GSNO reductase (lack of androgen). Our data suggest that when there is inadequate compensation for increased eNOS expression by decreased (androgen depletion-induced) GSNO-R activity, pulmonary vascular remodeling and pulmonary arterial hypertension will result. In this case, inhibition of androgen signaling in the lungs of female patients with progressive pulmonary arterial hypertension can be a treatment that will prevent upregulation of GSNO-associated remodeling genes, preventing the progression of pulmonary arterial hypertension in women.

20

25

30

In one embodiment, the present invention encompasses the use of androgens, either by inhalation or systemically, to treat diseases and disorders, including, but not limited to, asthma, cystic fibrosis, or related diseases and acute pulmonary arterial hypertension.

5 In another embodiment, the present invention encompasses the use of androgen receptor antagonists to treat diseases and disorders, including, but not limited to, progressive pulmonary arterial hypertension caused by excessive eNOS activity/estrogen, high flow states, chronic inflammation or chronic hypoxemia.

10 In one aspect, the dose and type of therapy can be titrated by measuring circulating or pulmonary GSNO reductase activity. That is, if increased S-nitrosoglutathione reductase activity is needed (for example, for chronic pulmonary arterial hypertension, using androgen depletion or inhibition), the dose of androgen inhibitor can be adjusted based on circulating GSNO reductase activity or GSNO reductase activity in a transbronchial biopsy; similarly, if decreased GSNO reductase is
15 needed (for asthma, cystic fibrosis, acute pulmonary arterial hypertension or related diseases of GSNO deficiency), the GSNO level in the airway, and/or the GSNO reductase activity in circulation or in the lung can be used to titrate the dose of androgen given.

20 Various aspects and embodiments of the invention are described in further detail below.

BRIEF DESCRIPTION OF THE DRAWINGS

25 **Figure 1**, comprising left and right panels, graphically depicts the gender differences in response to NAC indicators of PH. Treatments- Normoxia/untreated; NAC; and Hypoxia. The left panel indicates RV weight and the right RV pressure.

Figure 2, comprising left and right panels, graphically demonstrates that castration eliminates NAC-induced PAH. The left panel indicates RV weight and the right RV pressure. Treatments- Gonad intact; Castrated.

30 **Figure 3** graphically depicts that castration increases GSNO-R activity. The ordinate indicates [GSNO] remaining μM , and the abscissa GSNO-R activity.

Figure 4 is a schematic representation of an NAC model.

Figure 5 is a schematic representation of regulatory pathways involved in pulmonary hypertension and possible mechanisms for regulating the pathways.

Figure 6 is a schematic representation of the possible role of S-nitrosothiols and pulmonary hypertension.

5 **Figure 7** is a schematic representation of the possible role Gender and S-nitrosothiols and pulmonary hypertension.

DETAILED DESCRIPTION

Definitions

10 In describing and claiming the invention, the following terminology will be used in accordance with the definitions set forth below.

The articles “a” and “an” are used herein to refer to one or to more than one (i.e., to at least one) of the grammatical object of the article. By way of example, “an element” means one element or more than one element.

15 The term "about," as used herein, means approximately, in the region of, roughly, or around. When the term "about" is used in conjunction with a numerical range, it modifies that range by extending the boundaries above and below the numerical values set forth. For example, in one aspect, the term "about" is used herein to modify a numerical value above and below the stated value by a variance of 20%.

20 Marked gender discordance has been observed for decades in the incidence, morbidity and mortality associated with human pulmonary diseases. For example, among children, asthma is more common in boys; however, in adults, nearly 2/3 of patients with asthma are women. In the case of cystic fibrosis, overall mortality among women is nearly 1-2 years earlier than that of men, suggesting that female gender is a risk factor for more severe disease. In the case of pulmonary arterial hypertension of most causes, women are overall more susceptible than men. The cause of this gender discordance is not well understood. The present invention discloses that androgens have a specific effect to inhibit S-nitrosothiol breakdown in the lung; this effect can counterbalance estrogen-induced excess S-nitrosothiol production by endothelial nitric
25
30
oxide synthase and appears to be protective against asthma and cystic fibrosis. There is a balance between cellular S-nitrosothiol breakdown that is co-regulated by androgens

and estrogens and appears to be disordered in many patients—particularly women—
with pulmonary arterial hypertension. The present invention encompasses the use of
specific agonists and androgen mimetic effects—given by inhalation and/or
systemically—for the treatment of asthma, cystic fibrosis, pulmonary arterial
5 hypertension, and related lung diseases.

The activity of the enzyme, S-nitrosogluthathione (GSNO) reductase, is inhibited
in lung homogenates of male mice relative to female mice. Castration of the mice
results in an increase in activity; and administration of dihydrotestosterone a decrease in
the activity. These are activity effects more than effects on protein expression.

10 GSNO reductase activity regulates cellular levels of S-nitrosogluthathione.
GSNO, in turn, is responsible for airway and vascular smooth muscle relaxation, as well
as increased expression, maturation and function of mutant and wild-type cystic fibrosis
transmembrane regulatory proteins. An increase in S-nitrosogluthathione therefore
reverses the adverse effects of many CF-associated mutations, improves airway
15 hydration and relaxes pulmonary vascular smooth muscle. Therefore, the effect of
androgens, dihydrotestosterone, that we observed to inhibit GSNO reductase activity
will increase GSNO levels in the lung, and will provide a novel treatment option for
asthma, cystic fibrosis and key pulmonary arterial hypertension.

However, chronic, long-term, unregulated exposure to high levels of S-
20 nitrosothiols can result in upregulation of genes that cause pulmonary remodeling. This
is particularly true in the case of pulmonary arterial hypertension. There is a balance
between S-nitrosothiol production by endothelial nitric oxide synthase and S-
nitrosothiol breakdown by S-nitrosogluthathione reductase. In women, it is known that
there is increased endothelial nitric oxide synthase expression in the lung. The same
25 has been observed in female mice. This increased expression is balanced by lack of
inhibition of GSNO reductase (lack of androgen). Our data suggest that when there is
inadequate compensation for increased eNOS expression by decreased (androgen
depletion-induced) GSNO-R activity, pulmonary vascular remodeling and pulmonary
arterial hypertension will result. In this case, inhibition of androgen signaling in the
30 lungs of female patients with progressive pulmonary arterial hypertension can be a

treatment that will prevent upregulation of GSNO-associated remodeling genes, preventing the progression of pulmonary arterial hypertension in women.

We have observed that the exogenous S-nitrosothiol, S-nitroso-N-acetyl-cysteine, enters pulmonary vascular endothelial cells and causes upregulation of genes associated with pulmonary vascular remodeling. Administration to mice *in vitro* and *in vivo* causes these effects. Also, in male mice that are eNOS replete, the S-nitroso-N-acetyl-cysteine causes pulmonary vascular remodeling in pulmonary hypertension. eNOS is necessary for this effect (through transnitrosation reactions occurring in hemoglobin) and that eNOS deficient mice are not susceptible to pulmonary arterial hypertension that is caused by S-nitroso-N-acetyl-cysteine.

Of interest, however, female mice are not susceptible to pulmonary arterial hypertension caused by S-nitroso-N-acetyl-cysteine, though they have higher baseline pulmonary pressures than male mice. If the male mice are castrated, they are also protected from S-nitroso-N-acetyl-cysteine. If female mice are ovariectomized, they remain protected from S-nitroso-N-acetyl-cysteine, suggesting that it is not an increase in estrogen/female sex steroids that causes the protection: rather, it is lack of androgen (see Figures). Indeed, we have shown that androgen replacement in the castrated male mice causes them to be susceptible to pulmonary hypertension.

Preliminary data suggest that the overall mechanism is this (Figure 5). Estrogen increases eNOS expression. eNOS is co localized with S-nitrosogluthathione reductase in pulmonary cells. The absence of androgens counter balances the increased nitrosothiol production associated with increased eNOS expression by being permissive for increased GSNO reductase activity. eNOS allows S-nitrosylation of circulating proteins such as hemoglobin and albumin. These, through transnitrosation reactions, form SNOAC. The SNOAC enters lung cells forming GSNO because of high glutathione levels in the cells. Over the long-term, there is upregulation of GSNO-regulated genes causing the vascular remodeling associated with pulmonary hypertension. Thus, males, who have androgen-induced decreased GSNO reductase activity, are susceptible to the long-term gene regulatory effects of N-acetyl-cysteine and S-nitroso-N-acetyl cysteine and, potentially, other S-nitrosothiols to cause

pulmonary hypertension. Normal females are protected by virtue of their increased S-nitrosoglutathione reductase activity.

5 The mechanism appears to be a final pathway for pulmonary arterial hypertension. Chronic hypoxia can cause excessive offloading of nitrosothiols into the pulmonary vascular endothelium, causing remodeling because of allosteric effects of hemoglobin. Excess inflammation can cause dumping of nitrosothiols into the pulmonary vascular endothelium. High flow states, in which an increased number of circulatory nitrosothiols go through the pulmonary vascular endothelium in time, can cause pulmonary vascular remodeling by nitrosothiol dumping. Women with high eNOS activity who do not have adequate compensatory S-nitrosoglutathione reductase activity are particularly at risk.

10 Though androgens do not increase GSNO reductase expression, we have recently observed that it inhibits GSNO activity (Figure 1). This inhibition of S-nitrosoglutathione reductase activity would be good for asthma and cystic fibrosis (increasing GSNO levels), it would be good acutely for pulmonary hypertension, leading to decreased pulmonary vascular tone (perhaps suggesting why the female mice have higher pulmonary artery pressures at baseline). However, in the long-term, this excess in nitrosothiols upregulates hypoxia-associated genes.

15 We have previously published the work on N-acetyl-cysteine and S-nitroso-N-acetyl-cysteine causing pulmonary hypertension in male mice. However, the observation that female mice are protected, and the mechanistic information regarding androgens (castration, androgen replacement, ovariectomy) is novel and forms the basis of the invention.

BIBLIOGRAPHY

25 1. Palmer L, Doctor A, Chhabra P, Sheram ML, Laubach V, Karlinsey MZ, Forbes M, Macdonald T, Gaston B. S-Nitrosothiols signal hypoxia-mimetic vascular pathology. *J Clin Invest*, 2007;117:2592-2601.

2. U.S. Patent: "Inhibiting GSNO Breakdown"

30 The disclosures of each and every patent, patent application, and publication cited herein are hereby incorporated by reference herein in their entirety.

Headings are included herein for reference and to aid in locating certain sections. These headings are not intended to limit the scope of the concepts described therein under, and these concepts may have applicability in other sections throughout the entire specification.

- 5 While this invention has been disclosed with reference to specific embodiments, it is apparent that other embodiments and variations of this invention may be devised by others skilled in the art without departing from the true spirit and scope of the invention.

ABSTRACT

There is a gender discordance in many human lung diseases, including asthma, cystic fibrosis, and pulmonary arterial hypertension. This discordance affects incidence, morbidity and mortality. We have discovered a novel pathway by which androgens can be both beneficial and can have adverse effects in these lung diseases. This is a completely novel mechanism involving S-nitrosothiol metabolism in the lung.

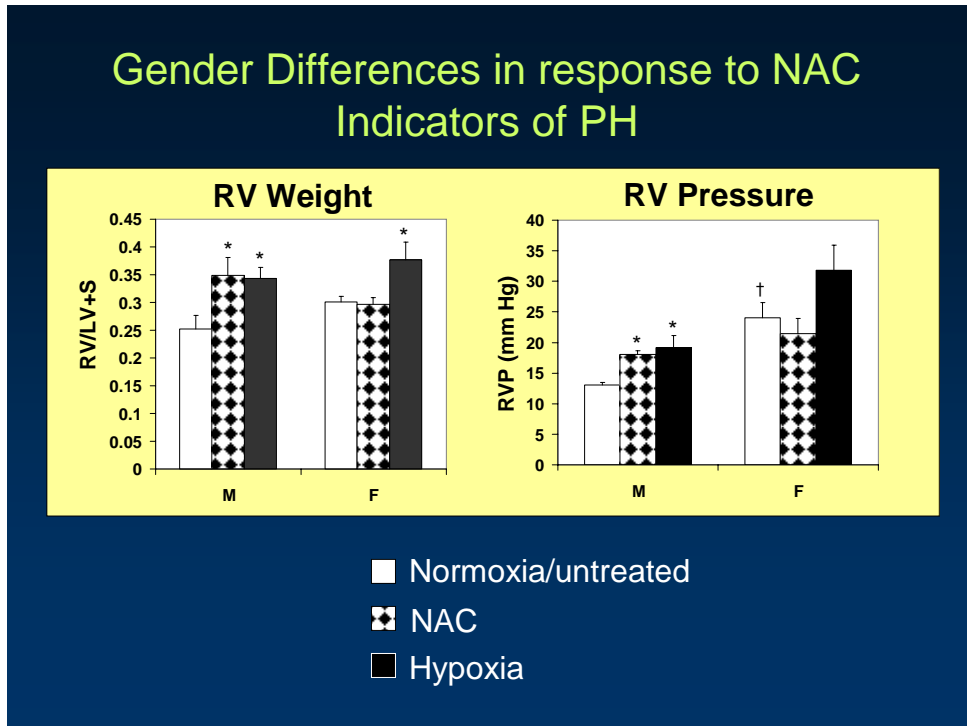


FIG. 1

Castration eliminates NAC-induced PAH

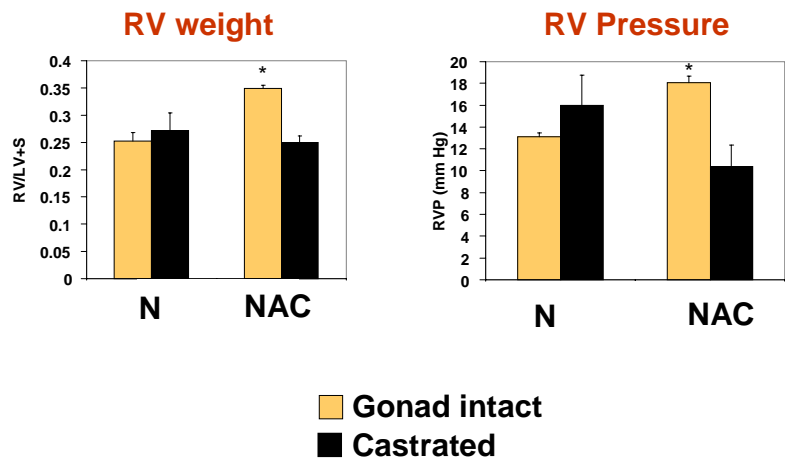


FIG. 2

Castration increases GSNO-R activity

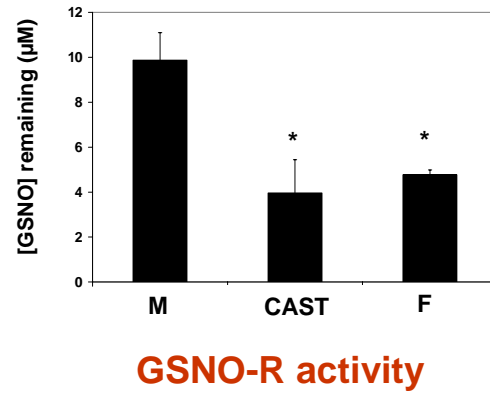


FIG. 3

NAC Model: Androgen Effects

1. Castration:
 - eliminates development of PH with NAC
 - right ventricular pressure
 - right ventricular weight
 - increases GSNO-R-Activity
2. Ovariectomy:
 - No effects (*data not shown*)
3. GSNO-R is regulated by androgens.

FIG. 4

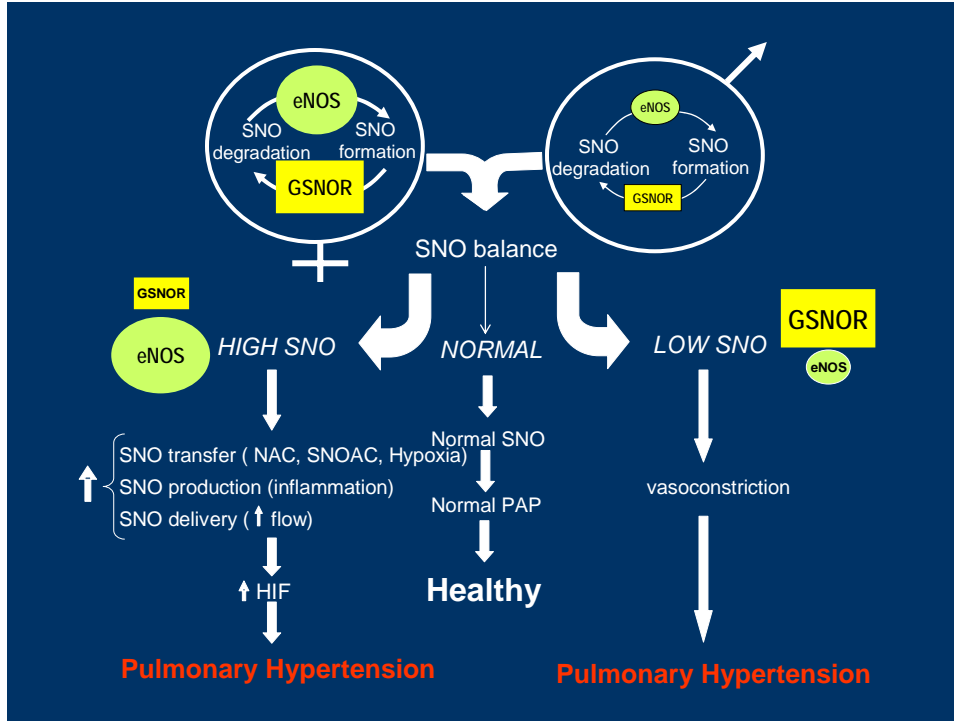


FIG. 5

S-nitrosothiols and Pulmonary Hypertension

Mismatch between SNO production and SNO degradation can cause pulmonary hypertension

1. SNO excess:
 - Inappropriate activation of transcription factors involved in PH (HIF-1, SP-3)
2. SNO depletion:
 - Inappropriate vasoconstriction

FIG. 6

Gender and S-nitrosothiols

SNO Bioavailability may be responsible, in part, for gender disparities.

1. SNO formation:
 - Estrogen known to regulate eNOS
2. SNO degradation:
 - Androgens downregulate GSNO-R activity
3. SNO excess:
 - NAC model → males develop PH

FIG. 7